

SEDIMENTOLOGY AND DIAGENESIS OF THE SHUAIBA FORMATION
(LOWER CRETACEOUS; APTIAN), GHABA NORTH
FIELD, OMAN

by

AbdulRahman A. Manan Al-Bastaki


T-4522

A thesis submitted to the Faculty and Board of Trustees of the Colorado School of Mines in partial fulfillment of the requirements for the degree of Master of Science (Geology).


Golden, Colorado

Date 11/17/93

Signed :



AbdulRahman A. Al-Bastaki

Approved :


Dr. John D. Humphrey
Thesis Advisor

Golden, Colorado

Date 11/17/93


Dr. Roger M. Slatt
Professor and Head,
Department of Geology
and Geological Engineering

ABSTRACT

The depositional environment, diagenetic history, and development and distribution of reservoir characteristics of the Lower Cretaceous (Aptian) Shuaiba Formation of central Oman are considered in this study. Specifically core descriptions, core plug and thin section inspection, and SEM investigations were performed on samples taken from Ghaba North Field. In addition, stable carbon and oxygen analyses of Shuaiba matrix and late cements were used to constrain the diagenetic history of the formation.

The Shuaiba Formation is subdivided into two major zones, the lower and upper. The lower zone was deposited in a shallow innershelf depositional setting under restricted circulation conditions. The upper Shuaiba zone was deposited in a shallow outershelf depositional setting under more open conditions. Spatial trends in the Shuaiba at Ghaba North indicate that rudist buildups were developed to the northeast of the field and a paleostrandline existed toward the southwest portion of the field.

Reservoir properties include macroporosity, microporosity, and horizontal permeability. In general, favorable reservoir properties decrease with depth in the Shuaiba cores and in a trend from the northeast to southwest in Ghaba North Field. The Shuaiba has little primary interparticle porosity due to its micritic nature. Macroporosity occurs as secondary moldic porosity developed after rudists. Development of macroporosity is controlled by the abundance of originally aragonitic rudists and

proximity to subaerial exposure surfaces. The reservoir hydrocarbon storage capacity is controlled by microporosity, which occurs as intercrystalline porosity within a micro-rhombic calcite matrix. Isotopic analysis indicates that this matrix was stabilized during interaction with meteoric diagenetic fluids. Microporosity increases or decreases in the Shuaiba due to the relative abundance of blocky-crystal framework texture versus crystal mosaic texture in the matrix. Presence of calcite neomorphic microspar in interpeloidal pore spaces reduces microporosity as well. These observations indicate that reservoir quality of the Shuaiba is very heterogeneous, and trends observed for the variation of microporosity with depth should be considered in any reservoir development plan.

Development of microporosity is the key to establishment of a suitable petroleum reservoir in the Shuaiba. Development of secondary moldic porosity enhances reservoir properties further. Exploration in the Shuaiba has historically been oriented toward location of favorable structures; however, recognition of two subaerial exposure surfaces in the Shuaiba at Ghaba North increases the potential for further exploration in the region. The first exposure surface is the regional unconformity separating the Shuaiba from the overlying Nahr-Umr Formation. The second is a localized subaerial exposure that developed at the top of a rudist bioherm in the upper Shuaiba zone. Similar events to those which created the second subaerial exposure surface may have occurred in other locations on the shelf, particularly toward the northeast from Ghaba North, due to the presence of abundant bioherms in the proximity of the rudist buildup. Subaerial exposure events are important for the development of conditions during which Shuaiba sediments could interact with meteoric waters. Matrix stabilization, the formation of intercrystalline microporosity, and the development of moldic macroporosity are all consequences of subaerial exposure.

TABLE OF CONTENTS

ABSTRACT	iii
LIST OF TABLES AND PLATES	viii
LIST OF FIGURES	ix
ACKNOWLEDGMENTS	xii
INTRODUCTION	1
Geological Setting	2
Regional Overview of the Shuaiba Formation	8
Correlation of the Shuaiba Formation Over the Persian Gulf	11
Development of Shuaiba Reservoir Properties	15
Ghaba North Field	17
General Description of the Shuaiba Formation in Ghaba North Field	21
Previous Work	22
METHODS OF STUDY	25
RESULTS	29
Petrology, Petrography and Reservoir Properties of the Shuaiba Formation in the GN-23 Well	29
Lithology and Sedimentology of the Shuaiba Formation in GN-23	29
Stratigraphic Variability of Allochemical Constituents	49
Stratigraphic Variability of Selected Reservoir Properties	54

Diagenesis of the Shuaiba Formation in GN-23	59
Diagenetic Features Observed in GN-23	62
Shuaiba Isotopic Analysis	77
Lithology and Reservoir Properties of the Shuaiba Formation in Other Wells in Ghaba North Field	80
The Shuaiba Formation in GN-13.....	80
The Shuaiba Formation in GN-2.....	83
The Shuaiba Formation in GN-1	84
DISCUSSION	86
Petrology, Petrography and Reservoir Properties of the Shuaiba Formation in the GN-23 Well.....	86
Inferred Depositional Environments of the Shuaiba Formation	86
Stratigraphic Variability and Relationships Among Allochemical Constituents.....	98
Controls on Reservoir Properties	101
Diagenesis of the Shuaiba Formation in GN-23	116
Diagenetic Features of the Shuaiba in GN-23	116
Stable Carbon and Oxygen Isotopic Analysis.....	123
Paragenetic Sequence of the Shuaiba Formation in GN-23	134
Lithology and Reservoir Properties of the Shuaiba Formation in Other Wells in Ghaba North Field	135
The Shuaiba Formation in GN-13.....	136
The Shuaiba Formation in GN-2.....	137
The Shuaiba Formation in GN-1	137

Correlation of the Shuaiba Formation Across Ghaba North Field.....	138
CONCLUSIONS AND RECOMMENDATIONS	142
Recommendations	145
REFERENCES CITED	147
APPENDIX 1	154
APPENDIX 2	158

LIST OF TABLES AND PLATES

	Page
Table 1. Reservoir Properties and Depths of the SEM samples	108
Plate 1. Core Description of the Shuaiba GN-23	pocket
Plate 2. Core Description of the Shuaiba GN-1	pocket
Plate 3. Core Description of the Shuaiba GN-2	pocket
Plate 4. Core Description of the Shuaiba GN-13	pocket
Plate 5. Photographic Record of the Shuaiba GN-23 Core	pocket

LIST OF FIGURES

	Page
1. Arabian Plate tectonic setting	3
2. Geotectonic components of the Arabian Peninsula	5
3. Stratigraphic column of Oman	7
4. Aptian paleogeographic map of the Arabian Peninsula	9
5. Trends of rudist buildups in the Persian Gulf	12
6. Fence correlation diagram of the Lower Cretaceous Persian Gulf formations	13
7. Location map of Ghaba North Field	18
8. Ghaba Salt basin configuration	19
9. Structure contour map of the Shuaiba at Ghaba North	20
10. Photomicrograph of an <i>Orbitulina</i>	31
11. Photomicrographs of green algae in the Shuaiba	33
12. Rudist variability in GN-23	50
13. Algae variability in GN-23	52
14. <i>Orbitulina</i> and other allochem variability in GN-23	53
15. Total measured porosity variability in GN-23	56
16. Macroporosity variability in GN-23	57
17. Microporosity variability in GN-23	58
18. Horizontal permeability variability in GN-23	60
19. Masked horizontal permeability variability in GN-23	61
20. Photomicrograph of partially cemented algae intraparticle pores	63
21. Photomicrograph of fine-crystalline calcite cement	65

22. Photomicrograph of fine patchy calcite cement.....	66
23. Photomicrograph of coarse-crystalline calcite cement	67
24. Photomicrograph of calcite syntaxial overgrowth on an echinoid.....	69
25. Photomicrograph of leaching in rudists	71
26. Photomicrograph of solution seams	72
27. SEM photograph of a partially cemented mold	74
28. Cross-plot of macroporosity versus horizontal permeability	75
29. SEM photograph of micro-rhombic calcite matrix	76
30. SEM photograph of matrix with a crystal mosaic texture	78
31. SEM photograph of matrix with a neomorphic calcite microspar	79
32. Cross-plot of $\delta^{13}\text{C}$ versus $\delta^{18}\text{O}$	81
33. Major types of rudists in the Cretaceous.....	89
34. Cross-plot of rudists versus algae in GN-23	100
35. Cross-plot of total measured porosity versus microporosity in GN-23	104
36. Cross-plot of <i>Orbitulina</i> and other allochems versus microporosity in GN-23.....	106
37. Cross-plot of rudists versus microporosity in GN-23	107
38. Cross-plot of rudists versus macroporosity in GN-23	110
39. Cross-plot of algae versus macroporosity in GN-23.....	111
40. Cross-plot of rudists versus horizontal permeability in GN-23	113
41. Cross-plot of microporosity versus horizontal permeability in GN-23	114
42. Cross-plot of total measured porosity versus horizontal permeability	115
43. $\delta^{13}\text{C}$ variation of the Shuaiba matrix in GN-23.....	124
44. $\delta^{18}\text{O}$ variation of the Shuaiba matrix in GN-23	125
45. Plot of $\delta^{18}\text{O}$ values of the late cement in the Shuaiba with depth in GN-23	132

T-4522

46. Plot of $\delta^{13}\text{C}$ values of the late cement in the Shuaiba with depth in GN-23 133

ACKNOWLEDGMENTS

My advisor, Dr. John D. Humphrey, provided me with guidance, encouragement, fruitful discussions, and invaluable help throughout this study. His office was always open for me and I was always pleasantly greeted even when his schedule was busy. For that, I am sincerely grateful. My thesis committee members, Dr. John B. Curtis and Dr. John Warne, provided support and encouragement and were helpful in reviewing the thesis.

Petroleum Development Oman (PDO) sponsored me in my post-graduate studies. I am particularly grateful to Keith Eastwood, who suggested I consider this project. I highly appreciate Christopher Mercadier's effort in helping me carry out this project during my visit to PDO during the summer of 1992.

I am thankful to John Skok in the Geology department of the Colorado School of Mines for helping me with the SEM.

I would like to acknowledge and thank Dr. AbdulRahman Alsharhan, my professor at the United Arab Emirates University, for his encouragement pursue my Master's degree.

I am extremely grateful to my parents, my brother Ibrahim, and the rest of my family for their love, support, and prayers.

Finally, I am deeply grateful to my wife, Maryam. She stood with me throughout this study and remained very supportive, patient and loving.

INTRODUCTION

The Shuaiba Formation (Lower Cretaceous; Aptian) is a prolific hydrocarbon reservoir in the Persian Gulf, in general, and in northern and central Oman, in particular, due to its petrographic characteristics, framework properties and diagenetic nature. Therefore, it is important to consider the evolution of its depositional and diagenetic environments and reservoir characteristics. This thesis will concentrate on the Shuaiba Formation reservoir in the Ghaba North Field in central Oman. The purpose of this study is to fully characterize the sedimentary facies distribution in the field by means of core description, thin section analysis and log study. In addition, characterization of the diagenetic history of the Shuaiba Formation in Ghaba North Field is a major component of the study. Emphasis will be placed on porosity evolution and relative timing of diagenetic events.

This study begins by presenting a general review of the geology of Oman in order to familiarize the reader with the regional geologic setting. In addition, a review of the Mesozoic stratigraphic section and depositional setting of the region and in Oman will be presented. Moreover, the environment of deposition and reservoir properties of the Shuaiba Formation will be correlated over the Persian Gulf region in order to establish a regional understanding of the formation. Next, Ghaba North Field will be discussed in this regional context. Previous work performed on the Shuaiba Formation in Ghaba North Field will be reviewed as background for this research. Methods and procedures of the work performed will be reviewed. The results obtained in this study will be presented

and then discussed in order to develop an understanding of the Shuaiba Formation in Ghaba North Field. Finally, conclusions regarding the depositional and diagenetic history of the Shuaiba and reservoir properties in the field will be presented.

Geological Setting

The Sultanate of Oman lies within the northeastern corner of the crustal plate known as the Arabian Plate (Fig. 1). The plate boundary lying north of Oman is a convergent boundary between the Arabian Plate and the Eurasian Plate. The compressional forces here formed the Zagros Mountains of Iran to the north. To the east of Oman, the plate margin lies beneath the Indian Ocean. Here, the Arabian Plate and the Australian/Indian Plate form a transform boundary called the Owen Fracture Zone. At the southern and western edges, the Arabian Plate is diverging from the African Plate, forming new oceanic crust along the line of the Red Sea and the Gulf of Aden (Clarke, 1990).

Following break-up of the Gondwana supercontinent at the end of the Paleozoic Era, an elongated ocean (Tethys Seaway) extended from the Caribbean in the west through the Mediterranean, Middle East, and the Indo-Pacific Area to the east. Northward plate tectonic motion subsequently brought Oman and the rest of the region from subpolar latitudes to an equatorial position along the southern margin of the Tethys. This new position in tropical latitudes, on the western side of an ocean basin, created

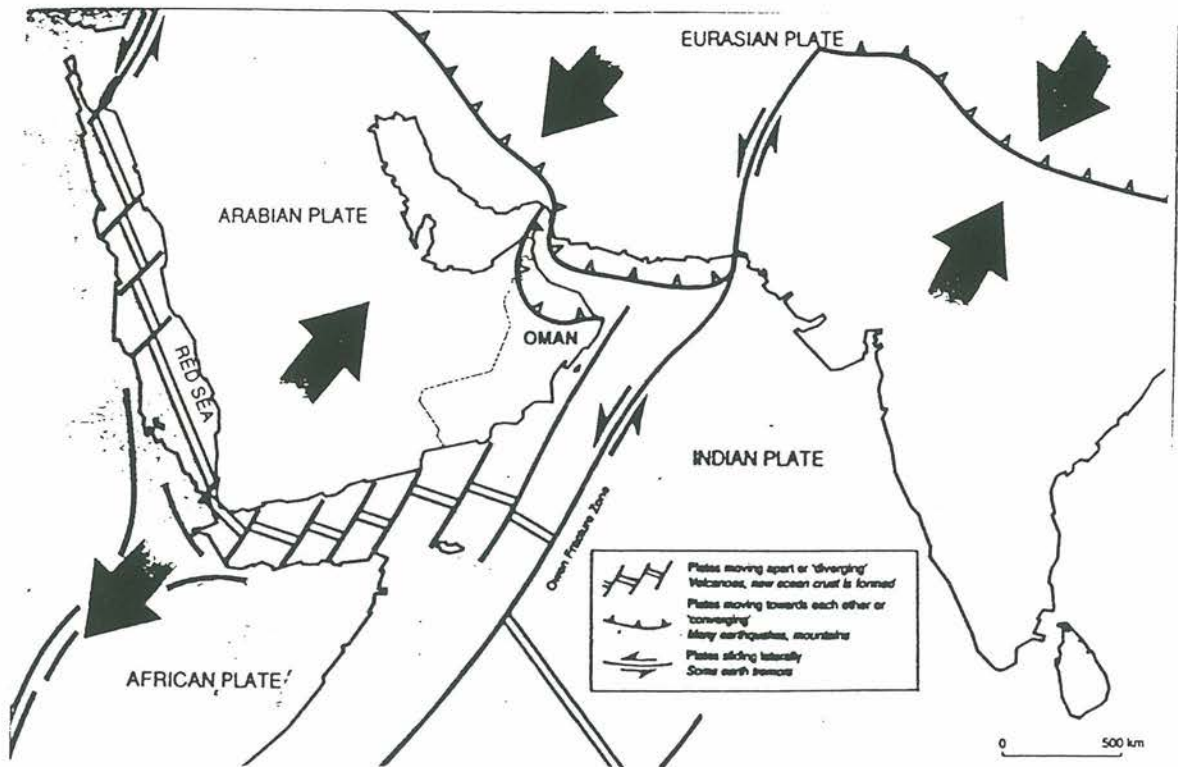


Figure 1. The Arabian Plate and Oman's plate tectonic setting (after Clarke, 1990).

favorable conditions for carbonate deposition in the region. Thus, the majority of sediments deposited in the Persian Gulf during the Mesozoic and Cenozoic are carbonates. These limestones and dolomites form most of the important reservoirs in the Middle East.

In order to place the stratigraphic section of Oman in its proper context, it is important to get an overview of the regional geology in the Arabian Peninsula. Generally, there are three main geotectonic components in the region (Fig. 2) (Powers et al., 1966) :

- 1) The Arabian Shield - Represents a complex area of Precambrian igneous and metamorphic rocks occupying the western and central part of the peninsula;
- 2) The Arabian Shelf - Extends northward and eastward of the Arabian Shield under a cover of continental and shallow marine Phanerozoic sediments, and;
- 3) The mobile belt of the Zagros and Oman Mountains lying north and northeast of the Arabian Shelf.

The deposition of carbonate and/or clastic rocks on the Arabian Shelf was controlled by the stability of the shelf and the Arabian Shield, which consequently resulted in the development of depositional basins (due to submergence of the shelf during relative sea-level rise). Furthermore, intraplate tectonics of the Arabian shield imposed broad flexures upon the Arabian Shelf sedimentary section (Alsharhan and Nairn, 1988). This resulted in the distribution of depressions (basins) on the shelf such as the Rubal Khali Basin, the Dibdibba Basin, the Northern Arabian Gulf Basin, and the

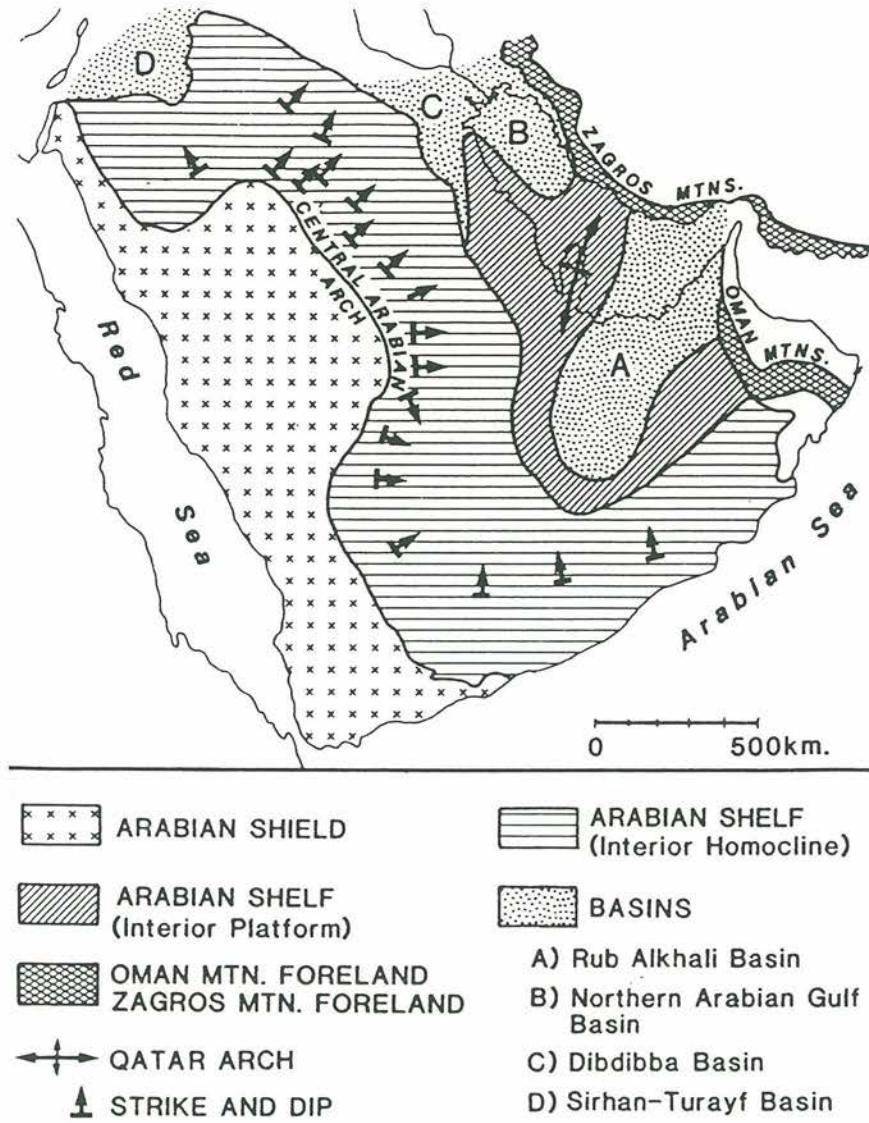


Figure 2. Geotectonic components and geologic setting of the Arabian Peninsula (after Powers et al., 1966; as referenced in Alsharhan and Nairn, 1986).

Sirhan-Turayf Basin (see Fig. 2). Moreover, the effects of the shield flexures also appear in the occurrence of arches such as the Central Arabian Arch and the Qatar Arch, which have played a key role in the changing lithology and facies development on the Arabian Shelf due to the recurrent rejuvenation of these flexural features during the Mesozoic and Cenozoic (Alsharhan and Nairn, 1988).

The Mesozoic stratigraphic section in Oman (Fig. 3) and the Persian Gulf is represented mainly by carbonate rocks. These rocks were deposited on the Arabian Shelf and indicate a period of relative stability. This stable shelf depositional environment was established during the Permian and continued through the Mesozoic (Alsharhan and Kendall, 1986). Deposition on this shelf was controlled by a series of transgressions and regressions during which were introduced a variety of sediments. Represented are deep-water mudstones and wackestones, shallow-water grainstones and packstones, as well as some evaporites. In Oman, many of these Mesozoic carbonates have maintained their primary porosities and permeabilities or had them enhanced via diagenetic processes. The result was the development of excellent hydrocarbon reservoirs, such as the Khuff Formation (Permo - Triassic), Sudair (Triassic), Mafraq (Lower Jurassic), Kharaib and Shuaiba Formations (Lower Cretaceous), and the Natih Formation (Middle Cretaceous).

Cretaceous carbonates of the Persian Gulf are generally shallow-water deposits that prograded across the Arabian Shelf (Alsharhan and Nairn, 1988). The Cretaceous section is generally divided into three major subdivisions in this region: the Lower Cretaceous Thammama Group (Berriasian to Aptian; referred to as Kahamah Group in Oman), the Middle Cretaceous Wasia Group (Albian to Turonian), and the Upper

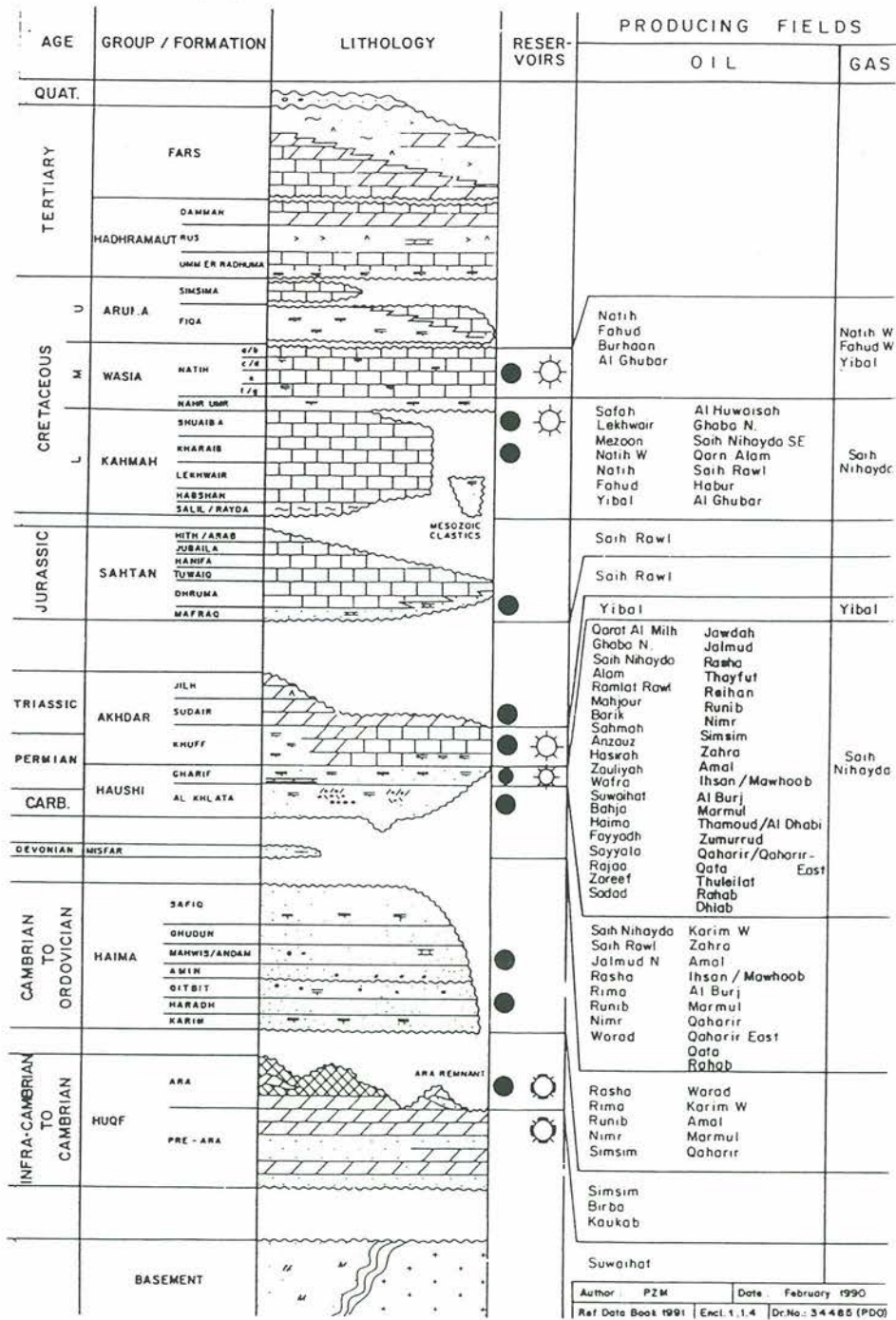


Figure 3. Stratigraphy of Oman and hydrocarbon distribution (after PDO, 1991).

Cretaceous Aruma Group (Coniacian to Maestrichtian) (Alsharhan and Nairn, 1986; Clarke, 1988).

In general, a simple carbonate ramp model has been proposed to characterize the rocks of the early Cretaceous in the Gulf (Murriss, 1980). Based upon this model, the succession of depositional environments (Fig. 4) during that period begins with alluvial and coastal plain sedimentation in western Saudi Arabia, bordering the exposed part of the Precambrian massif. Moving eastward, supra- and intertidal carbonate flats give way to lagoonal and open shelf environments, upon which shoals, biohermal accumulations, and intrashelf basins developed (Connaly and Scott, 1985).

Regional Overview of the Shuaiba Formation

Generally, the Arabian Peninsula depositional environments formed during the early Cretaceous, and specifically during the Aptian, were favorable for carbonate sediment deposition. These deposits are characterized by coral, algal and rudist colonies which grew along the Arabian Shelf (Alsharhan and Nairn, 1986). These sediments would eventually provide prolific carbonate reservoirs in the United Arab Emirates, Oman, Qatar, and Saudi Arabia in the southern part of the Persian Gulf. However, there was an increased influx of detrital material during the Hauterivian and Barremian which displaced the area of carbonate deposition eastward of Saudi Arabia (Alsharhan and Nairn, 1986).

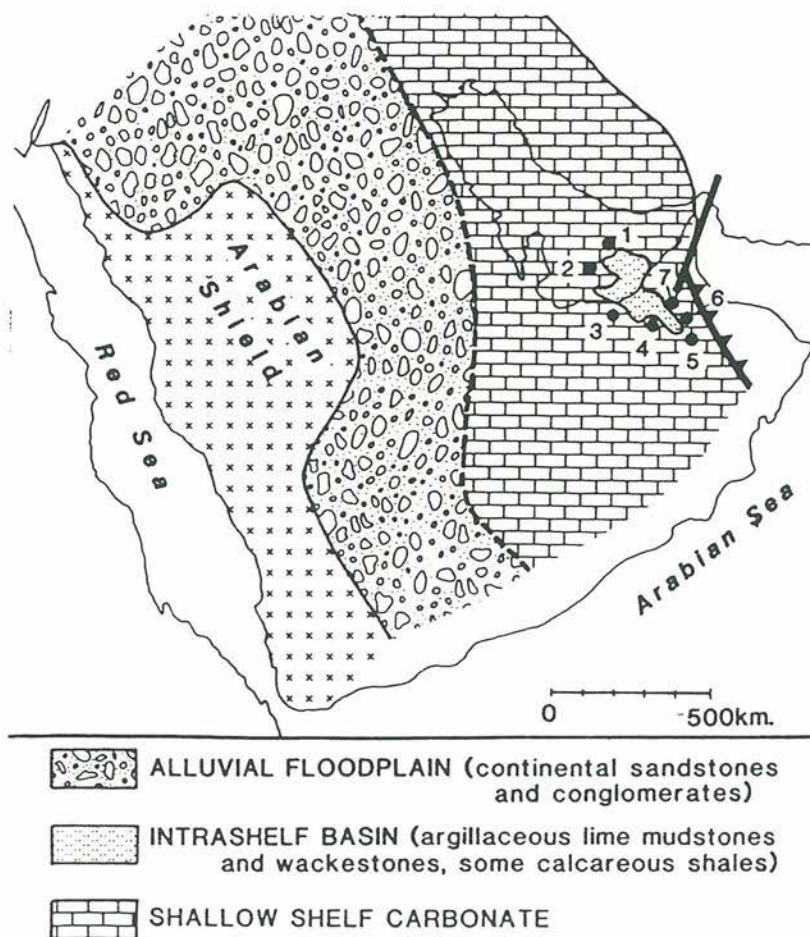


Figure 4. Aptian paleogeographic map of the Arabian Peninsula (after Alsharhan and Nairn, 1986). Numbers refer to locations of oil fields.

The region as a whole during the early Cretaceous is characterized by shelf carbonate deposition, with relatively low amounts of argillaceous materials, mostly confined to the north and east. Westward of Saudi Arabia, clastic shoreline facies mark the margin against the Precambrian rocks of the Arabian Shield (Powers et al., 1966) (Fig. 4).

Two carbonate cycles are recognized in the Lower Cretaceous of the region, with each cycle shallowing upward. The first cycle ends after the lower Hauterivian and is capped by the top of the Habshan Formation. The end of the second cycle is marked by deposition of the Shuaiba Formation which indicates establishment of a shallow-water carbonate depositional environment over most of the area (Alsharhan and Nairn, 1986).

The Shuaiba Formation, the unit of interest for this thesis, is Aptian in age and is the uppermost formation of the Lower Cretaceous Thammama Group. The Shuaiba Formation is named after the town of Shuaiba, located just east of Basra in southern Iraq. It was first used by P. M. Rabanit in 1951 in an unpublished report for the Iraqi Petroleum Company (Alsharhan, 1985; Clarke, 1988). Type locality for the Shuaiba Formation is the Basra Petroleum Company Zubair # 3 well in Iraq (Alsharhan and Nairn, 1986; Clarke, 1988). The Shuaiba Formation represents shelfal limestone deposition, extending in the subsurface over much of the Gulf from Iraq to central Oman and outcropping in northern Oman. It was deposited during an extensive marine inundation of the northern Arabian Shield, which extended into the southeast of the Rubal Khali Basin, and was marked by a series of thick rudist grainstone buildups (Alsharhan, 1985). Murriss (1980) believed that during the Aptian, in the southern part of the Persian Gulf

and United Arab Emirates in particular, the intrashelf basin of Abu Dhabi had developed and the fringing shelf-margin rudist buildups grew where conditions were favorable and created the prolific Shuaiba reservoir. The Shuaiba rudist buildups comprise a narrow belt which extends through Abu Dhabi in the United Arab Emirates to Oman, Saudi Arabia, and offshore Qatar (Fig. 5), where many oil fields in these countries produce from the Shuaiba Formation (Alsharhan, 1985).

Correlation of the Shuaiba Formation over the Persian Gulf

The Shuaiba Formation, which was deposited on the Arabian Shelf as a shallow-marine platform carbonate sequence, extends over most of the area as mentioned previously. Slight differences in Shuaiba Formation characteristics are caused by differences in water depths. Therefore, different facies of the Shuaiba can be correlated over the Gulf (Fig. 6).

In the southern part of the Persian Gulf, particularly in Oman, the United Arab Emirates, and Qatar, Alsharhan and Nairn (1986) described the Shuaiba depositional environment as a shelf platform. Furthermore, in Oman it is described as a shallow to deep platform. In the United Arab Emirates, the depositional environment was a shallow shelf with rudist and algal deposits that rimmed the Abu Dhabi intrashelf basin where the deposition of Bab member occurred over Zakum area in Abu Dhabi. The Bab member is comprised by deep sediments equivalent to the Shuaiba Formation (Aldabal and Alsharhan, 1989). According to Clarke (1988), the Shuaiba Formation in Oman shows a full cycle of carbonate sedimentation, which reflects a shallow to deep and then to

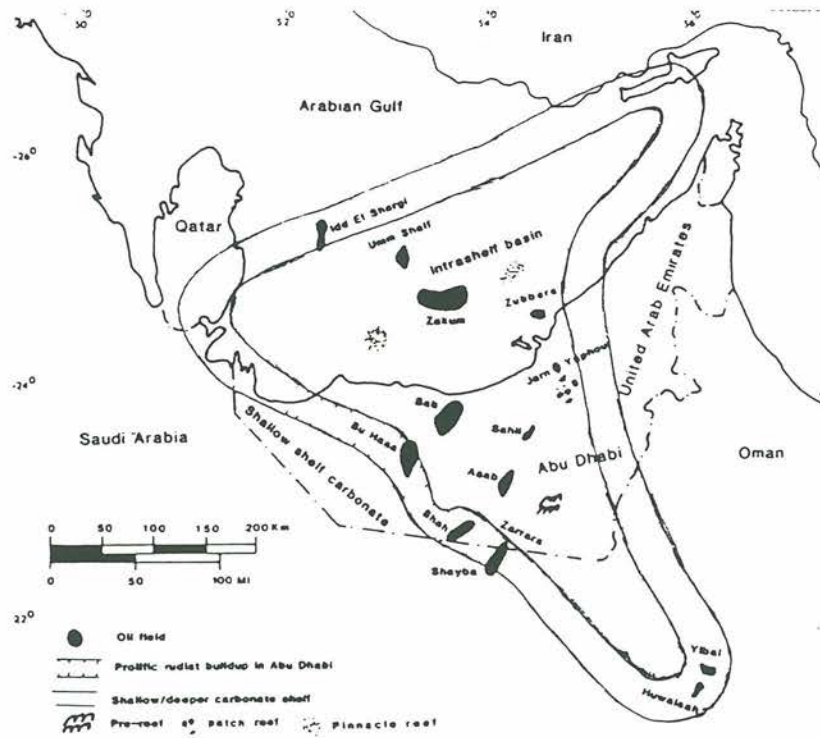


Figure 5. Approximate trend of rudist buildups in the southern part of the Persian Gulf (after Alsharhan, 1985).

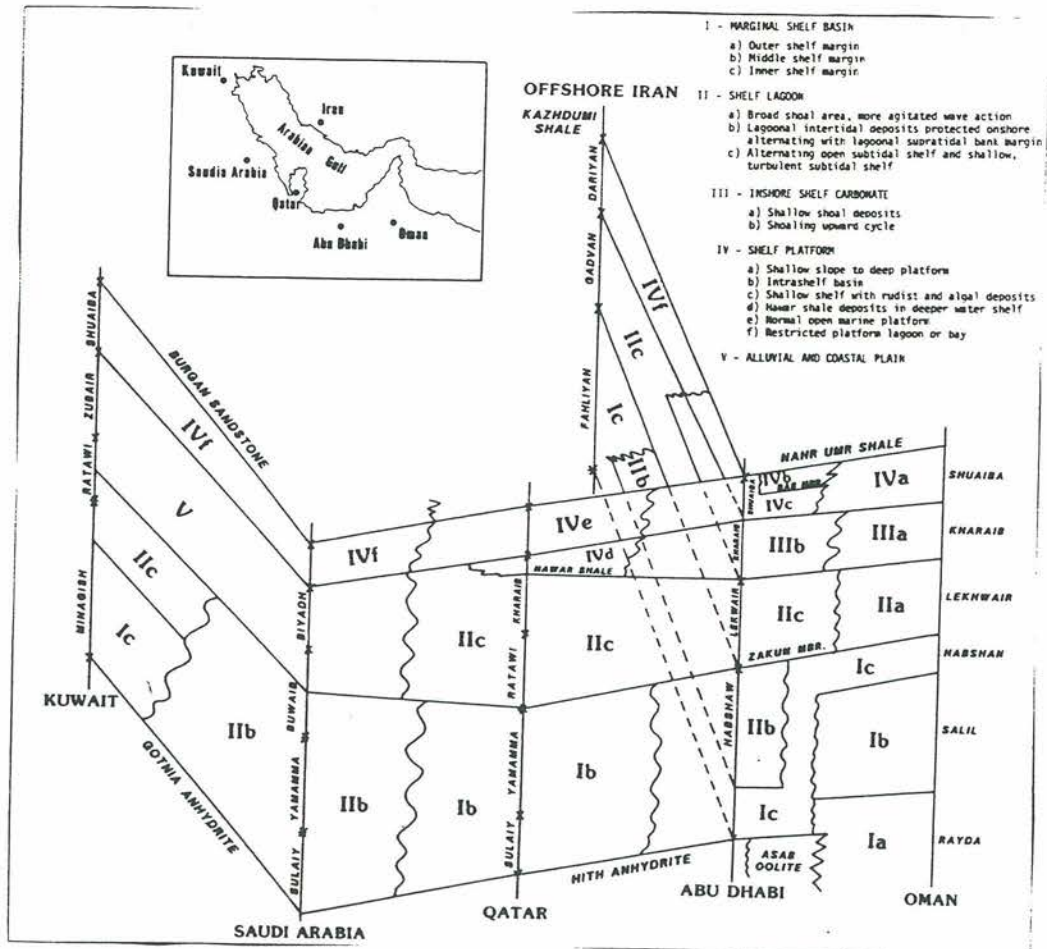


Figure 6. Fence diagram showing facies variation of the Shuaiba Formation and other Lower Cretaceous formations across the Arabian Peninsula and Iran (after Alsharhan and Nairn, 1986).

shallow shelf deposition. It is subdivided into two parts, the lower and upper. The lower part is described as an algal (*Bacinella*) skeletal wackestone to boundstone. This passes up into argillaceous carbonates, which then grade-up into cleaner foraminiferal, and sometimes rudist-rich, wackestones to packstones. This upper part of the Shuaiba then persists to the top of the formation (Clarke, 1988). The Shuaiba in Oman and the United Arab Emirates overlies the Kharai Formation which consist of shallow shoal deposits on an inshore carbonate shelf. In Qatar, the Shuaiba represents a normal open shelf platform. Here it overlies the Hawar shale which represents the spreading of clastic sediments into Qatar at the end of the second carbonate cycle in the early Cretaceous (Alsharhan and Nairn, 1986).

The Shuaiba Formation in the northern part of the Persian Gulf, which includes Saudi Arabia and Kuwait, represents restricted platform lagoons or bays. Here, it overlies the Biyadh sandstone in Saudi Arabia and Zubair Formation (interbedded shale and sandstone) in Kuwait. These formations represent an invasion of a clastic wedge from the west and northwest during the Hauterivian and Barremian (Alsharhan and Nairn, 1986).

The Shuaiba is terminated in the southern part of the Gulf by a shale seal called the Nahr-Umr Formation, the lower formation in Wasia Group of the Middle Cretaceous. The Nahr-Umr Formation (Albian) records a shift to a mixed siliciclastic-carbonate system. Pratt and Smewing (1993) believe that it was deposited during the drowning event of the shelf in the Albian. The generation of detrital influx of the Nahr-Umr was due to uplift on the west side of the platform. The large-scale evolution of the margin in the central Oman Mountains, which was driven by tectonic processes, imposed major

sedimentological changes to the platform in generating the siliciclastics of the Nahr-Umr. This tectonic episode led to a reduction in the calcium carbonate generating capacity of the shelf, causing shallow-water facies to be abruptly overlain by deeper water facies (Pratt and Smewing, 1993). A regional unconformity, representing erosion or non-deposition of the middle Aptian section, marks the contact between the Shuaiba formation and the overlying Nahr-Umr in this area (Harris et al., 1984). In the northern part of the Persian Gulf, the Shuaiba is overlain by Burgan sandstone. In offshore Iran across the Gulf, the equivalent of the Shuaiba is called the Dariyan Formation which is made of a massive, crystalline, occasionally chalky limestone (Mina et al., 1967, as referenced in Alsharhan and Nairn, 1986), and it represents restricted platform lagoons or bays.

The Shuaiba can be correlated over the Gulf area; however, it shows variations in depositional facies. It occurs as massive and chalky limestones in the northern part of the Gulf and offshore Iran; however, in the southern Gulf region, it represents high-energy limestones. It is this southern part of the Persian Gulf where the favorable Shuaiba reservoir facies occur (Aldabal and Alsharhan, 1989).

Development of the Shuaiba Reservoir Properties

Reservoir quality of the Shuaiba depends upon the texture and depositional environment, porosity modification by diagenetic processes, and fracture development (Alsharhan, 1987). Porosity and permeability development is known regionally along the Shuaiba Formation - Nahr-Umr unconformable boundary because of subaerial exposure

and leaching of the chalky rock. In addition, better opportunity for reservoir development is achieved by the presence of depositional relief underlying the unconformity (Wilson, 1975). Essentially, leaching of rudist buildups and fracturing in the Shuaiba Formation, which is common in skeletal particles, have improved the porosity and permeability of the reservoir. Therefore, the Shuaiba shows high reservoir quality where it comprises maximum thickness of rudistid sediments (Alsharhan, 1985).

Overall, there are three main factors which have influenced the Shuaiba as an exploration target in the Persian Gulf and especially in the southern region (Frost et al., 1983) :

- 1) Development of the Abu Dhabi intrashelf basin with its deep open marine sediments. These are recognized as minor source rocks for the Shuaiba reservoir. The presence of the intrashelf basin established conditions for a buildup-prone belt around the basin.
- 2) Rising sea level in the early Aptian enhanced vertical aggradation of the rudist buildups.
- 3) Subaerial exposure in the middle Aptian (over a period estimated to be about 1.5 m.y.) and associated meteoric water leaching formed secondary porosity in the skeletal debris of rudists and other allochemical constituents of the Shuaiba.

In addition to the Bab member, which was deposited in the intrashelf basin of Abu Dhabi, argillaceous limestone and calcareous shale of the Upper Jurassic Dukhan (Hanifa) Formation are likely sources of the Shuaiba oil (Pratt and Smewing, 1993). The

Nahr-Umr possesses no or poor source rock characteristics which might be due to the low preservation potential of sedimentary organic carbon.

Ghaba North Field

Ghaba North Field is located in central Oman (Fig. 7), and was discovered in 1972. The field produces from two main horizons; the fractured Shuaiba Formation (Aptian) and the sandstone/shale Garif Formation (Lower Permian). Since development of the field in 1975, twenty-three wells have been drilled; thirteen in the Shuaiba and ten in the Garif. Current net production of the field is 200 m³ / d from the Shuaiba lithologies and 600 m³/d from the Garif reservoir (Gallagher et al., 1990).

Ghaba North Field is situated in what is called the Ghaba Salt Basin (Fig. 8) (PDO report, 1992). This basin and other salt basins, such as Fahud Salt Basin, developed in the Arabian Peninsula subsequent to the Najd Orogeny (terminated 520 Ma). Great thicknesses of Precambrian to early Paleozoic clastics, salts, and marine carbonates accumulated in the Ghaba Salt Basin (Alsharhan and Kendall, 1986). Abundant structures formed by salt tectonism in this basin have developed prolific oil traps in the area, such as the Marmul Field in southern Oman.

The structural setting of the Ghaba North Field (Fig. 9), obtained primarily from seismic data, indicates a faulted, 9 by 5 km NW-SE trending anticline at the deeper Garif Formation level. In addition, an anticlinal structure, 15 by 8 km trending NE-SW with a fractured and faulted crest, occurs at the shallower Shuaiba Formation level (PDO report, 1992). The structure has probably formed by deep seated Ara Salt movement. Moreover,

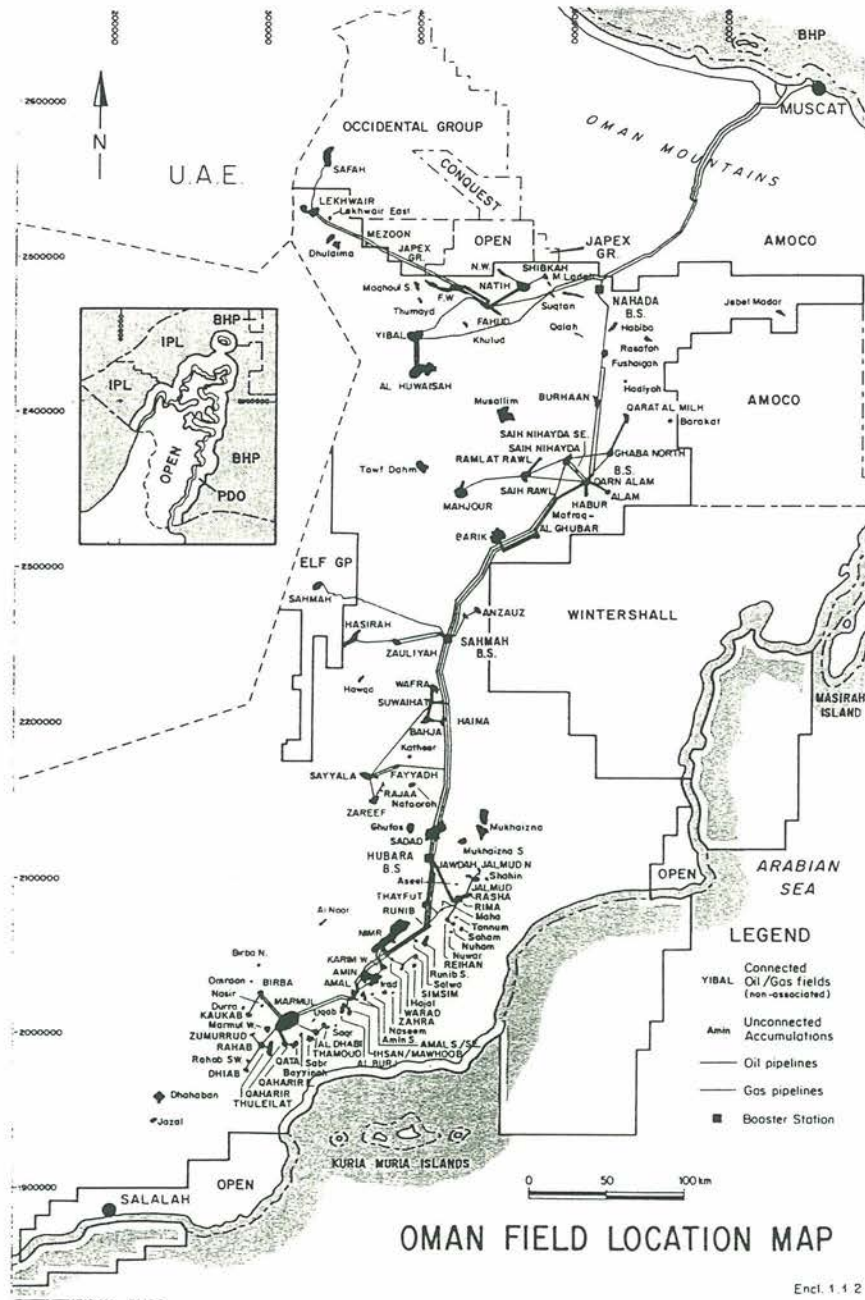


Figure 7. Ghaba North Field location map (after PDO, 1991).

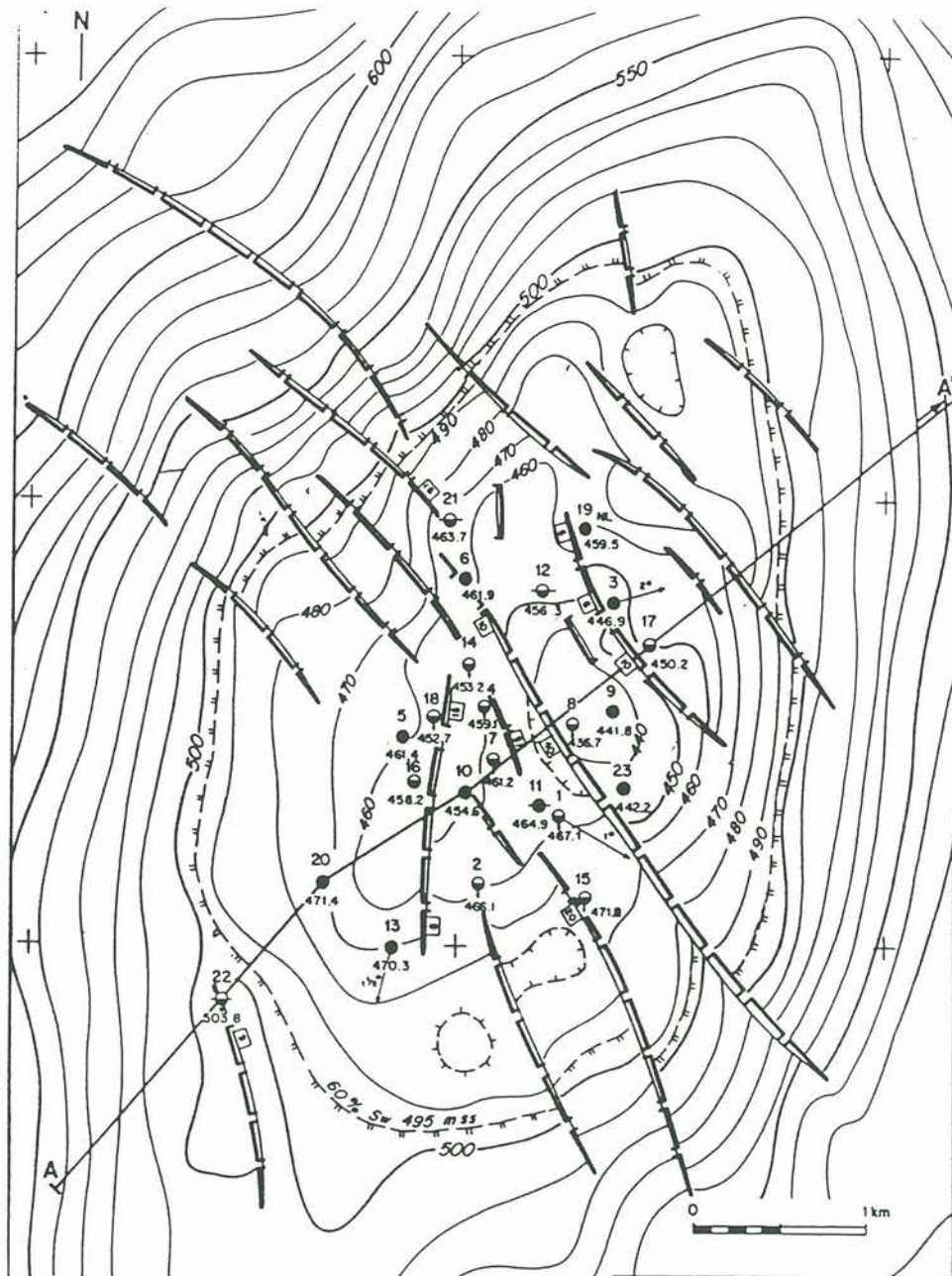


Figure 9. Structure contour map on top of the Shuaiba Formation and well locations in Ghaba North Field (after PDO, 1992).

stresses caused by the salt movement, together with wrench faulting associated with the Maradi Fault Zone (Fig. 8), created a NE-SW striking fault system consisting of normal faults (Uitentuis, 1981).

General Description of the Shuaiba Formation in Ghaba North Field

The Shuaiba Formation in Ghaba North Field overlies limestone of the Kharaiab Formation (Lower Cretaceous; Barremian) and is overlain by a seal of calcareous shales and marls of the Nahr-Umr Formation (Albian), the lowermost member of the Wasia Group (Middle Cretaceous). In general, the Shuaiba Formation in Oman is subdivided into a transgressive unit (lower Shuaiba) and a regressive unit (upper Shuaiba) (Freake and Witt, 1972; and Engel, 1989). Apart from the Al Huwaisha Field, in which the upper Shuaiba is described as rudist grainstones, the majority of the upper unit of Shuaiba reservoirs is described as high porosity/low permeability bioclastic wackestones and packstones with chalky matrix (Mattes and Wynne, 1984).

According to a PDO report (1992), the Shuaiba Formation in Ghaba North Field is 65 m thick and is described as rudist-rich pack/boundstones which were deposited in an open shallow-marine, relatively high-energy environment. The rudistid zones alternate with chalky, algal-rich wackestones deposited in a partly restricted, relatively low-energy environment. The rudist-rich intervals are thicker and become more abundant towards the top of the formation. Selective leaching created good inter- and intragranular porosity in these intervals; thus, they form the best reservoir zones. However, reservoir productivity is primarily a function of open fracture development (PDO report, 1992).

The upper pay zone of the Shuaiba has an average porosity of 31%, and possesses a matrix permeability of about 10 md and about 100 md fracture permeability (PDO report, 1992).

Previous Work Performed on the Shuaiba Formation in Ghaba North Field

The Shuaiba Formation has been the subject of only cursory, reconnaissance study at the Ghaba North Field (PDO report, 1992). Gallagher et al. (1990), studied GN-23 core and subdivided the formation into three zones. From the bottom to the top, these are :

- Zone 1 : 40 m thick and described as a chalky wackestone with nodular algal locally cemented horizons, characterized by low permeabilities (< 10 md).
- Zone 2 : 10 m thick and described as a chalky wackestone with bedded rudist-rich layers, characterized by low to moderate permeabilities (10 to 100 md).
- Zone 3 : 15 m thick and described as bioclastic, leached wacke/packstones with rudist-rich, leached boundstones layers, characterized by low to high permeabilities (from 10 to over 100 md).

The studies of Uitentuis (1981) and Frikken (1982) of other cores available from the field (cores GN-1, GN-2, and GN-13) have shown that the Shuaiba Formation consists mainly of chalky wackestones alternating with pack- and mudstones and occasional grainstones. These studies have interpreted the environment of deposition of the Shuaiba as a shallow-marine, protected, somewhat restricted setting in which shoals (rudist bioherms) and tidal channels (normally graded lag deposits over a scour) could

develop. Moreover, matrix porosity predominates the Shuaiba and favorable reservoir properties decrease toward the bottom of the formation. Mercadier (1990) has correlated the Shuaiba between GN-23 and GN-13. He suggested that the sedimentological evidence of the Shuaiba interval in GN-13 suggests that it is stratigraphically located below the third zone in the GN-23 core.

According to Uitentuis (1981), the Shuaiba oil in the Ghaba North Field is of 28° API. Moreover, he suggested that the Shuaiba oil is a mixture of two possible hydrocarbon sources; the Huqf Group (Precambrian to Lower Cambrian), generating high sulfur low API crude, and a source rock in the Haushi Group (Permian), generating high API crude.

The Shuaiba Formation in this field is characterized by vertical or high-angle extensional fractures trending NW-SE to N-S, most of which are parallel to the fault pattern on the Ghaba North anticline. These fractures, important for reservoir quality, are on the order of 5 to 10 m long (Gallagher et al., 1990). Mercadier's (1990) FMS study of the GN-23 core showed that these high angle extensional fractures are laterally extensive in the reservoir because they cut across the large diameter core of GN-23 from one side to the other. In addition, core and FMS studies show that these fractures form an open, interconnected network through the Shuaiba and underlying Kharaib Formation (PDO report, 1992). Due to this fracture network and the strong aquifer of the Kharaib, water has invaded the fractures of the Shuaiba and displaced oil. Therefore, to improve oil production by draining oil from the oil-rich matrix of the Shuaiba a new mechanism is proposed. This mechanism is called Gas Oil Gravity Drainage (GOGD) and it involves

drainage of oil from the matrix by surrounding it by a gas-filled fracture system
(Gallagher et al., 1990).

METHODS OF THE STUDY

As mentioned previously, only a reconnaissance study of depositional features has thus far been undertaken for the Shuaiba Formation at Ghaba North Field. With the exception of a descriptive accounting of the porosity, no systematic study of the diagenesis has been performed. In order to understand the controls on porosity evolution and the development of reservoir quality, this study focuses on the sedimentological history and diagenesis of the Shuaiba Formation.

The work is concentrated on a single core from Ghaba North Well # 23. This core, taken in 1990, is 50 m long and 19.5 cm in diameter and is still in good condition. This large-diameter core affords an excellent opportunity for megascopic study. Moreover, there are three other available cores from this field; GN-1, GN-2, and GN-13 (see Figure 9 for locations), all of which are 10.2 cm in diameter. Cores from the first two wells were taken in 1972, and the third was taken in 1980.

During the summer of 1992, core descriptions were performed (plates 1, 2, 3, and 4), and core samples were taken in Oman. Eighty-five core samples were taken from core GN-23 at an approximate interval of half a meter. All representative facies were sampled in GN-23, with the emphasis being on recognition of sediment types, bounding features, and diagenetic phases. Based on the detailed sampling in the GN-23, representative samples were also taken from the other three cores for comparison.

Thirteen, four, and eight representative samples were taken from the cores GN-1, GN-2, and GN-13, respectively. These samples were marked, packaged, and brought to the Colorado School of Mines. In addition, there are Gamma Ray-Neutron-Density logs for all of the wells mentioned above. Copies of these logs were brought back from Oman.

During the fall of 1992, the laboratory portion of this research was started. The core samples were described using the binocular microscope in order to augment the original core descriptions completed in Oman. Thin sections were prepared, some were stained, and all were examined using standard transmitted-light petrography. A sedimentary facies framework for the deposition of the Shuaiba at Ghaba North Field was established by the core descriptions and the binocular microscope inspection. Thin section petrography has further clarified sedimentary environments and microfacies. In addition, petrographic study has established relative timing of diagenetic events in order to characterize porosity evolution. Importantly, petrography has determined the timing of hydrocarbon migration to the reservoir.

Five samples from the GN-23 core were chosen for a Scanning Electron Microscope (SEM) investigation. Three of these samples belong to intervals with high porosities and two belong to intervals with relatively low porosities. These high and low porosity intervals alternate with each other from the bottom of the core to the top. These samples were first cleaned by using a toluene solvent. The samples were stirred and the toluene was replaced every few hours several times. These samples were mounted to a stub and coated by a thin coating of gold. The broken surfaces of these samples were inspected by the SEM in an attempt to understand variations of the porosity in GN-23 with depth. This study has helped in analyzing the occurrence of microporosity and in

characterizing matrix textures in the Shuaiba, enhancing our understanding of the reservoir properties and constancy in Ghaba North.

Stable carbon and oxygen isotopes on whole rock and component samples helped in delineating diagenetic events. Samples for stable carbon and oxygen isotopic analyses of matrix and cements in the Shuaiba GN-23 core were collected. The samples of micro-rhombic calcite matrix of the Shuaiba were extracted by drilling a transect across the face of slabbed plugs, taken from the core, with a dental drill. All types of facies were sampled because samples were taken from all eighty-four samples of the GN-23 core. Large components, such as skeletal fragments and coarse-crystalline cements were avoided so that the resultant powders would be from finer components of each facies (matrix, pellets, and fine grains). The isotopic composition of these powders is assumed to be representative of the micro-rhombic calcite matrix because this fabric dominates the matrix. The powdered samples of the matrix were treated by toluene in order to leach out the hydrocarbons in order to avoid interference in the analyses of the matrix. Separate samples of coarse-crystalline calcite cements were collected as well. All samples were prepared for isotopic analysis by off-line extraction of CO₂. Samples were dissolved in 100% orthophosphoric acid at 90°C. The evolved CO₂ was purified through a water trap and collected in sample tubes. Stable carbon and oxygen isotopes were analyzed on a VG Micromass 602E mass spectrometer according to standard procedures outlined in McCrea (1950). Isotopic ratios are expressed in the standard delta notation and are given relative to PDB standard in per mil (‰) notation. Precision on blind duplicates for 10% of the samples yields a mean half range of 0.20‰ for δ¹⁸O and 0.07‰ for δ¹³C.

The qualitative descriptive and temporal studies on the Shuaiba Formation were enhanced by the isotopic analysis. Environments of diagenesis were determined by the stable isotope analysis. These studies then provided a framework within which a detailed paragenetic sequence was developed. Recognition of trends in porosity evolution through diagenetic studies will aid in the development of predictive models for future Shuaiba exploration/exploitation.

Changes in the reservoir characteristics have been correlated across the field by extending the reservoir core subdivisions in GN-23 to the other available cores in the field. Correlation of reservoir properties across the field is important for development of the Ghaba North Shuaiba reservoir.

RESULTS

Petrology, Petrography And Reservoir Properties of the Shuaiba Formation in the GN - 23 Well

This chapter covers the results and the observations deciphered in this study about the Shuaiba Formation in the Ghaba North Field from the GN-23 well. These results and observations were obtained by integrating the data which were collected from the core, plugs, thin sections and scanning electron microscope lab work. There are many results recognized here that will help in developing an understanding about the nature of the Shuaiba Formation in this field, which subsequently will help in establishing a model for reservoir evolution of the Shuaiba Formation.

Lithology and Sedimentology of the Shuaiba Formation in GN-23

The Shuaiba Formation will be subdivided into thirty-one intervals starting at the bottom of the core and working up. Each interval shows certain characteristics that distinguish it from the other intervals. These include the lithologic texture, allochemical constituents and the abundance of each major allochem relative to the matrix and to other allochems. These abundances were estimated by examining the core, plugs and thin sections that cover each interval. Each interval is described in both macro-scale and micro-scale terms. The macro-scale represents description of the core and plugs, whereas

the micro-scale description is based on the thin sections. In addition, cement types and occurrence will be described for each interval. Macroporosity, which is defined as all visible porosity whether observed in the core, plugs or thin sections, will be described to indicate its type and distribution. Moreover, hydrocarbon occurrence and distribution will also be described. Subsequently, this will help in establishing trends observed in the Shuaiba Formation.

Interval I.- This interval starts at the bottom of the core at a depth of 644.80 m and ends at a depth of 643.10 m. On macro-scale, this interval consists of a light brown wackestone with nodular intraclasts of wackestone and few subvertical extensional fractures, with a hardground at the top of the interval. However, in thin section, this interval appears dominantly as a packstone. This interval is dominated by a group of small-sized forams, which include millioids, uniserial, and biserial forams (or the combination of two), peneroplids and few agglutinated and spiral forams. In addition, the relatively larger *Orbitulina Sp.* benthic foram (Fig. 10) with rare ostracodes, echinoids and sponge spicules. These constituents form about 20% of the rock in this interval. These allochems are present in a micritic to peloidal matrix. Cementation is minimal and occurs as patchy, very fine calcite cement. It occurs as intraparticle cement within forams and ostracodes. In addition, there is a calcite microspar in interpeloidal pore spaces. Echinoids show syntaxial calcite overgrowths. Hydrocarbon staining of this interval is very low and it occurs only in remaining matrix's microporosity. Macroporosity in this interval is almost totally absent, and hydrocarbon occupies the microporosity only.

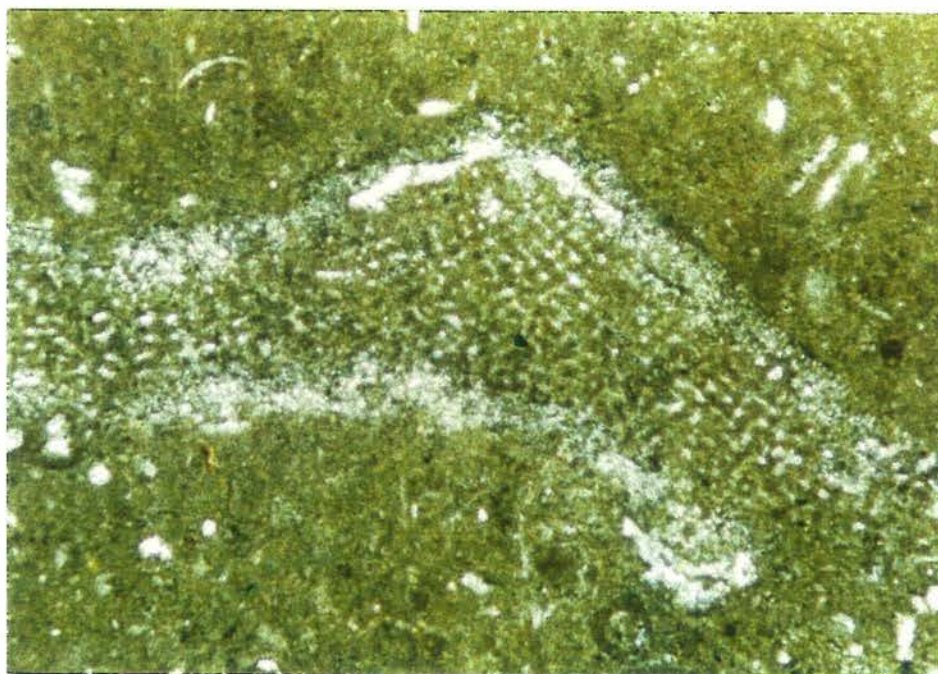


Figure 10. An *Orbitulina* benthic foram in a wackestone matrix. Note fine-crystalline calcite cement in intraparticle pores of the foram. Field of view is 3 mm.

Interval II:- This interval extends from a depth of 643.10 m to 641.50 m. From a macro-scale perspective, it is described as a wackestone with algal layers and nodules.

However, again, thin section study indicates that this interval dominantly consists of packstones. This interval is dominated by green algae, which encompass about 20% of the rock. Most of the algae is identified as *Bacinella Sp.*, with minor *Lithocodium Sp.* (Fig. 11) (Johnson, 1969). *Orbitulina* and other small forams form about 10% of the allochems. Moreover, there are some intraclasts and small rudist fragments which form less than 5% of the allochems. These allochemical constituents are present in a micritic matrix. The cementation is patchy and occurs as a very fine calcite cement filling intraparticle pores of the algae and forams. In addition, there are syntaxial calcite overgrowths on some echinoids, along with replacement or recrystallization of probable small rudist fragments which are outlined by micritic envelopes. There is a slight hydrocarbon staining and it occurs within matrix microporosity and remaining algal intraparticle pore spaces. Macroporosity is nearly absent, with the hydrocarbon occurring only in the microporosity.

Interval III.- This interval begins at a depth of 641.50 m and ends at 639.20 m. This interval is described as a floatstone of nodular green algae. From a micro-scale perspective, this interval has a wacke- to packstone texture. It consists of 20% algae and less than 10% of *Orbitulina* and other small forams. Moreover, there are small fragments of rudists in this interval with an abundance of about 5%. The matrix is peloidal to micritic. The algal nodules are cemented by a very fine calcite cement which appears patchy because it is constrained to these nodules. This calcite fills algae and

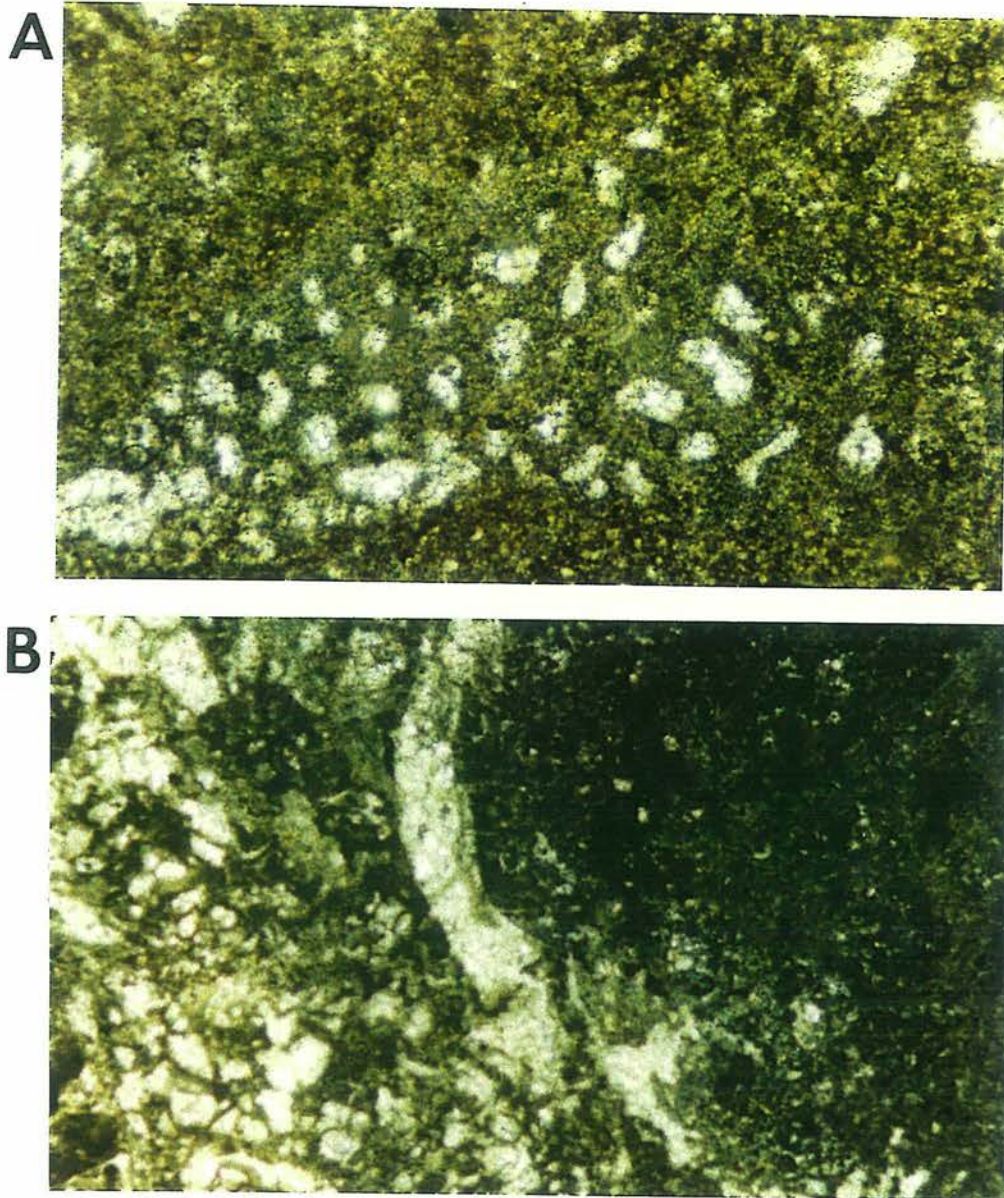


Figure 11. Green algae in the Shuaiba Formation. A. *Lithocodium* algae with fine-crystalline calcite intraparticle cement. Field of view is 1.5 mm. B. *Bacinella* algae encrusting on/or trapping a recrystallized rudist fragment. Note cement in intraparticle pores of the algae. Field of view is 3 mm.

foram intraparticle pores and is characterized by subhedral crystals with an increase in their sizes toward the center of the pores. Some of the rudist fragments are outlined by micritic envelopes and replaced by calcite. Calcite also occurs as overgrowths on echinoids and as microspar in interpeloidal pore spaces. Hydrocarbon staining is very low and it occurs in some of the matrix micropores or within algal intraparticle porosity and along solution seams. Macroporosity is nearly absent.

Interval IV.- This interval extends from a depth of 639.20 m to 636.80 m. It is described as a wackestone, characterized by the occurrence of algal nodules that become increasingly layered toward the top of the interval. There are also few scattered rudist fragments floating in a micritic matrix. A hardground occurs at the top of this interval and separates it from the fifth interval. The micro-scale texture is described as a packstone. This interval consists of 15% algae and 10% *Orbitulina* and few other small forams. Rudist fragments are small in size and make up about 5% of the allochems. Moreover, there are minor peloids and intraclasts. The matrix is micritic. A very fine calcite cement is observed and it occurs within the intraparticle pore spaces of the algae. Rudist fragments are either neomorphosed or recrystallized to a calcite spar and outlined by micrite envelopes. Calcite cements are also present as overgrowths on echinoids and as microspar cementing interpeloidal pore spaces within the intraclasts. Hydrocarbons occur in some micropores of the matrix and along solution seams and at grain contacts. In addition, hydrocarbons occur within the intraparticle pores of partially cemented algae. Nevertheless, hydrocarbon staining is low and macroporosity is scarce.

Interval V.- This interval starts at a depth of 636.80 m and ends at 635.30 m. This interval is described as an algal floatstone to algal boundstone. The micro-scale texture

of this interval is described as a packstone. Algae make up about 20% of the allochems, with less than 10% *Orbitulina* and other small forams. The rudists and rudist fragments have an abundance between 5 and 10%. These allochems are present in a micritic matrix. The algal layers trap or bind rudists and rudist fragments together. These algal layers are characterized by abundant calcite cements. These cements occur as replacement of rudist fragments and they occur within the intraparticle pores of algae. However, some rudist fragments were simply neomorphosed. Calcite cements collapse breccias within some of these layers. Some echinoids have calcite overgrowths on them. Hydrocarbon occurs in micropores of the matrix, some algal intraparticle pores and at some grain contacts. Still, the hydrocarbon staining and the macroporosity are low.

Interval VI.- This interval starts at 635.30 m and ends at a depth of 633.75 m. This interval is described as a wackestone and is characterized by horse-tail compaction features. The micro-scale texture is described as a packstone. This interval consists of 10% algae and 10 to 15% *Orbitulina* and other small forams. Rudists and rudist fragments comprise 5 to 7% of the rock. The matrix is micritic. Internal pore spaces of rudists have been filled by geopetal fabrics and the remaining spaces are either cemented by sparry calcite or microspar cement. Some calcite cements also occur as replacements of rudist fragments, which are outlined by micrite envelopes. In addition, algal intraparticle pores and a few very fine fractures are cemented by calcite. Hydrocarbon staining and macroporosity are still low. Where it occurs, hydrocarbon is observed in micropores of the matrix, some algal intraparticle pores, at grain contacts, along solution seams, and hydrocarbons also stain rudist and *Orbitulina* intraparticle porosity.

Interval VII.- This interval extends from 633.75 m to a depth of 633.50 m. It occurs as a highly cemented rudist rudstone. The micro-scale texture is a packstone. This interval consists of 20% rudists and rudist fragments and of 5 to 10% algae. Moreover, there are *Orbitulina*, peloids and some breccias or intraclasts present in this interval. These intraclasts may have been sourced from the hardground that occurs at the top of the previous interval. These allochems occur in a peloidal matrix. Cementation is very extensive and occurs as medium to coarse, euhedral to subhedral calcite cements which increase in size toward the center of the pores. These cements fill molds of rudist fragments, algal intraparticle pores and cement fractured rudist fragments, some of which appear floating in calcite cements. Most of the rudists are neomorphosed and their internal spaces are filled by cements and geopetal fabrics. The macroporosity is very low and hydrocarbon is only present in some algal intraparticle pores and at grain contacts.

Interval VIII.- This interval begins at a depth of 633.50 m and ends at 632.70 m. The lithology is a wackestone with numerous solution seams. The micro-scale texture is a wacke- to packstone. This interval is composed of 10 to 15% algae and 10 to 15% *Orbitulina*. There are less than 5% small rudist fragments present in this interval. It is characterized by a micritic matrix. There is a very fine calcite patchy cementation that occurs within algal intraparticle pores. Some echinoids have calcite overgrowths on them. Rudist fragments in this interval are neomorphosed. Macroporosity is low; however, hydrocarbon is observed in micropores of the matrix, algal intraparticle pores, along solution seams, and it stains some *Orbitulina*.

Interval IX.- This interval ranges from 632.70 m to 632.40 m. This interval is an algal boundstone with few subvertical extensional fractures. The micro-scale texture appears

as a wacke- to packstone. It contains greater than 35% algae and 5% *Orbitulina*. The algae is mostly composed of *Bacinella* with minor *Lithocodium*. There are less than 5% rudist fragments present in this interval. The matrix is micritic. Algal intraparticle pore spaces are cemented by very fine calcite spar which occur as equant crystals and increase in size toward the center of these pores. These cements have a patchy appearance in the core and the plugs. Calcite cement also occurs as syntaxial overgrowths on some echinoids. Hydrocarbon is present in partially cemented algal intraparticle pores, micropores of the matrix and along solution seams. The macroporosity of this interval is still considerably low.

Interval X.- This interval starts at a depth of 632.40 m and ends at 630.50 m. This interval is a wackestone with algal nodules and a few scattered rudists and rudist fragments. The micro-scale texture is a pack- to wackestone. This interval consists of 10% algae and 10% *Orbitulina*. Rudist fragments form about 5% of the rock. Rudist infills contain peloidal intraclasts and minor small forams. The matrix is described as peloidal to micritic. Most of the rudists are preserved, but there are some have been replaced. The latter are replaced by calcite and outlined by micritic envelopes, some of which are fractured. There are algal intraparticle pores, borings in rudist fragments and shelter porosity that have all been cemented by calcite. Some echinoids show calcite overgrowths on them. Macroporosity is low, but hydrocarbon is present in algal intraparticle pores and it stains *Orbitulina* and some rudist infills.

Interval XI.- This interval starts at 630.50 m and ends at a depth of 629.50 m. This interval is an algal boundstone with wispy algae laminations and few scattered algal nodules and rudist fragments. The micro-scale texture of this interval is described as a

wacke- to packstone. It consists of 30% algae and 10% *Orbitulina* with minor other small forams and ostracodes. Rudist fragments are small and present as less than 5%. This interval has a micritic matrix. Algal intraparticle pores are cemented by a patchy very fine sparry calcite cement. In addition, calcite cements fill borings in some rudist fragments and shelter porosity beneath others. The rudist fragments themselves are either neomorphosed or recrystallized. Some echinoids show calcite overgrowths on them. Macroporosity is still low; however hydrocarbon is observed to be concentrated along solution seams and stains *Orbitulina*. Hydrocarbon also occurs in micropores of the matrix and algal intraparticle pores.

Interval XII.- This interval begins at a depth of 629.50 m and ends at 628.30 m. This interval is a wackestone with few algal nodules and rudist fragments. The micro-scale texture is a wacke- to packstone. It consists of 10 to 15% algae and 15% *Orbitulina*, with minor other small forams and peloids. In addition, there are 5% rudist fragments scattered in the micritic matrix of this interval. A very fine calcite cement occurs in algal intraparticle pores. This cement has a patchy occurrence. Moreover, a neomorphic calcite microspar fills interpeloidal pore spaces. Some rudist fragments are clearly neomorphosed. Since the macroporosity is low, it is obvious that hydrocarbon occurs within the microporosity. Hydrocarbon is present in micropores of the matrix, partially cemented algal intraparticle pores and stains some of the *Orbitulina*.

Interval XIII.- The interval ranges from a depth of 628.30 m to 628.00 m. It is a rudist rudstone with very extensive cementation. The micro-scale texture is a packstone. It contains less than 5% algae and 10% *Orbitulina* with a few other small forams and ostracodes. Rudists are the main constituents of this interval, with an abundance

percentage between 25 and 30%. The matrix is micritic. Some rudists have been replaced by calcite cements. These cements increase in crystal size toward the center of the pores. Rudists may contain peloidal infills. Interpeloidal pore spaces of these infills are cemented by neomorphic calcite microspar. Calcite overgrowths are observed on some echinoids. The extensive cementation observed in this interval has almost occluded all the macroporosity. Nevertheless, hydrocarbon stains some rudist infills where it occurs along intercrystalline porosity. Hydrocarbons also occur in micropores of the matrix.

Interval XIV.- This interval starts at 628.00 m and ends at a depth of 626.50 m. This interval is a wackestone and is characterized by horse-tail compaction features and algal nodules. It is characterized by a packstone texture in thin section. The interval contains 15% algae and 15% *Orbitulina* with minor other small forams and mollusks. There are 5% rudist fragments present in this interval with some peloidal intraclasts or rudist infills. All these allochems are present in a micritic matrix. Algal intraparticle pores are cemented by a very patchy fine sparry calcite cement. Neomorphism of some rudist fragments is observed along with calcite overgrowths on some echinoids. Broken micrite envelopes are floating in calcite cements. Hydrocarbon occurs in micropores of the matrix, in some algal intraparticle pores, at grain contacts and along solution seams. This interval, as the previous ones, has a low macroporosity.

Interval XV. - The interval ranges from 626.50 m to a depth of 625.45 m. The lithology is a rudist rudstone which is interrupted by wackestone intervals. This interval is characterized by packstone and wackestone micro-scale textures. It consists of less than 5% algae and 10% *Orbitulina*, with peloids and some ostracodes. It contains 15 to 20%

rudists. The matrix is peloidal or micritic, corresponding to the packstone or the wackestone intervals, respectively. The intensity of cementation differs between the two textures. The wackestone intervals are only slightly cemented, unlike the highly packed intervals which are heavily cemented. The latter contains higher amounts of rudists. Some of the rudist fragments are fractured, outlined by micritic envelopes and replaced by calcite cements. Calcite cements also fill microfractures and occur as overgrowths on echinoids. Interpeloidal pore spaces are cemented by calcite neomorphic microspar. The macroporosity and hydrocarbon staining are low. Hydrocarbon is present in micropores of the matrix, along solution seams and stains some *Orbitulina*.

Interval XVI.- This interval starts at a depth of 625.45 m and ends at 622.80 m. This interval is a wackestone with abundant solution seams, which appear as horse-tail compaction features. It is also characterized by the presence of algal nodules and few scattered rudists. The texture is a wackestone to packstone. It consists of 10% of algae and 15% *Orbitulina* with a few other small forams, peloids and intraclasts. Rudists and rudist fragments form 5 to 8% of the allochemical constituents. The matrix of the interval is micritic. Calcite cementation has a patchy appearance and corresponds to the algae and the rudists. It occurs in algal intraparticle pores and cements internal pore spaces within rudists. The rudists themselves are neomorphosed. Calcite cements also occur as overgrowths on echinoids and as neomorphic microspar in interpeloidal pore spaces. Macroporosity is low; however, it is slightly better in this interval than the previous ones. Hydrocarbon stains *Orbitulina* and occurs along solution seams and at grain contacts. It is also present in micropores of the matrix and in partially cemented algal intraparticle pores.

Interval XVII.- This interval begins at a depth of 622.80 m and ends at 621.15 m. The lithology is a rudist rudstone with algal nodules and is interrupted by wackestone intervals. There are a few subvertical fractures present at the base of the interval. In thin section, it has a packstone texture. It consists of less than 10% algae and 15% *Orbitulina* and small forams. Rudists and rudist fragment abundance is between 10 and 15%. The matrix is micritic. There are some recrystallized rudists; however, the majority are preserved. A very fine sparry calcite is found in algae and foram intraparticle pores and in borings in some *Orbitulina*. In addition, echinoids show calcite overgrowths on them. Hydrocarbon stains *Orbitulina* and rudist infills and occurs along solution seams. It also occurs in micropores of the matrix and in partially cemented algal intraparticle pores. The macroporosity of the interval is low.

Interval XVIII.- The interval ranges from 621.15 m to a depth of 619.45 m. The lithology is a wackestone with horse-tail compaction features. It has a packstone texture in thin section. It contains 10% of algae and greater than 15% *Orbitulina*, with a few other small forams and peloids. It has less than 5% rudist fragments. These allochemical constituent are present in a peloidal to micritic matrix. The characteristics of the cementation are analogous to the ones in the previous interval. The macroporosity of this interval is low. Hydrocarbon stains *Orbitulina* and occurs along solution seams, in algal intraparticle pores and micropores of the matrix.

Interval XIX.- This interval starts at a depth of 619.45m and ends at 619.05 m. The lithology is a rudist rudstone. The micro-scale texture of this interval is a packstone. It contains 5% algae and 10 to 15% *Orbitulina*, with minor small forams, peloids and mollusks. Rudists and rudist fragments form 15 to 20% of the allochemical constituents.

The matrix is peloidal to micritic. Rudists are either neomorphosed or replaced by calcite cements and outlined by micritic envelopes. A shelter beneath a rudist fragment has been partially filled by a geopetal fabric and the rest of the pore space is filled by a neomorphosed calcite spar. One *Orbitulina* foram has experienced partial leaching and subsequent cementation by calcite fills the leached part. Algal intraparticle pores are also cemented by calcite spar. There is a slight increase in the macroporosity, but it is still low. Hydrocarbon stains *Orbitulina* and rudist infills and occurs in partially cemented algal intraparticle pores and along solution seams.

Interval XX.- The interval ranges from 619.05 m to a depth of 618.05 m. It is a wackestone with algal nodules and is characterized by thick solution seams of concentrated clay or silt-sized insoluble residue. There is a very sharp contact between this interval and the previous one. In thin section, this interval has a packstone texture. It contains 10 to 15% algae and 15% *Orbitulina*, with minor amounts of other forams, peloids and few ostracodes. There is less than 5% rudist fragments in this interval. These allochems are present in a peloidal matrix. In addition to the preserved rudist fragments, there are some replaced ones. Calcite cements occur in rudist infills, in algal intraparticle pores and as overgrowths on echinoids. Hydrocarbon stains *Orbitulina* and rudist infills, and occurs within micropores of the matrix. Hydrocarbon also occur within algal intraparticle pores and in molds of rudist fragments or microfractures. The macroporosity is low.

Interval XXI.- This interval starts from a depth of 618.05 m and ends at 617.00 m. It is described as a rudist boundstone with algal nodules and has a subvertical fracture at the base of the interval. In thin section, it has a wacke- to packstone texture. It consists of 10

to 15% algae and 10% *Orbitulina* and peloids. Rudist and rudist fragments are abundant and form up to 20% of the allochems in this interval. The matrix is micritic and becomes peloidal toward the top of the interval. Partially cemented rudist molds in this interval show, for the first time, the presence of macroporosity in appreciable amounts. This macroporosity reaches about 8% . Hydrocarbon migration into these pores has preserved them and prevented their total occlusion by cements. These rudist molds are partially cemented by calcite and outlined by micritic envelopes. Nevertheless, there are some other rudists that have either been preserved or neomorphosed. Calcite cements are also present in algae intraparticle pores and as overgrowths on echinoids. Hydrocarbon occurs in partially cemented rudist molds and algal intraparticle pores and in micropores of the matrix. Hydrocarbons also stain some rudist infills and *Orbitulina* and is present along solution seams and at grain contacts.

Interval XXII.- The interval extends from 617.00 m to a depth of 614.40 m. This interval is a wackestone which is characterized by algal nodules that become layered toward the top of the interval. In addition, there are some thin beds of rudists that interrupt this sequence. It has a wackestone micro-scale texture. It contains 15 to 20% algae and 15% *Orbitulina* and peloids. This interval has less than 5% rudist fragments. The matrix is generally micritic but it is interrupted by peloidal matrices. Most of the rudist fragments are preserved although there are some leached fragments. The molds of these leached rudist fragments are partially cemented by calcite. There is extensive cementation by very fine sparry calcite which corresponds to the algae in the wackestone intervals. On the other hand, sparry calcite is patchy in the rudist beds. These cements are observed to occur in algal intraparticle pores and as overgrowths on echinoids. Interpeloidal pore spaces are cemented by neomorphic calcite microspar. The

macroporosity is lower in this interval than the previous one and it equals about 5%. Hydrocarbon occurs along solution seams and in partially cemented rudist fragments molds and algal intraparticle pores and in micropores of the matrix.

Interval XXIII.- This interval starts from a depth of 614.40 m and ends at 613.65 m. It is a rudist boundstone with a subvertical extensional fracture at the top of the interval. The micro-scale texture of this interval is a packstone. It consists of 5% algae and 5 to 10% *Orbitulina*. Rudists are abundant and form 20% of the allochemical constituents. The matrix is micritic. This interval possesses considerable macroporosity which reaches about 8%. This macroporosity occurs as moldic porosity after rudists. These molds are partially cemented by calcite. Algal intraparticle pores and borings in some *Orbitulina* are cemented by calcite as well. Hydrocarbon stains some rudist infills and occurs in the moldic porosity, algal intraparticle pores and micropores of the matrix.

Interval XXIV.- The interval extends from 613.65 m to 612.77 m. This interval is a wackestone with solution seams and subvertical extensional fractures which correspond to some cemented intervals in the lower part of the interval. It has a wackestone micro-scale texture. It consists of 5% algae and 15% *Orbitulina*, with minor small forams and peloids. In addition, it contains less than 5% rudist fragments. The matrix is described as micritic. There is a very fine sparry calcite cement that occurs in algal intraparticle pores and has a patchy appearance from the macro-scale perspective. Echinoids show syntaxial calcite overgrowths on them. The macroporosity in this interval is low. Hydrocarbon stains *Orbitulina* and occurs along solution seams and in algal intraparticle pores and micropores of the matrix.

Interval XXV.- This interval begins at a depth of 612.77 m and ends at 610.42 m. This interval is identified as an algal boundstone with solution seams and algal nodules and layers. These nodules and layers of algae bind or trap rudists within them. This interval is capped by a possible hard ground. The micro-scale texture is a packstone. It consists of greater than 30% algae and 10% *Orbitulina* and peloids. The algae are identified as: green algae, the majority of which are *Bacinella* with some *Lithocodium*. Rudist fragments are present as about 5% of the constituents of this interval. The matrix is micritic to peloidal. At the base of the interval, cementation by very fine sparry calcite appears as patchy and then increases dramatically toward the top. This phenomenon has led to the reduction of porosity toward the top of the interval. Algal intraparticle pores are characterized by partial calcite cementation at the base of the interval which becomes more intense toward the top. Rudist fragments have created shelter porosity which is now cemented by calcite. Echinoids show syntaxial calcite overgrowths. Macroporosity of this interval reaches about 5% and corresponds to the partially cemented algal intraparticle pores. Hydrocarbon occurs in algal intraparticle pores, micropores of the matrix and along solution seams.

Interval XXVI.- The interval ranges from 610.42 m to 609.45 m. It is identified as a rudist boundstone with a hardground at the base and an erosional surface at the top. The latter is overlain by a wackestone interval without any lag deposits. In thin section, this interval has a packstone texture. It contains less than 5% algae and 5 to 10% *Orbitulina* with minor small forams, peloids and intraclasts or rudist infills. Rudists and rudist fragments are very abundant in this interval and form about 30% of the allochemical constituents. The matrix is micritic to peloidal. This interval possesses a macroporosity of about 10% due to the presence of a considerable amount of rudist molds which were

formed by leaching. Rudists are either neomorphosed or partially cemented by calcite and outlined by micritic envelopes. Calcite cements also occur in algal intraparticle pores and borings in some rudist fragments. Interpeloidal pore spaces are cemented by a neomorphic calcite microspar. Hydrocarbon stains rudist infills and occurs in rudist molds, micropores of the matrix and at grain contacts.

Interval XXVII.- This interval starts at a depth of 609.45 m and ends at 608.12 m. It is described as a wackestone from both the macro and micro-scale perspective. It contains less than 10% algae, 15% *Orbitulina* and peloids and less than 5% small rudist fragments. The matrix is micritic. A very fine sparry calcite cementation of algal intraparticle pores has a patchy appearance in the slabbed core. Macroporosity is low and hydrocarbon occurs only in micropores of the matrix.

interval XXVIII.- This interval starts at 608.12 m and ends at 606.80 m. It is identified as a rudist rudstone with algal nodules and horse-tail compaction features. The lower contact of this interval is a possible hardground. It has a packstone micro-scale texture. The allochems consist of 10% algae and 10% *Orbitulina* and peloidal intraclasts within rudist infills. This interval also contains about 20% rudists and rudist fragments. The matrix is peloidal to micritic. The macroporosity is estimated as high as 10% and corresponds to the partially cemented rudist molds. Rudists are either preserved or leached out. The rudist molds are partially to completely cemented by calcite. Algal intraparticle pores and pore spaces within rudist infills are cemented by calcite. Interpeloidal pore spaces are filled by a neomorphic calcite microspar. Hydrocarbon occurs in rudist molds, micropores of the matrix, along solution seams and at grain contacts.

Interval XXIX.- The interval ranges from 606.80 m to 602.17 m. The lithology is a rudist floatstone with algal nodules. The micro-scale texture is a wackestone to packstone. It consists of 15% algae and 15% *Orbitulina*, with minor small forams, mollusks, peloids and intraclasts. It contains 10% rudists and rudist fragments. The matrix is peloidal to micritic. Rudists are either neomorphosed or replaced partially or completely by calcite spar and outlined by micritic envelopes. In general, the rock samples appear to be unconsolidated, with lots of rubble in this interval. The cementation is not that intense, but there are some cemented portions. In these portions, cementation by calcite occurs in algae intraparticle pores and fills fine fractures in the intraclasts. The macroporosity reaches about 7% and is present as moldic or fracture porosity. The fracture porosity occurs as subvertical extensional fractures that occur in the cemented portions of this interval, especially toward the top. Hydrocarbon occurs in the above mentioned macroporosity, in algal intraparticle pores and in micropores of the matrix.

Interval XXX.- This interval begins at 602.17 m and ends at a depth of 600.40 m. It is described as a rudist boundstone with a graditional contact at the base. The micro-scale texture is a packstone. It contains 5% algae and 10% *Orbitulina*, with minor small forams, peloids and intraclasts or rudist infills. Rudists and rudist fragments have an abundance percentage between 25 to 30%. The matrix is peloidal. The macroporosity is high and reaches 13% due to the presence of rudist molds. These rudist molds are only partially cemented by calcite and are outlined by micritic envelopes. Some of the pores are lined with calcite cement crystals. Some rudist fragments have calcite cements in shelters beneath them. Algal intraparticle pores are cemented by sparry calcite as well. There are brecciated intraclasts or collapse breccias floating in calcite cements. Interpeloidal pore spaces are blocked by neomorphic calcite microspar. Echinoids are

rimmed by calcite overgrowths. Hydrocarbon is present in rudist molds, algal intraparticle pores and micropores of the matrix. Moreover, hydrocarbon stains *Orbitulina* and occurs along solution seams and at grain contacts.

Interval XXXI.- The interval ranges from 600.40 m to a depth of 596.00 m. The lithology of this interval is a rudist boundstone. It contains an unconsolidated rubble interval at the base and few subvertical fractures. From the micro-scale perspective, this interval has a packstone texture. It consists of less than 5% algae and 15% *Orbitulina*, with minor small forams, intraclasts, peloids and ostracodes. Rudists and rudist fragments are very abundant and are present in an abundance percentage between 25 and 30%. This interval has a peloidal matrix. An interesting observation in this interval is that there are some thin layers of mudstone or wackestone, represented by samples such as #83 at 597.37 m, which interrupt the rudist boundstone of this interval. This interval possesses the highest macroporosity percentage among all the previous intervals, and is estimated between 15 and 20%. This due to the presence of abundant rudist molds resulting from leaching. These molds are outlined by micritic envelopes and some of them are only partially cemented by calcite. A few other rudists have been neomorphosed. Cementation has a patchy appearance and corresponds to the portions with abundant allochems. In these portions, calcite cements occur in algal intraparticle pores and as overgrowths on echinoids. Interpeloidal pore spaces are cemented by neomorphic microspar. Hydrocarbon staining in this interval is the most intense. It occurs in rudist molds, micropores of the matrix, algal intraparticle pores and interpeloidal pore spaces. This interval is the uppermost of the Shuaiba Formation in GN-23. It is overlain by the Nahr-Umr Shale Formation (Albian). There is a regional unconformity, which represents erosion or non-deposition during the Middle Aptian, that

marks a lithological change from shallow shelf limestones of the Shuaiba Formation to overlying shallow shelf clastics of the Nahr-Umr Formation (Harris et al; 1984).

Stratigraphic Variability of Allochemical Constituents

This section presents the variability observed in the major allochemical constituents throughout the GN-23 core. Allochem percentages are plotted versus depth in meters. These allochem percentages represent the abundance in each interval relative to other allochems and to the matrix. Allochem abundance was estimated in the core, plugs and thin sections that cover each interval. These plots are very useful in establishing a stratigraphic subdivision of the Shuaiba Formation in GN-23. The thirty one intervals of the Shuaiba Formation here are grouped into two major zones with very distinctive petrographic and sedimentologic characteristics due to the variability of rudists, algae, *Orbitulina* and other allochems with depth. The variability of each one of these allochems will be presented separately.

Rudists.- By observing the rudist percentage plot versus depth (Fig. 12), the subdivision of the Shuaiba Formation into two zones is easily identified. The lower zone extends from the bottom of the core to a depth of 619.45 m where the separation between this zone and the upper zone occurs. The lower zone, in general, is characterized by its lower content of rudists and rudist fragments which average about 7%. However, there are few thin intervals within the lower zone that possess higher rudist percentages. In general, the rudist content of this zone increases toward the top. The upper zone extends from above 619.45 m to the top of the Shuaiba Formation, which occurs at 596.00 m in this

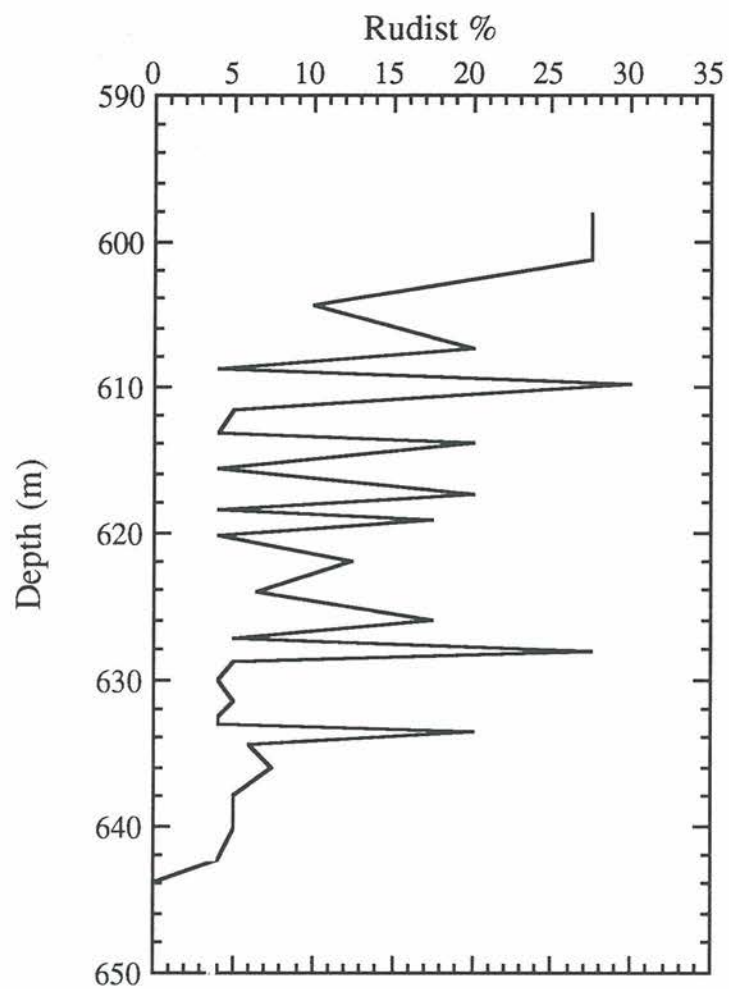


Figure 12. Variability of rudist abundance with depth in the Shuaiba Formation GN-23 core.

core. This zone is characterized by rudist-rich intervals alternating with some rudist-poor intervals. The rudist-rich intervals show abundance percentages as high as 30%, while the rudist-poor intervals show percentages as low as 4%. The average rudist percentage in the upper zone is greater than 12%. The Shuaiba Formation, in general, shows a trend of increasing rudist abundance toward the top of the core. Additional characteristics of these two zones will be reviewed in the following sections.

Algae.- The two zones mentioned above are clearly deciphered from the plot of algae percentage versus depth (Fig. 13). The boundary between the lower and the upper zones occurs again at 619.45 m. In this plot, the two zones show a similar trend, where the algae start at the base in low abundance, and increases gradually until a maximum percentage of about 30 to 35%. There is then a gradual decrease in the percentage toward the top of the zones. However, the lower zone possesses a higher average percentage of algae, (reaching about 15%) than the upper zone, which contains an average percentage of less than 10%. Therefore, the Shuaiba Formation, in general, shows a decreasing algae abundance toward the top of the core.

Orbitulina And Other Allochems.- The other allochems mentioned here include a group of forams other than the benthic *Orbitulina* and are smaller in size, along with ostracodes, peloids, echinoids, sponge spicules and mollusks. The small foram group includes benthic forams such as millioids, uniserials, biserials, peneroplids, fusulinids, agglutinated forams and a few others. The total abundance percentages of all these allochems in each interval are plotted versus depth in Figure 14. This plot again shows the two zones of the Shuaiba Formation, with the separation occurring at 619.45 m. The characteristics of the of the lower and upper zones regarding allochem variability trends

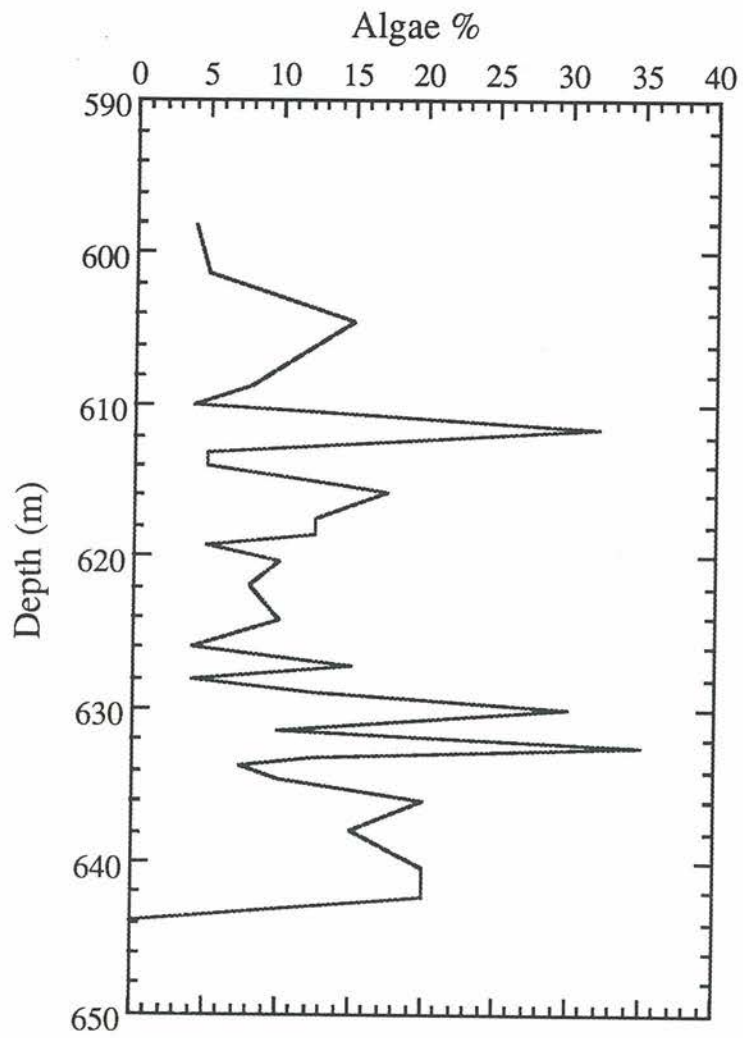


Figure 13. Variability of algae with depth in the Shuaiba Formation GN-23 core.

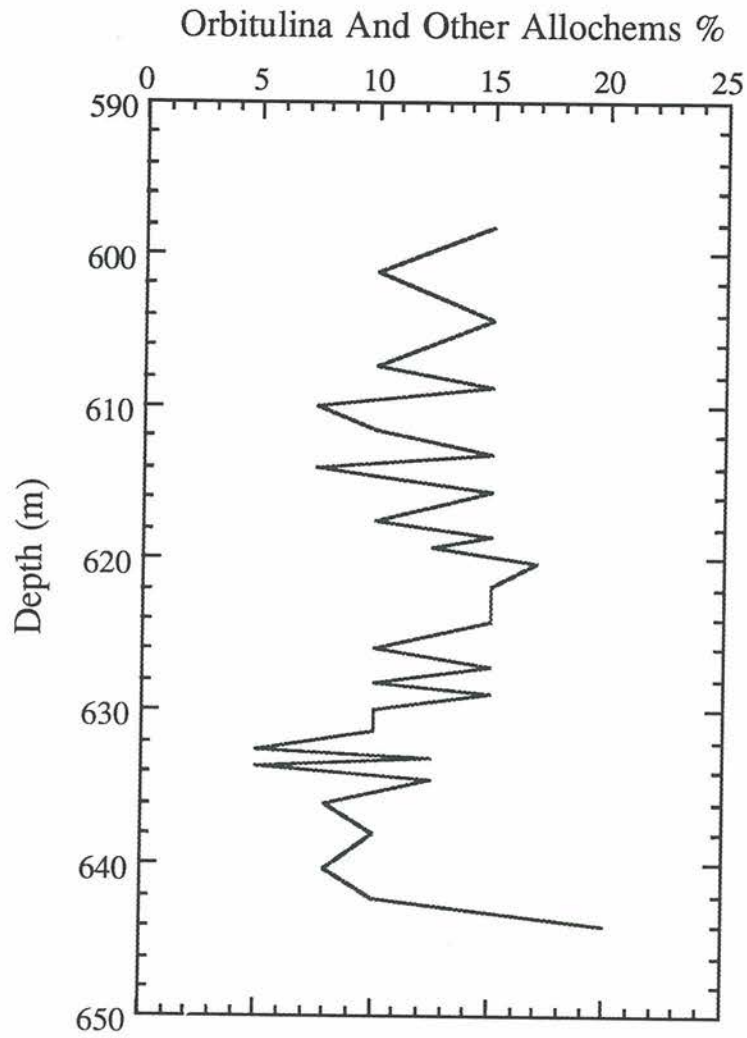


Figure 14. Variability of *Orbitulina* plus other allochems with depth in the Shuaiba Formation GN-23 core.

appear to be opposite to that of algae abundance. Here, both zones start with high abundance of allochems at the base, which then decreases gradually until a minimum percentage of about 5 to 7% is reached. There is then a gradual increase in the percentages toward the top of each zone. However, the lower zone possesses a lower average percentage (about 10%) than the upper zone, which contains an average of greater than 12%.

Stratigraphic Variability of Selected Reservoir Properties

Reservoir properties considered in this section include total measured porosity, macroporosity, microporosity and horizontal permeability. Total measured porosity and horizontal permeability were obtained from a Core Laboratories report (PDO; 1990). This report includes measurements and analyses performed on the GN-23 Shuaiba core and was presented to PDO in 1990. Grain volume, for plugs taken from the core, was determined by helium injection using a Helium Porosimeter. Subsequently, the total measured porosity and grain density of each plug were calculated. Macroporosity represents the porosity observed and estimated for each of the thirty one intervals in the Shuaiba Formation from the core, plugs and thin sections in this study. Microporosity percentages are calculated from the difference between the total measured porosity and the estimated macroporosity for each interval. Each of these reservoir properties is plotted versus depth in order to evaluate the reservoir heterogeneity. These plots are consistent with plots of allochem variability in subdividing the GN-23 core into two separate zones. The boundary between the lower and the upper zones is observed to occur again at 619.45 m.

Total Measured Porosity.- The lower and the upper zones have similar characteristics regarding total measured porosity variation (Fig. 15). Both of these zones start with high total measured porosity at the base, which then decreases gradually through the middle sections of the zones. A gradual increase in the porosity then occurs as the top of each zone is approached. However, the lower zone has a lower average total porosity (27 %) than the upper zone, which has an average of greater than 30%. Thus, the Shuaiba Formation, in general, shows a trend of increasing total measured porosity toward the top of the core. Moreover, the Shuaiba Formation, as a whole, possesses very high porosities.

Macroporosity.- From the plot of macroporosity values versus depth (Fig. 16), it is obvious that the lower zone of the Shuaiba formation possesses a lower macroporosity (average equals 5 %). This value appears to be relatively constant over all the lower zone except for few intervals which show even lower values. The macroporosity increases gradually above 619.45 m, where the boundary between the two zones occurs, toward the top of the Shuaiba Formation. The upper zone is characterized by a higher macroporosity average (estimated to be greater than 8%) and it reaches a maximum of greater than 15% at the top of the zone, which is the top of the Shuaiba.

Microporosity.- The plot of microporosity values versus depth (Fig. 17) is analogous to the plot of the total measured porosity variation with depth (Fig. 15). The same porosity variation trends are seen in this plot. However, the microporosity averages for the lower and the upper zones are smaller than the total measured porosity averages. This is due to the fact that the total porosity represents the sum of the macroporosity and the

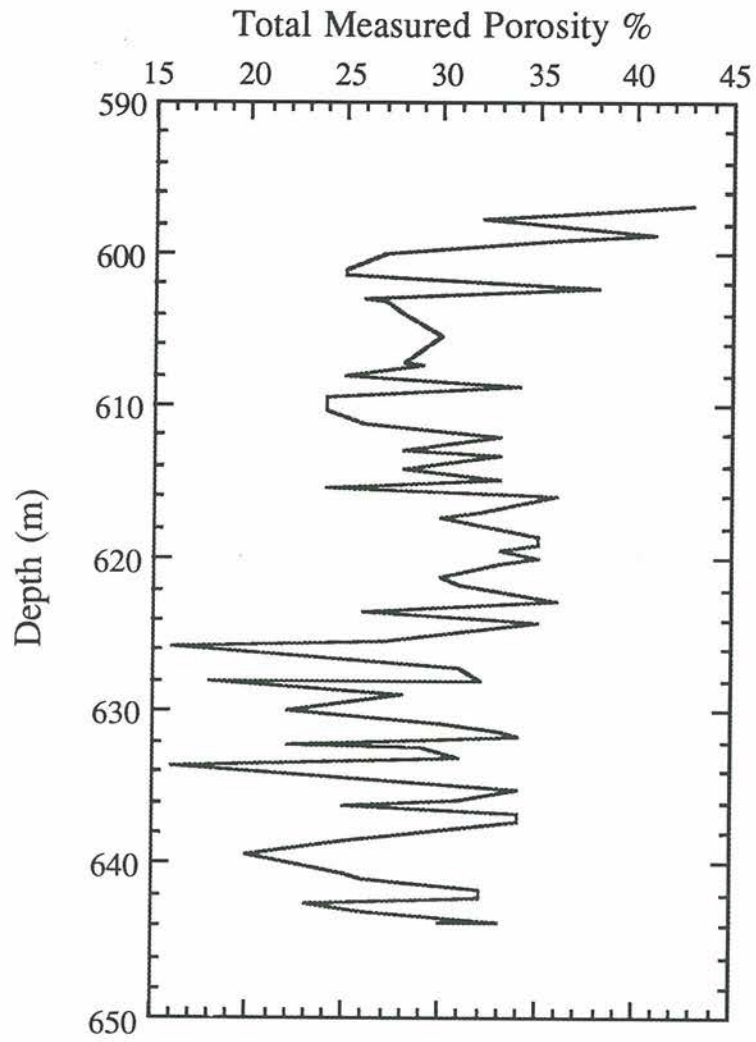


Figure 15. Variability of total measured porosity with depth in the Shuaiba Formation GN-23 core.

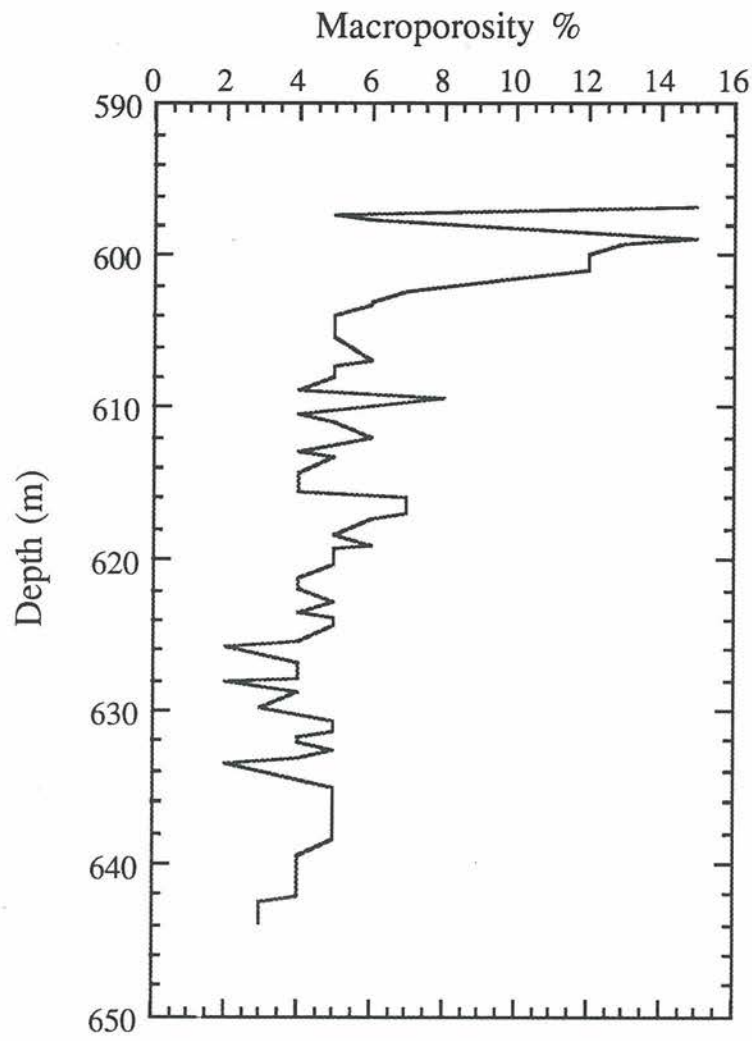


Figure 16. Variability of macroporosity with depth in the Shuaiba Formation GN-23 core.

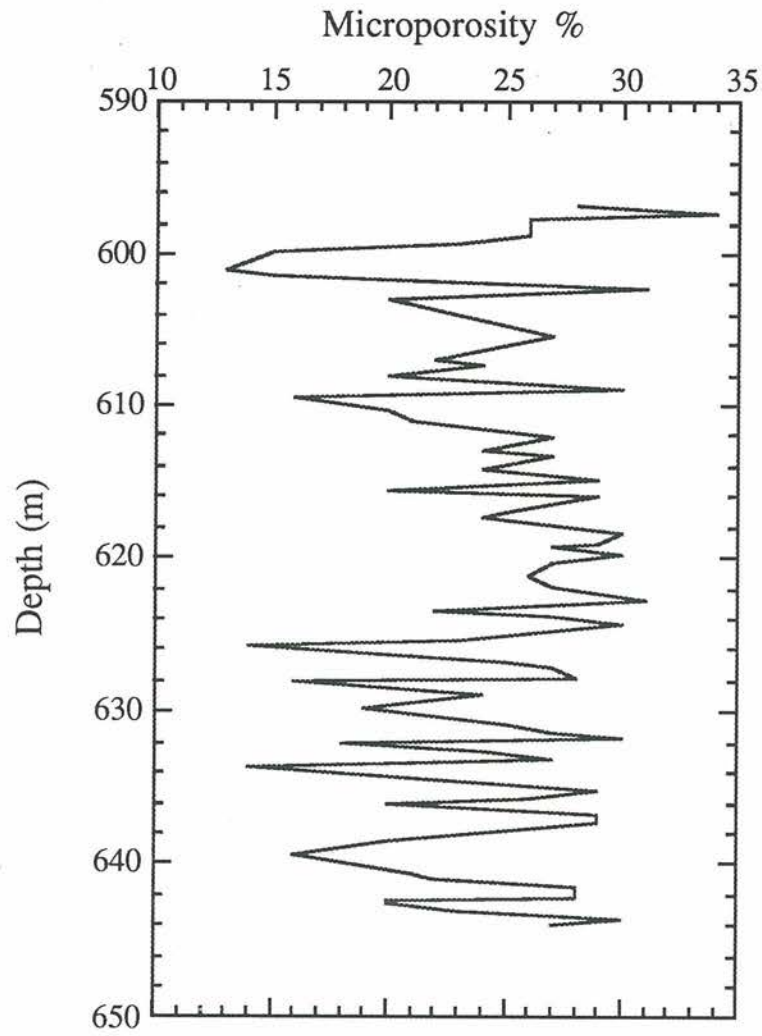


Figure 17. Variability of microporosity with depth in the Shuaiba Formation GN-23 core.

microporosity. The lower zone, in this plot, possesses an average of about 23% whereas the upper zone shows an average of about 25%.

Horizontal Permeability.- The horizontal permeability values, which are measured in millidarcies, is plotted versus depth in Figure 18. In general, the Shuaiba Formation is characterized by very low permeability values. The permeability is lower at the bottom of the core and becomes slightly higher toward the top of the formation. By masking the permeability values of greater than 35 md (Fig. 19), we obtain a better representation of the variation in permeability through the lower and the upper zones of the Shuaiba. The lower zone, which occurs below the 619.45 m boundary, possesses horizontal permeability values of less than 10 md, reaching 10 md at the top of the zone. The upper zone shows higher permeability values with an average estimated to be greater than 25 md. Moreover, in this zone, the values increase dramatically toward the top until it reaches values greater than 200 md (Fig. 18).

Diagenesis of the Shuaiba Formation in GN - 23

Studying the diagenesis of the Shuaiba Formation is essential for understanding the development of the reservoir in Ghaba North Field. In this section, diagenetic petrographical observations and geochemical data will be presented. This will help in developing the diagenetic history of the reservoir and evaluating the evolution of its reservoir properties. Petrographic description and occurrence of all types of cements in the formation, although described briefly in the first section of this chapter, will be reviewed in a diagenetic context. Geochemical data, which include stable carbon and

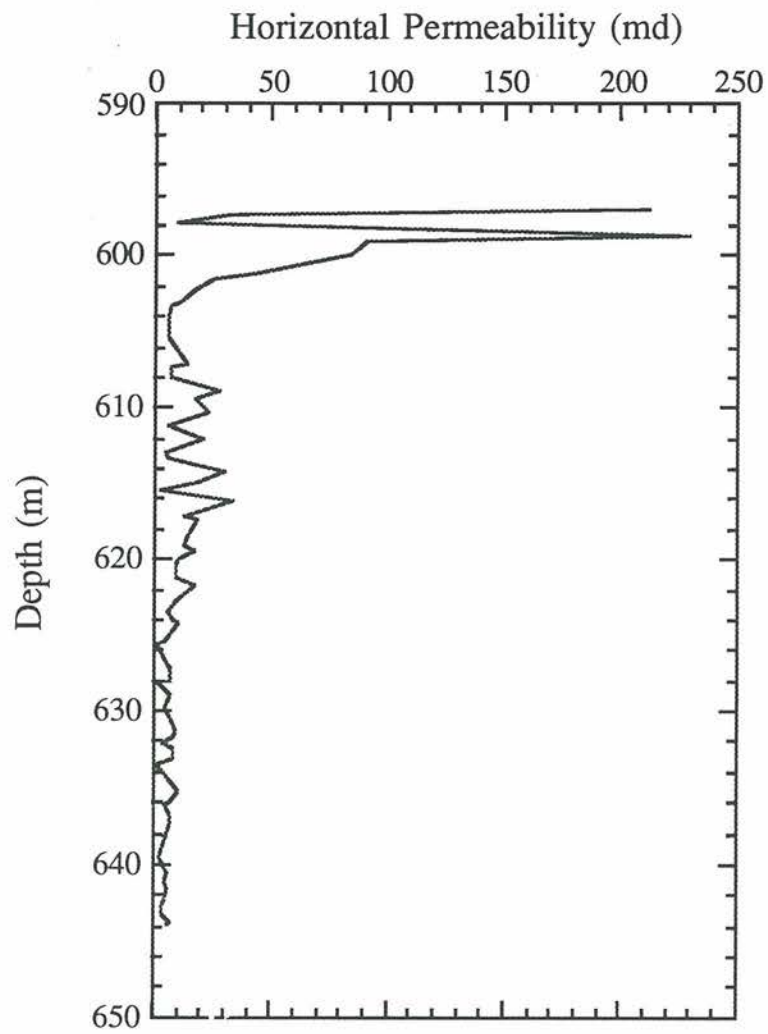


Figure 18. Variability of horizontal permeability with depth in the Shuaiba Formation GN-23 core.

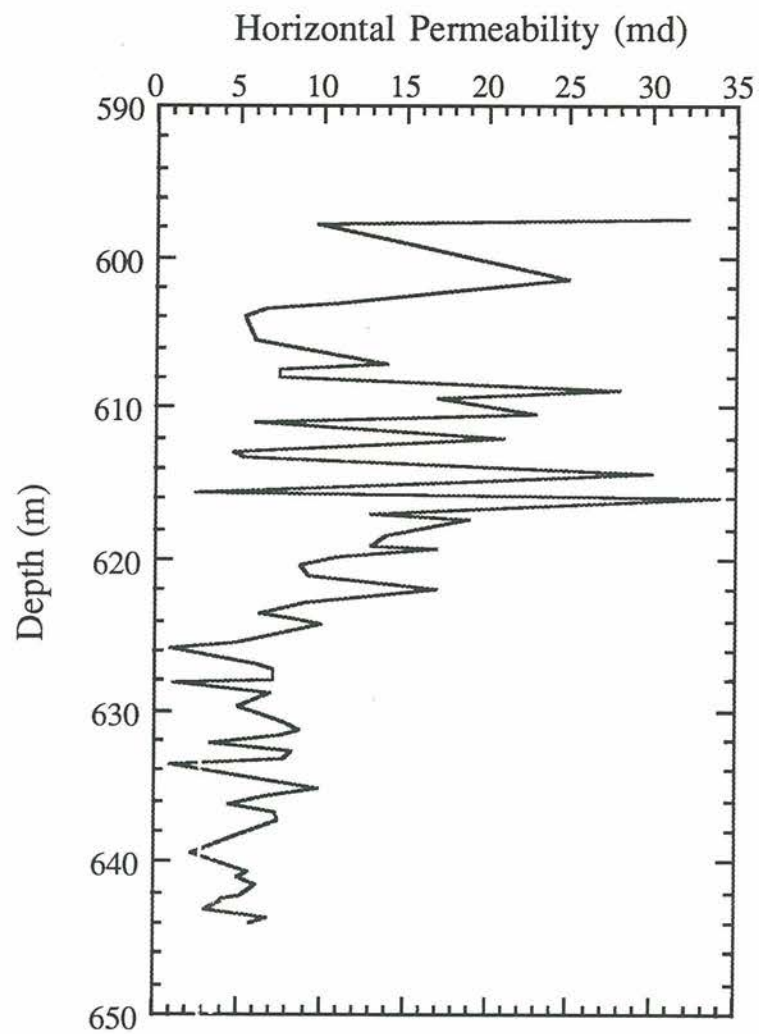


Figure 19. Variability of horizontal permeability with depth in the Shuaiba Formation GN-23 core.

oxygen analyses of matrix and late cements, will be presented in order to help constrain the diagenetic history.

Diagenetic Features Observed in the GN-23 Shuaiba Core

Diagenetic features of the Shuaiba include cements, micro-rhombic calcite matrix, leaching and other diagenetic fabrics. Each of these will be presented and evaluated separately.

Cements In The Formation.- Cementation in the Shuaiba Formation, in general, is not very well developed because there is only minor primary interparticle porosity in such muddy and wacke sediments. However, some cementation is observed in the Shuaiba in the GN-23 core. These cements are calcitic in composition but with variable morphologies. Cementation patterns vary with depth and facies of the Shuaiba. These cements will be described and their relation to the facies and variation with depth will be shown.

There are, in general, two major types of calcite cements observed and described in the petrology and petrography section of this chapter. These and other diagenetic features were mentioned in the description of the sedimentology and facies of GN-23. The first type of calcite cement occurs as a fine-crystalline calcite, and the second occurs as a coarse-crystalline pore filling calcite. The fine-crystalline calcite cements occur in intraparticle pores of algae, *Orbitulina* and other forams, as well as within microfractures, borings, shelter porosity and primary interparticle pores. These cements partially to completely fill the pores. In the partially filled pores (Fig. 20), the fine-crystalline calcite

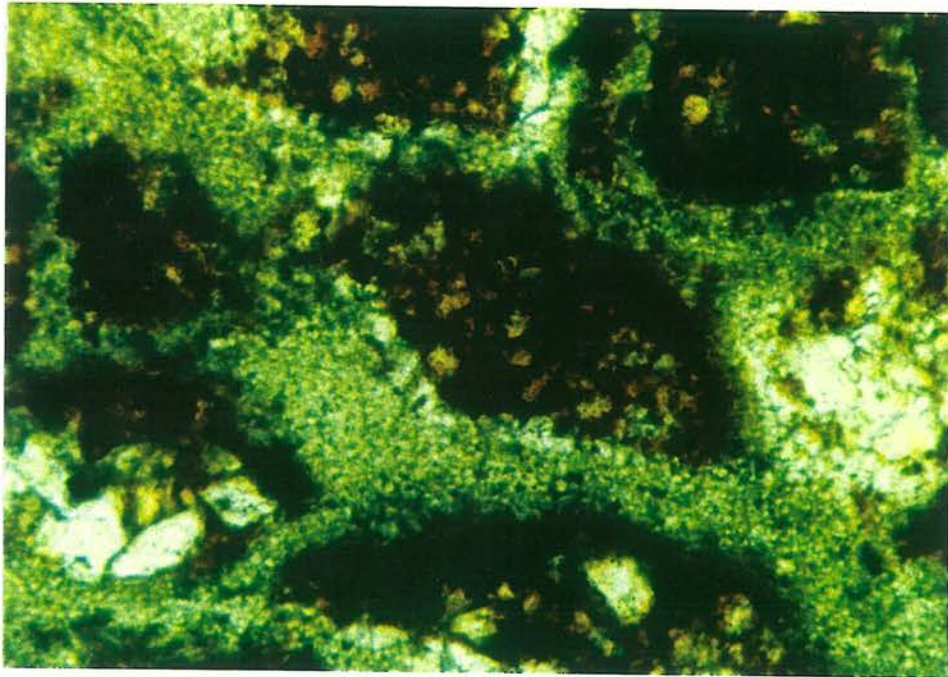


Figure 20. Algal intraparticle pores filled partially by fine-crystalline calcite cement and hydrocarbon. Field of view is 800 μm .

crystals line the pores and the remainder is filled by hydrocarbons. These fine-crystalline calcite cements show an increase in crystal size toward the center of the pores (Fig. 21). In general, the calcite crystals of this cement type are subhedral to euhedral in shape. Interestingly, this fine-crystalline calcite cement has a patchy appearance in the core and plugs. This is due primarily to the localization of cements within algae intraparticle pores, and therefore it corresponds to the distribution of algae in the Shuaiba (Fig. 22).

The other cement type is the coarse-crystalline calcite, which occur predominately in molds of rudists and rudist fragments, and in primary intraparticle pore spaces of rudists and other macropores. These cements consist of coarse, equant-blocky, subhedral to euhedral calcite crystals. The size of these crystals also increases toward the center of the pores. In some samples, this cement type encases broken micritic envelopes, rudists fragments and brecciated matrix fragments (Fig. 23). Importantly, these coarse-crystalline calcite cements are more abundant at depths below 619.45 m than above it in the GN-23 core. Moreover, below this depth, all the rudist-rich intervals in the core appear highly cemented by this cement. Here, it completely fills any available macroporosity. On the other hand, there are many examples of partially filled macroporosity above 619.45 m.

Thus, in general, the fine-crystalline calcite cements are patchily distributed throughout the core, but are more abundant below 619.45 m due to higher abundance of algae (see Fig. 23). In addition, the coarse-crystalline calcite cements are also more abundant below 619.45 m and correspond mostly to rudist-rich intervals.

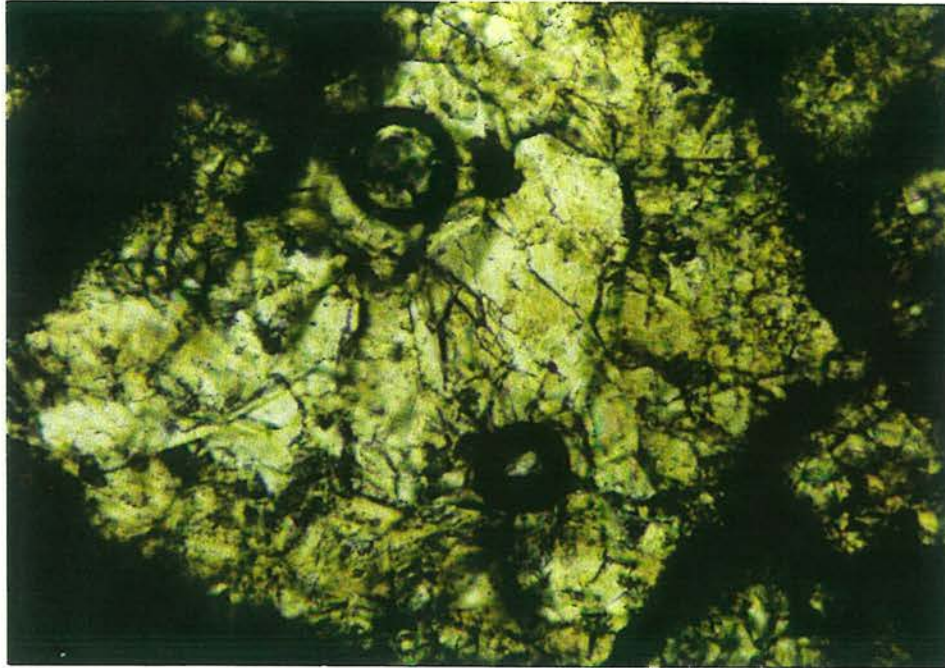


Figure 21. Algal intraparticle pore filled by fine-crystalline calcite cement which increases in crystal size toward the center of the pore. Field of view is 800 μm .

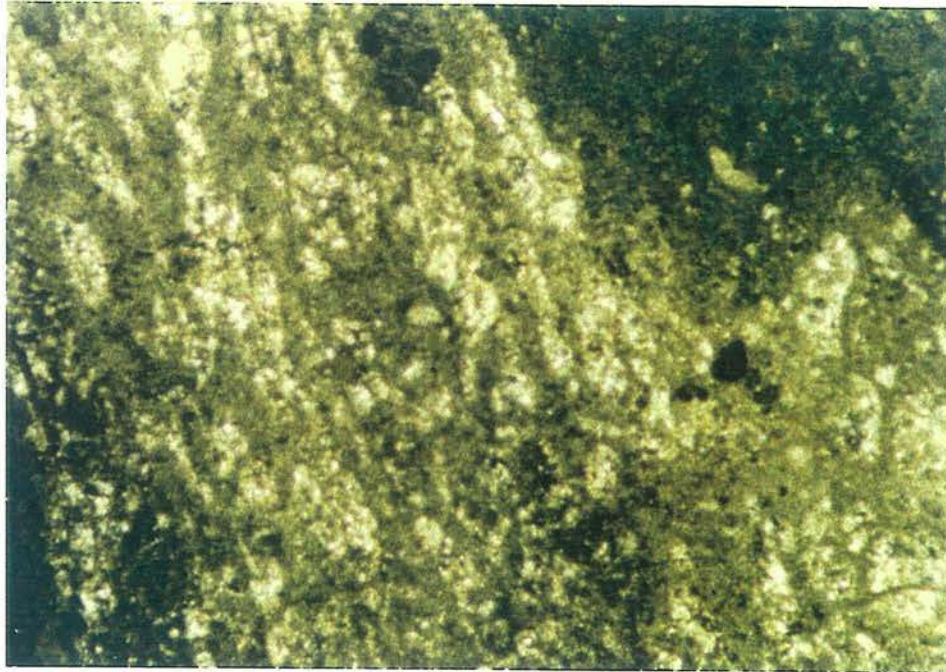


Figure 22. Photomicrograph of thin section showing the relation between patchy fine-calcite cement and algal intraparticle pores. Note that epoxy stained only the parts of matrix without algae. Field of view is 3 mm.



Figure 23. Coarse-crystalline calcite cement encasing rudist fragments, micritic envelopes and matrix fragments. This indicates the late nature of this cement. Field of view is 3 mm.

Other Diagenetic Features In The Shuaiba.- In addition to calcite cements described above, there are other diagenetic features in the GN-23 Shuaiba core that can be observed. These features include hardgrounds, solution seams, micritic envelopes, calcite overgrowths, calcite microspar, and replacement, recrystallization and neomorphism of rudists and rudist fragments. Occurrence of these features and their variation with respect to facies and/or depth will be presented.

Micritic envelopes are very common features in the Shuaiba thin sections. These micritic envelopes mostly outline rudists and rudist fragments, or mollusc fragments if present. In some cases, these envelopes were spalled and broken and appear to be floating in the coarse-crystalline calcite cements (see Fig. 23). In other cases, the micrite envelopes surround recrystallized fragments or molds of rudists.

Syntaxial calcite overgrowths on echinoid plates are very common in the Shuaiba (Fig. 24). These occur on most echinoid plates regardless of the depth or facies.

Neomorphic calcite microspar occurs in some intervals of the Shuaiba. This microspar is mostly confined to interpeloidal pore spaces, wherever these peloidal matrices occur. In addition, neomorphic microspar also cements some of the matrix microporosity. Microspar cements reduce the total measured porosity of the intervals in which they occur.

Several hardgrounds were observed in the Shuaiba GN-23 core. These hardgrounds are mostly overlain by rudist-rich facies (such as rudist rudstones or boundstones). These hardgrounds were accompanied, in some cases, by the occurrence of intraclasts in the overlying facies. In addition, there are some boring into the

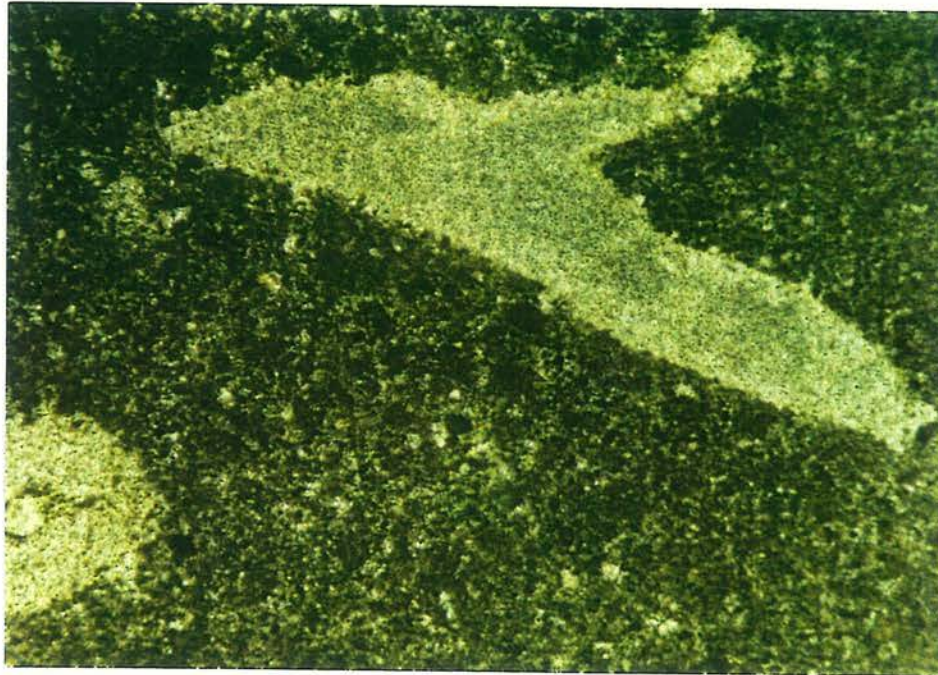


Figure 24. An echinoid plate floating in a wackestone matrix showing calcite overgrowths. Field of view is 3 mm.

hardground surfaces (such as the hardground which occurs at 619.45 m [see GN-23 core photographic record; plate 5]). This occurrence is a very important feature which separates two lithologic units and its significance will be discussed later.

Rudists and rudist fragments in GN-23 are either preserved or leached. Preserved rudists are either replaced or recrystallized. Almost all of the rudists and rudist fragments below the 619.45 m boundary are preserved with no signs of leaching. Here, some rudists were replaced and their wall microstructures were preserved, and some were recrystallized with no preservation of wall microstructures. These rudists and rudist fragments are outlined by micritic envelopes. Moreover, there are some neomorphosed rudists. These cannot be categorized as either replaced or recrystallized and show irregular crystal boundaries. Rudist internal pore spaces show geopetal fabrics and extensive cementation by coarse-crystalline calcite cements below 619.45 m. Above 619.45 m, there is obvious evidence from the core, plugs and thin sections (Fig. 25) for dissolution and leaching. However, there are still some preserved rudists and rudist fragments above this depth.

Solution seams (Fig. 26) are very abundant in the Shuaiba Formation in the Ghaba North Field. These are described as drapes of dark clay sized organic residuals (non-argillaceous), some of which have a fabric which has been termed "horse-tail". In general, these solution seams seem to be more abundant in facies or intervals which are poor in coarse-grained constituents.

Leaching And Dissolution.- As mentioned above, leaching of rudists and rudist fragments and development of secondary moldic porosity is an obvious phenomenon in

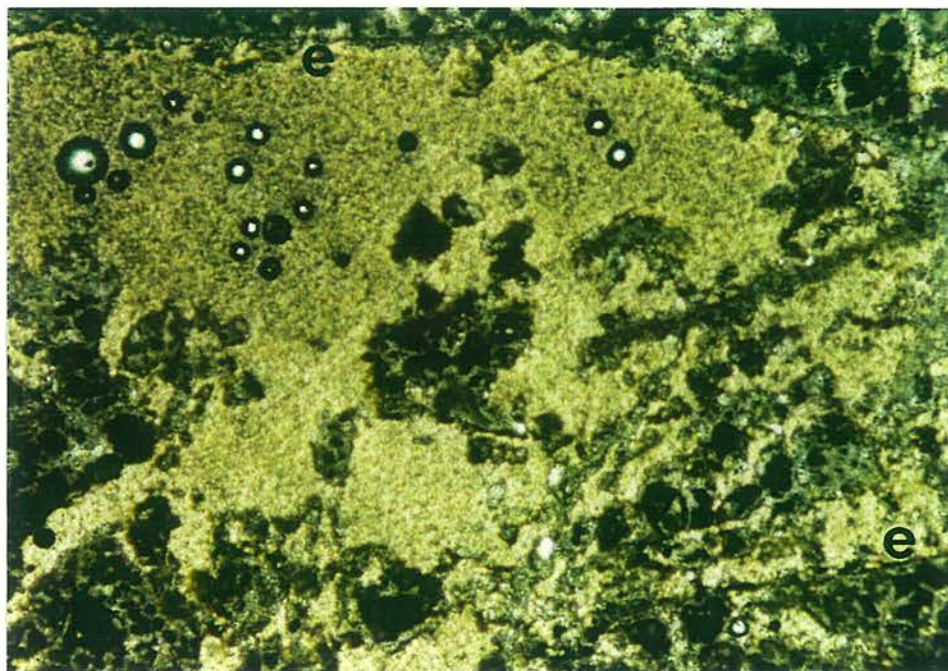


Figure 25. Photomicrograph of rudist leaching in the Shuaiba. Note micritic envelopes (e) outlining the mold. Field of view is 3 mm.

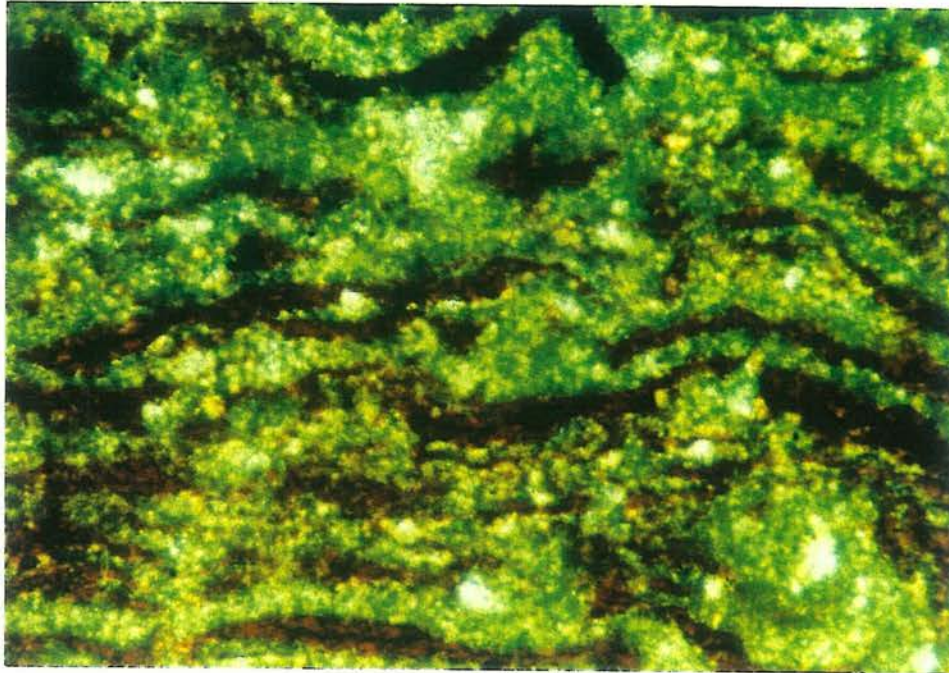


Figure 26. Photomicrograph of solution seams in the Shuaiba. Note concentration of hydrocarbons along these seams. Field of view is 800 μm .

the Shuaiba GN-23 core. These leaching features are present in the core above the 619.45 m boundary. This moldic porosity is either present as whole molds, now filled by hydrocarbon, or as partially cemented molds. The latter have coarse-crystalline calcite crystals growing in them (Fig. 27). The development of this moldic porosity has resulted in an obvious increase in the macroporosity (Fig. 16) and the horizontal permeability (Fig. 19). There is a positive linear covariance between these two reservoir properties, as shown in Figure 28. Importantly, dissolution and leaching features are observed to be intense and abundant below distinct stratigraphic boundaries and decrease with depth away from them. These boundaries are the regional unconformity, which occurs at the top of the Shuaiba and separates it from the overlying Nahr-Umr Shales, and the erosional surface described at the top of the twenty sixth interval at a depth of 609.45 m.

Micro-Rhombic Calcite Matrix.- In addition to the macroporosity observed in the Shuaiba GN-23 core, which includes moldic secondary porosity and late-tectonic open macrofractures, there is microporosity within the matrix which accounts for most of hydrocarbon storage capacity in the reservoir. The SEM study of the Shuaiba matrix revealed that it is composed of micro-rhombic calcite crystals with abundant intercrystalline microporosity (Fig. 29). These micro-rhombs have equant shapes and appear growing in open pore spaces without any evidence of formation as coating on pre-existing microparticles. Sometimes, these micro-rhombic calcite crystals show partial smoothing of their corners and edges, which reflect limited dissolution. The intercrystalline microporosities of the matrix are in the order of 5 to 10 μm . In addition, there are relatively larger micropores approaching 62 μm . These are secondary in nature, include micromolds and microvugs. There are two types of textures observed in the

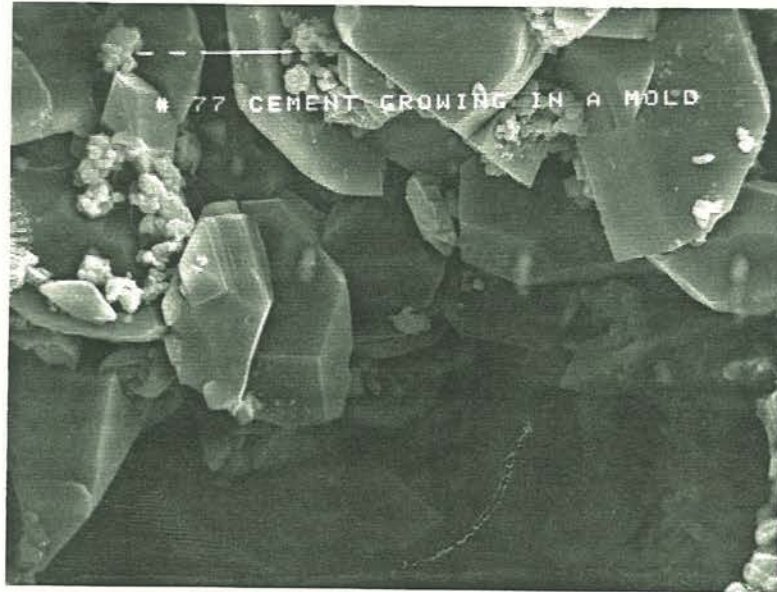


Figure 27. SEM photograph of a mold (probably of a rudist fragment) with coarse-crystalline calcite crystals growing into the void and partially cementing it. Long bar in the photo is 10 μm .

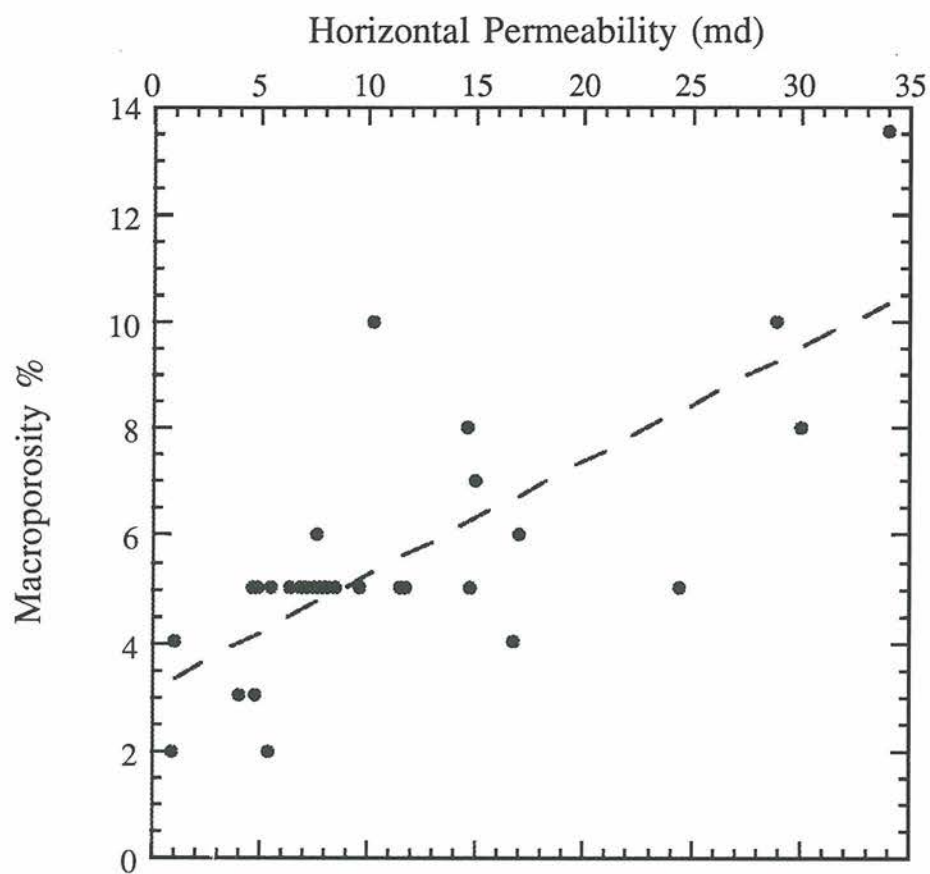


Figure 28 Cross-plot of macroporosity versus horizontal permeability in the Shuaiba Formation GN-23 core. Dashed line represents the overall trend.

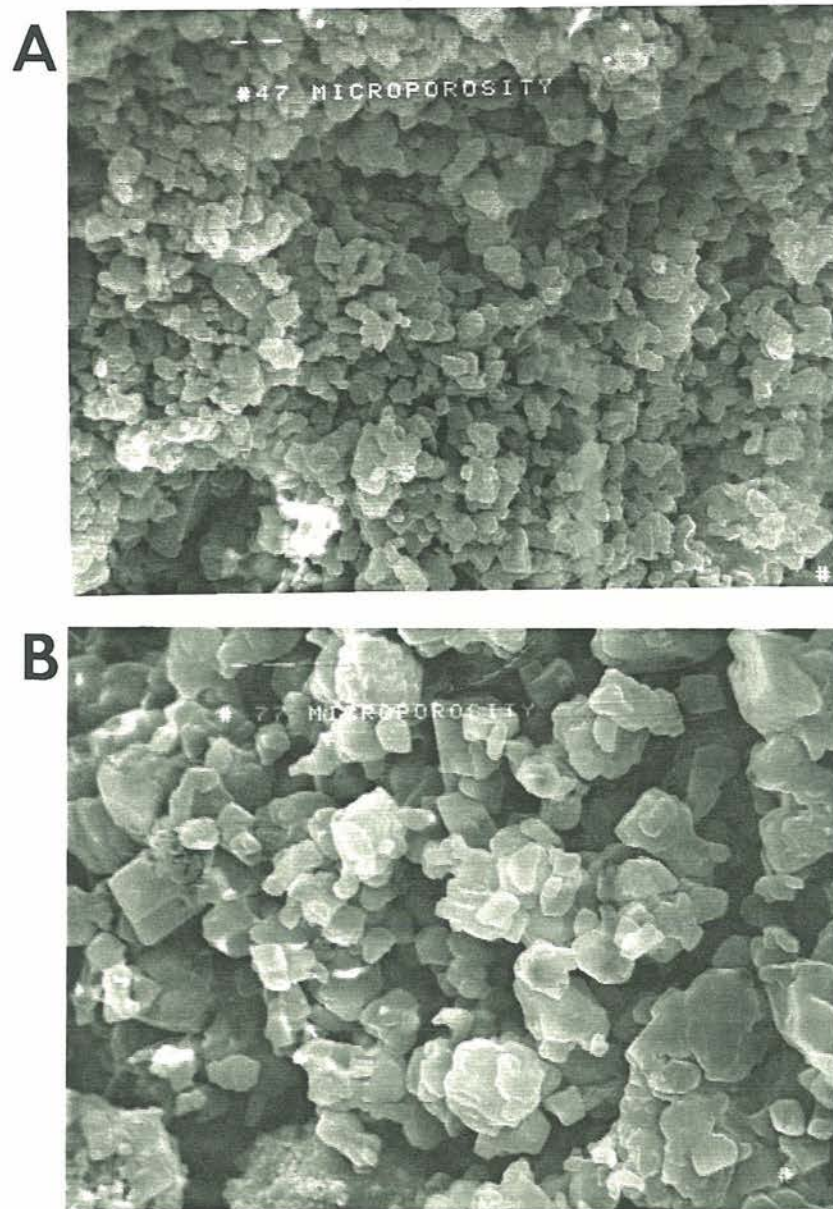


Figure 29. SEM photographs of micro-rhombic calcite matrix and intercrystalline microporosity in the Shuaiba. Photos are of broken sample surfaces. A. Sample #47 from a depth of 618.49 m in GN-23. B. Sample #77 from a depth of 601.06 m in GN-23. Second bar from the right, in both photos, is 1 μm .

Shuaiba matrix from SEM inspection; a blocky-crystal framework texture (Fig. 29) and a crystal mosaic texture (Fig. 30). Moreover, there is variation in the amount of microporosity with depth (Fig. 17). Five samples were chosen for SEM investigation from different depths in the core. These are samples #2, 19, 47, 77 and 81. Samples #19 and 77 correspond to intervals with relatively low microporosities, whereas the other three samples belong to intervals with high microporosities. High microporosity intervals alternate with low microporosity intervals. Sample #19 (Fig. 31) possesses low microporosity due to the presence of neomorphic calcite microspar blocking and healing some of the intercrystalline microporosity of the peloidal matrix. Moreover, sample #77 possesses low microporosity due to the presence of the two matrix textures within the sample. The blocky-crystal framework texture possesses higher intercrystalline microporosity than the crystal mosaic texture. The latter possesses very low microporosity due to the presence of well-developed subhedral to euhedral calcite crystals with straight and curvilinear boundaries.

The Shuaiba Isotopic Analysis

Eighty four samples of micro-rhombic calcite matrix, covering all the plugs taken from the GN-23 core, were analyzed for stable carbon and oxygen isotopes. Only four samples of the late coarse-crystalline calcite cements were analyzed for stable carbon and oxygen isotopes. This is due to the lack of sufficient amount of cement in the plugs, especially above 617 m. All four cement samples were from depths below 617 m. Isotopic data are tabulated in appendix 2. The $\delta^{13}\text{C}$ of the micro-rhombic calcite matrix

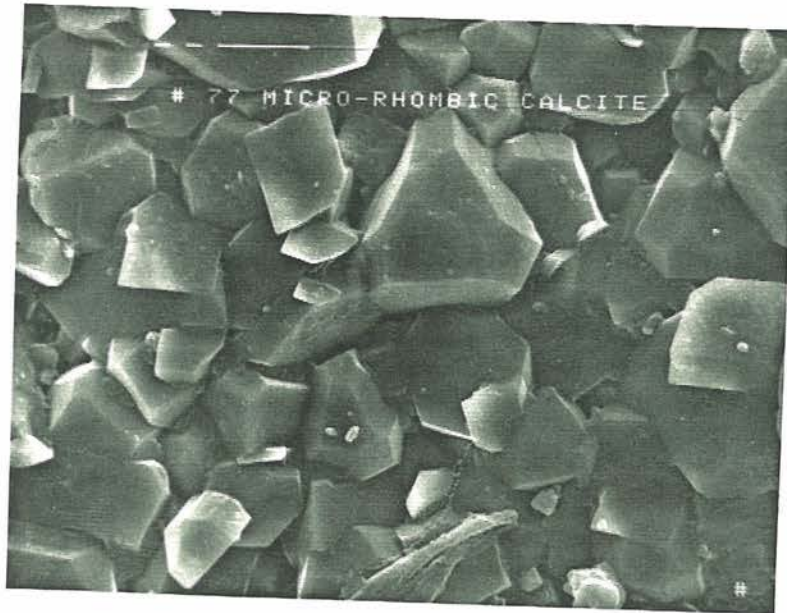


Figure 30. SEM photograph of the Shuaiba matrix in sample #77 with a crystal mosaic texture. See text for discussion. Long bar in the photo is 10 μm .



Figure 31. SEM photograph of a broken surface of sample #19 from a depth of 633.6 m in GN-23. It shows the presence of neomorphic calcite microspar healing some of the microporosity of this sample. Long bar in the photo is 10 μm .

ranges from +3.11 to +5.95‰ and $\delta^{18}\text{O}$ range from -7.31 to -4.10‰ (all relative to PDB) (Fig. 32).

Lithology and Reservoir Properties of the Shuaiba Formation in other Wells in Ghaba North Field

In addition to the GN-23 core, there are three other available cores from the Ghaba North Field. These are the GN-13, GN-2, and the GN-1 cores. Core descriptions were performed and representative samples from these cores were taken based on the detailed sampling in GN-23. This section describes the sedimentology of the Shuaiba Formation observed in these three cores, using core descriptions and thin section inspection. Observations from these other cores will help in the recognition of variation in the Shuaiba Formation across the field. Reservoir properties of the Shuaiba from these cores will be presented as well, in order to identify lateral variations in the reservoir characteristics over the field. Poor recovery in these three additional cores limits the amount of useful information that can be obtained. Missing intervals in these cores reduces the degree to which vertical variations and trends can be deciphered.

The Shuaiba Formation in GN-13

The recovered Shuaiba core from this well is separated by missing intervals into three sections. The lower section starts at 661.40 m and ends at 652.70 m. From the bottom of this section to a depth of 654.50 m, the Shuaiba is comprised of wackestone

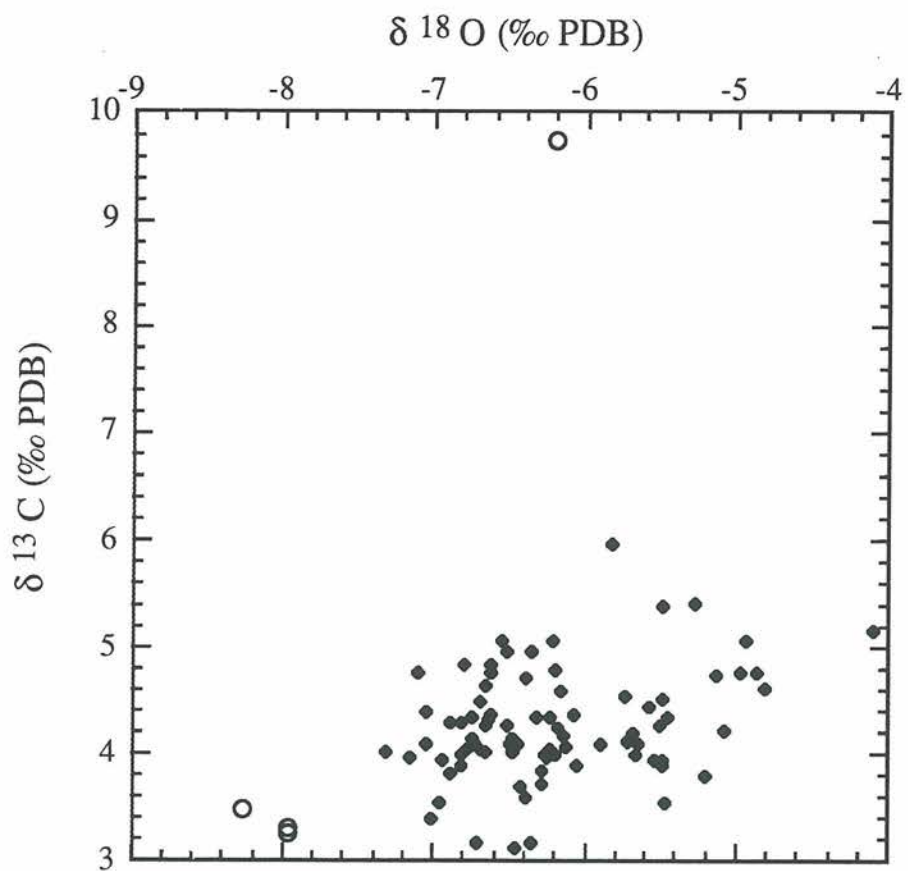


Figure 32. Cross-plot of $\delta^{13}\text{C}$ versus $\delta^{18}\text{O}$ of the Shuaiba matrix (solid diamonds) and late calcite cements (open circles) in GN-23 core.

intervals which contain *Orbitulina* with other small benthic forams, ostracodes, echinoids, some peloids and a few small rudist fragments. These intervals alternate with packstone to wackestone intervals which contain, in addition to the above constituents, scattered algal nodules. From 654.50 m to the top of the lower recovered section in this well, the Shuaiba is composed of two alternating facies; floatstone and wackestone facies. The floatstone intervals contain preserved or recrystallized fragments of rudists and algal nodules which float in a wackestone matrix. Macroporosity in these intervals is almost absent, and hydrocarbon occupies only the microporosity. Calcite cementation of intraparticle pores of algae has a patchy distribution.

The middle recovered section of GN-13 covers the interval from 650.10 m to 643.50 m. This section is comprised of wackestone to packstone/wackestone intervals which are composed of *Orbitulina* and other small forams, ostracodes, echinoids, peloids, molluscs, algae, and fragments of rudists. However, this sequence is interrupted by two intervals which show cut and fill features. The first occurs between 648.50 m and 648.20 m, and is described as a cemented wackestone with normal grading. The other occurs between 646.05 m and 645.30 m, and is described as a scour filled with a rudist/gastropod rudstone to floatstone. Apart from minor fenestral porosity, corresponding to the interval with the normal grading, and a solution cavity filled partially by blocky-calcite cements, there is minimal macroporosity. Hydrocarbon primarily occurs in the microporosity and along solution seams. Rudists and rudist fragments are either preserved, neomorphosed or recrystallized. Algae nodules are cemented by very fine calcite cements.

The upper recovered section of the Shuaiba from this well occurs between 620.25 m and 619.50 m. This section includes the regional unconformity between the Shuaiba and Nahr-Umr, which occurs at 619.60 m. The Shuaiba observed here is analogous to the wackestone facies with the scattered algal nodules described earlier in the previous sections.

The Shuaiba Formation in GN-2

The Shuaiba Formation in this core is separated by missing intervals into two recovered sections. The lower recovered section extends from 637.75 m to a depth of 632.60 m. The Shuaiba here is comprised of wackestone intervals alternating with floatstone intervals. The wackestone intervals are composed of *Orbitulina* and other small forams, echinoids, sponge spicules, peloids, rare ostracodes, skeletal fragments of molluscs, a few small rudist fragments, and scattered algal nodules. The floatstone intervals contain similar constituents, but higher percentages of rudist fragments. The latter are either preserved or partially replaced by calcite cements. Hydrocarbon occurs in the microporosity and along solution seams. Intraparticle pores of algae are cemented by subhedral calcite crystals, which increase in size toward the center of the pores.

The upper recovered section of the Shuaiba covers the interval from 615.50 m to 614.30 m. It includes the unconformity between the Shuaiba and the Nahr-Umr Formations, which occurs at 614.35 m. The Shuaiba here is analogous to what is described in the lower recovered section in this well. However, the floatstone intervals

here possess complete shells of rudists, which show obvious leaching. The unconformity here is underlain by an algal boundstone.

The Shuaiba Formation in GN-1

The recovered Shuaiba in this well is separated by missing intervals into four sections. The lower section extends from a depth of 646.90 m to 643.85 m. The Shuaiba here is composed of wackestone intervals separated by a floatstone interval. The wackestone intervals are comprised of *Orbitulina* and other small benthic forams, echinoids, sponge spicules, ostracodes, peloids, algal nodules, and a few small fragments of rudists scattered in the matrix. The floatstone interval contains, in addition to the above constituents, rudist shells scattered in the matrix. Macroporosity is almost absent, and hydrocarbon occupies micropores of the matrix only. Rudists are either preserved or recrystallized. In addition to geopetal fabrics in internal pore spaces of the rudists, blocky coarse calcite cements fill the rest of the pore spaces. Fine fractures in these intervals are cemented by calcite as well.

The second recovered section in this well covers the interval from 634.10 m to 630.75 m. The Shuaiba here is represented by algal boundstone intervals with some scattered rudist fragments trapped within the algae. These algal boundstones alternate with packstones and wackestones composed of *Orbitulina* and other small forams, echinoids, peloids, ostracodes, and skeletal fragments of rudists and other allochems. These wackestone intervals are characterized by very clear burrowing and horse-tail

compaction features. Macroporosity is very low and hydrocarbon is concentrated along solution seams and in the microporosity.

The third recovered section extends from 628.00 m to 624.95 m. It is composed of a wackestone interval which consists of alternating layers of wackestone with algal nodules and layers of bioclastic wackestones with compaction features and obvious burrowing. The allochemical constituents here are similar to the previously described wackestone intervals in this core. A floatstone interval with preserved rudist fragments occurs at the top of this section. Only minor macroporosity is observed here, occurring as shelter porosity and partially cemented algae intraparticle pores. Calcite cements fill rudist internal pore spaces and the intraparticle pores of algae. The latter has a patchy distribution through the core.

The upper recovered section of the Shuaiba in GN-1 covers the interval from 623.00 m to 617.30 m, where the boundary between the Shuaiba and the overlying Nahr-Umr occurs. In addition to the presence of the small allochemical constituents which are described above, the Shuaiba here is dominated by rudists and rudist fragments. Thus, it consists primarily of rudist floatstones and rudstones, which are interrupted from time to time by thin wackestone intervals. Some of these wackestones are thinly laminated and are characterized by calcite cementation and fine subvertical cemented fractures. A hardground with borings occurs at 621.20 m and separates a wackestone interval from an overlying floatstone to rudstone interval. Calcite cementation of internal pore spaces of the rudists and replacement of some of their shells is more extensive at the base of the section. Macroporosity increases toward the top of the section. Macroporosity occurs as molds of rudists and rudist fragments, some of which are partially cemented by calcite.

DISCUSSION

Petrology, Petrography and Reservoir Properties of the Shuaiba Formation in the GN-23 Well

This section discusses the importance and the application of the results obtained in this study regarding sedimentology, petrology and reservoir characteristics of the Shuaiba Formation. The primary objective of this discussion is to establish a model for the environments of deposition of the Shuaiba Formation. Reservoir characteristics will be evaluated in order to understand reservoir heterogeneity and controls on its variability.

Inferenced Depositional Environment of the Shuaiba Formation

The Shuaiba Formation was deposited on the stable Arabian Shelf, which was established during the Permian and continued through the Mesozoic (Alsharhan and Kendall, 1986). During the Early Cretaceous, there was the gradual establishment of a ramp-type carbonate depositional setting related to a rise in sea level (Murriss, 1980). In general, the Shuaiba is represented by shallow-water deposits which prograded across the shelf (Alsharhan and Nairn, 1988). The Shuaiba was deposited during an extensive marine inundation of the shelf and was marked by a series of thick rudist grainstone buildups (Alsharhan, 1985). In this section, sedimentologic and petrographic features described in GN-23 will be used in order to understand the depositional environment and

facies mosaic in the Ghaba North area, central Oman. The biofacies and lithofacies observed in the Shuaiba will be interpreted from a depositional perspective.

Interval I.- This interval was most likely deposited in a very restricted shallow marine environment, probably in an interior shelf setting behind a barrier or buildup. This interpretation is based on the abundance of wackestones lacking coarse-grained constituents. Limited circulation in this setting led to high-salinity conditions through evaporation. This can be inferred from the dominance of miliolids and other small benthic forams among the allochemical constituents of this interval.

Interval II.- The presence of the green algae as a major constituent of this interval indicates a slightly deeper setting than the previous interval. Green algae occur predominately in protected shelf settings within the photic zone (Scoffin, 1987). The two types of calcareous green algae recognized here, *Bacinella* and *Lithocodium*, are characteristic of the Lower Cretaceous and typical in the Middle East (Johnson, 1969).

Interval III.- Depositional conditions for this interval are similar to the previous one. Sedimentological differences include the presence of algal nodules in place of layered algae and an increase in the amount of rudist fragments present. This likely indicates a higher depositional energy in a setting that is more proximal to rudist buildups.

Interval IV.- A similar setting to the two previous intervals is indicated here; however, there is a decrease in the energy of the environment because algae is present as nodules at the base and then becomes layered toward the top. The presence of only a few small fragments of rudists indicates that this facies is still far from the buildup.

Interval V.- This facies shows evidence of increasing proximity to the buildup or an increase in the energy of the setting. This is due to the presence of greater amounts of rudists and rudist fragments. These were transported from the buildup, by wave action, to the interior shelf setting. The fact that there are both preserved and recrystallized rudists indicates that these were sourced from different types of rudists with different original mineralogy. Different types of rudists live in different environmental settings. Rudists with an original high-Mg calcite (HMC) mineralogy are easier to stabilize to calcite than rudists with aragonitic mineralogy. Aragonitic rudists are more susceptible to leaching and recrystallization or replacement. There are many types of rudists present in the Shuaiba Formation (Fig. 33), such as requienids, monopleurids, caprotinids and caprinids that thrived during the Lower Cretaceous (Wilson, 1975; Hamdan and Alsharhan, 1991). Monopleurids and requienids predominate in the shelf lagoonal setting, whereas caprinids and caprotinids are dominant in the barrier setting (Hamdan and Alsharhan, 1991). In addition, the shells of caprinids and caprotinids are formed from aragonite, whereas monopleurid shells are made of calcite (Borgomano, 1991). The presence of cemented collapse breccias in this interval indicates that they were formed by the collapse of some voids formed due to dissolution by undersaturated diagenetic fluids at the surface or subsequent to burial. Cementation of the breccias indicates that these are late cements introduced subsequent to mechanical compaction at depth.

Interval VI.- The allochemical constituents, sedimentological signatures and petrographic textures of this interval are indicative of deposition on the shallow shelf mentioned above. The presence of green algae and abundant wackestones indicate restricted circulation conditions.

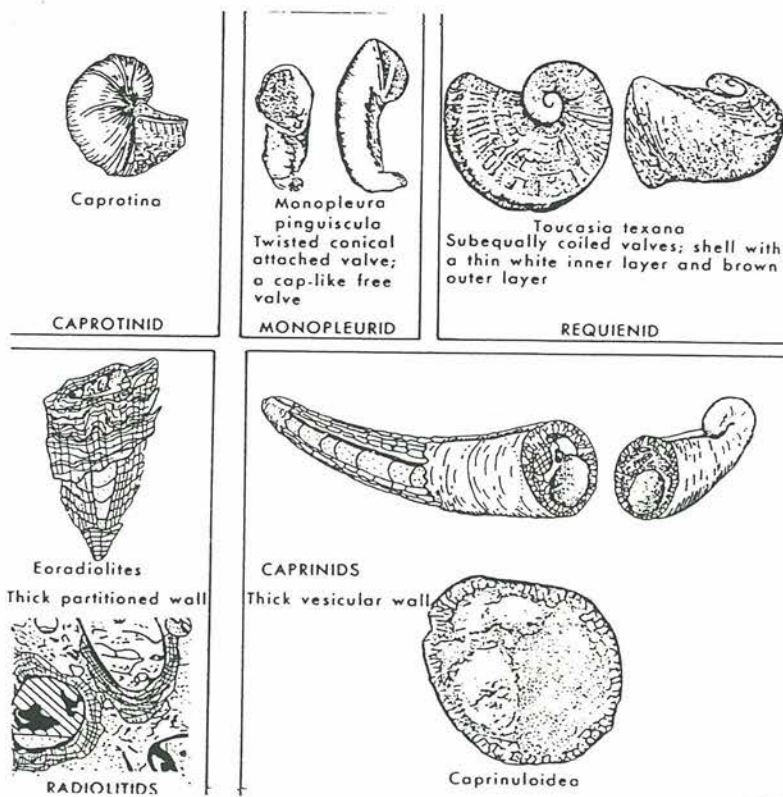


Figure 33. Major types of Cretaceous rudist bivalves (after Wilson, 1975).

Interval VII.- This interval is thin, only 25 cm thick, and is abundant in rudists and rudist fragments. Therefore, it might represent a storm bed that was deposited during a major storm event which transported large amounts of rudists and rudist fragments from the buildup to the protected shelf. More evidence for rudist transportation comes from the fact that their shells are found to be broken and not in growth position (Hamdan and Alsharhan, 1991).

Interval VIII.- This interval represents the same depositional conditions as the sixth interval. These two intervals were interrupted by the storm event which led to the deposition of the seventh interval.

Interval IX .- Since green algae thrive in a calm shelf setting within the photic zone (Scoffin, 1987), and since there are only few rudist fragments present in this interval, the development of these algal boundstones indicates deposition in a shallow shelf setting with restricted water circulation.

Interval X.- The presence of algal nodules rather than algal layers and the presence of some rudists and rudist fragments in this interval indicates that the energy conditions here are slightly greater than the previous interval.

Interval XI.- This interval is similar to the ninth interval and represents the same depositional conditions.

Interval XII.- This interval is analogous to the tenth interval. Therefore, it is obvious that algal boundstone intervals, such as the ninth and the eleventh intervals, are alternating with wackestone and packstone intervals, such as the tenth and the twelfth intervals. This

likely indicates slight fluctuations in depositional energy level on the shelf on which deposition occurred.

Interval XIII.- This interval represents another thin storm bed, which was deposited by transporting large amounts of rudists and rudist fragments in a short period of time. The extensive cementation which is observed in this interval is due to the presence of abundant rudists, which increases its potential to later leaching and cementation.

Interval XIV.- This interval, which is similar to the twelfth interval, represents deposition under normal conditions on the shelf after the interruption by the storm event responsible for the deposition of the last interval. The presence of calcite spar cementing broken rudist micrite envelopes indicates that the rudist fragments were leached early in the diagenetic history of the rock prior to later mechanical compaction and cementation.

Interval XV.- The presence of alternating, thin rudist-rich beds with wackestone beds within this interval suggests that the rudist-rich beds are storm beds. The occurrence of recrystallized and brecciated rudist fragments, which are outlined by micritic envelopes, indicate that compaction of these rudists was followed by a recrystallization event.

Interval XVI.- The presence of abundant solution seams in this interval, marked by very fine-grained insoluble residue, indicates that there has been volume loss due to chemical compaction.

Interval XVII.- This interval represents a rudist mound that was established on a preexisting high on the shelf. This rudist boundstone is over a meter and a half thick, with rudists in erect or recumbent growth positions. Preservation of most of the rudists

indicates that they are monopleurids, which have an original calcite mineralogy (Borgomano, 1991).

Interval XIII.- This interval represents return to typical shallow-water shelfal deposition, demonstrated by the presence of algae, *Orbitulina* small forams and rudist fragments in a peloidal to micritic matrix.

Interval XIX.- This interval either represent another storm bed or a rudist bioherm. Some of the rudists appear to be in growth position. This rudist mound or bioherm might have developed on a preexisting high on the shelf.

Interval XX.- The typical shelfal deposits of this interval are separated from the biohermal facies of the last interval by a sharp contact. This contact might be a hardground indicating a period of non-deposition, which was followed by relative deepening of the water during which the deposition of this interval occurred.

Interval XXI.- This interval is a meter thick and is analogous to the nineteenth interval, representing a rudist mound or bioherm. The increasing presence of such bioherms in the shelf setting shows a trend of increasing proximity to the buildup at the shelf edge, and an increase in more favorable water circulation. The abundance of rudists is increasing, as is their occurrence in growth position. The occurrence of some leached out rudist molds, which are only partially cemented by calcite, indicates that hydrocarbons migrated into these macropores, preventing total occlusion of the porosity by calcite cementation.

Interval XXII.- This interval represents a typical shallow water shelfal facies that was interrupted by thin rudist storm beds. The relation between macroporosity and the abundance of rudists is demonstrated by the lower percentage of both rudists and

macroporosity relative to the previous interval. However, these storm beds still show some leaching of the rudists which supports the assumption that macroporosity is controlled by the presence of rudists.

Interval XXIII.- This represents another example of a rudist bioherm that developed in the shelf setting. Biohermal sediments are enclosed within wackestone intervals above and below, which represent adjacent inter-mound deposition.

Interval XXIV.- This interval interrupts the overall upward trend to more open-water circulation conditions. Sediments here may represent return to shallow, restricted shelf conditions. Alternatively, these sediments may merely represent inter-mound deposits. In either case, the complexity of the facies mosaic present on the Shuaiba shelf at Ghaba North is clearly demonstrated.

Interval XXV.- This interval is another example of the complexity of the depositional setting because it is dominated by green algae which thrive in shallow water with restricted to partially restricted circulation. The algal boundstone of this interval, in addition to the hardground at the top, may have provided a substrate for the development of the rudist bioherm of the next interval. The presence of partially cemented intraparticle algal pores supports the assumption that hydrocarbons migrated early enough to prevent total occlusion of the porosity.

Interval XXVI.- The hardground which caps the previous interval acted as a stable substrate for the development of the rudist bioherm facies of this interval. The bioherm is overlain by a subaerial exposure surface that likely led to the development of fresh water

diagenetic environment. This may be verified by stable isotopic analysis. This will be discussed in a later section.

Interval XXVII .- The sedimentology, allochemical constituents and petrographic textures are characteristic of a shallow-water protected shelfal environment. It lacks coarse-grained constituents and sedimentary structures such as layering. This interval may represent relatively deeper-water deposits laid down on top of the subaerial exposure following relative sea-level rise.

Interval XXVIII.- Following subaerial exposure and deposition of deeper-water facies of the previous interval, sedimentation returned to primarily rudist bioherm deposition. This interval represents good water circulation and relatively high-energy conditions.

Interval XXIX .- This rudist rudstone facies represents deposition on the flanks of the rudist bioherm of the pervious interval. The rudists are not in growth position and they appear as debris in the core. In addition, this interval contains less rudists than the previous one and it contains more algal nodules, forams and matrix. The rubbly nature of this interval is due to the sparse cementation of the matrix microporosity. This is due to early hydrocarbon migration into these micropores, ceasing the cementation process before complete occlusion of the porosity.

Interval XXX .- The rudist boundstone facies of this interval represents another rudist bioherm with very high macroporosity values due to the presence of abundant rudist molds.

Interval XXXI.- The occurrence of rudist bioherms alternating with wackestone and muddy facies within this interval is indicative of deposition on a shelf interior setting and

not at a shelf edge. The wackestone facies occurs as interbiohermal deposits in the shelf setting. Favorable reservoir properties and hydrocarbon staining are at a maximum here due to the presence of a regional unconformity at the top of the Shuaiba Formation. This unconformity was a subaerial exposure surface through which potential diagenetic fluids intruded the formation and caused leaching of the rudists and matrix stabilization.

Biofacies of the Shuaiba Formation in GN-23.- Reviewing the sedimentology and petrography of the Shuaiba Formation in GN-23 led to identification of three biofacies and two lithofacies. Each biofacies is characterized by specific types of allochems, but the boundaries between these biofacies are transitional and may display faunal mixing. These biofacies are as follows:-

1. Foram Biofacies: This biofacies is dominated by *Orbitulina* and small benthic forams, such as miliolids, uniserial and biserial forms, peneropolids, agglutinated and spiral forams. This biofacies is represented by the first interval in GN-23. The faunal assemblage is indicative of a restricted to partially restricted shallow-shelf setting. This biofacies lacks any rudists or rudist fragments, which are indicative of more energetic conditions. However, the presence of such a faunal assemblage in the foram biofacies requires that the environment be "healthy" and rich in nutrients.
2. Algae-Foram-Rudist Fragment Biofacies: This biofacies is characterized by abundant green algae (*Bacinella* and *Lithocodium*), *Orbitulina*, small forams and small-sized rudist fragments. In addition, there are a few scattered whole rudists in this biofacies. Skeletal debris of echinoderms and mollusks is common as well. The algae are either present as nodules or layers. This faunal assemblage is indicative of a restricted to partially restricted shallow-shelf setting. However, in this case, the presence of rudist fragments

indicates that water-circulation conditions are slightly better than the previous biofacies. This indicates that the depositional site on the shelf is closer to the shelf edge or the rudist buildups, due to the presence of transported rudist fragments.

3. Rudist-*Orbitulina* Biofacies: Domination of rudists is obvious and these are, in general, present in growth position. The benthic foram *Orbitulina* is abundant in this biofacies; however, small benthic forams are rare or absent. This biofacies is characterized by low percentages of algae and, if present, these are found as nodules only. This biofacies is indicative of a less restricted, much shallower shelf setting. It represents deposition in the proximity of the rudist buildups at the shelf edge or pre-existing high.

Lithofacies Of The Shuaiba Formation.- The two identified lithofacies of the Shuaiba Formation in GN-23 reflect the complexity of the depositional environment in the Ghaba North Field during the Aptian. The lithofacies are distinguished from each other in the core by certain properties depending on the facies mosaic they contain. The Shuaiba Formation in GN-23 can be described, in general, as shallow-water shelfal deposits; however, the lithofacies observed here differ in their biofacies, sedimentology, abundance of major allochemical constituents of the formation and reservoir characteristics. This is due to the depositional site that each lithofacies represents on the shelf. These lithofacies are as follows:

1. Inner Shelf Lithofacies: This lithofacies is represented by the foram biofacies and the algae-foram-rudist fragment biofacies. This lithofacies was deposited on the far side of the shelf, away from the shelf edge. Therefore, it is indicative of shallow waters but with partial restriction of circulation. It is represented in the Shuaiba Formation by the lower zone which starts from the bottom of the first interval and ends at the top of the

eighteenth interval, which occurs at 619.45 m. In general, this zone is dominated by algal boundstone facies alternating with packstones and wackestones, but this sequence is interrupted from time to time by some rudist-rich storm beds.

2. Outer Shelf Lithofacies: This lithofacies is represented by the rudist-*Orbitulina* biofacies. It was deposited in a site proximal to the shelf edge. Thus, the lithofacies is indicative of much shallower waters and more open circulation conditions than in the inner shelf lithofacies. This lithofacies is represented in the Shuaiba Formation by the upper zone which begins at the base of the nineteenth interval and ends at the top of the thirty-first interval, which is the top of the Shuaiba in GN-23 (596.00 m). In general, this zone is dominated by rudist boundstones, rudstones and minor rudist floatstones. Thus, it is formed by stacking rudist bioherms on top of each other and is interrupted by interbiohermal floatstone facies. Reservoir characteristics of the inner and outer shelf lithofacies will be discussed in a following section.

In conclusion, the Shuaiba Formation in GN-23 is represented by the inner shelf lithofacies, from the bottom of the core to a depth of about 619.45 m, which is indicative of a restricted shallow-shelf setting. This lithofacies is overlain by the outer shelf lithofacies, from a depth of 619.45 m to the top of the Shuaiba, which is indicative of a shallower, more open-shelf setting. Therefore, there is a trend of shallowing upward in this core which ends by a drop in sea-level and subaerial exposure at the time of the Middle Aptian which is represented now by the regional unconformity between the Shuaiba and the Nahr-Umr Formation (Harris et al., 1984).

Stratigraphic Variability and Relationships Among Allochemical Constituents

Following the review of results and observations obtained from plotting major allochemical constituents of the Shuaiba Formation versus depth, it is useful to interpret these plots and observe the relations among these allochemicals. This will enhance our understanding about the lower and upper zone characteristics. In addition, it will provide more evidence for the interpretation of the environment of deposition which was reviewed in the previous section. Reservoir characteristics of each zone will be recognized through observation of the relations between the allochemical constituents.

Rudists.- The lower and upper zones have both been deposited in the same general depositional setting, which is a shallow protected shelf. This is based on the results and observations obtained regarding the sedimentology of the Shuaiba Formation in GN-23. Nevertheless, each one of these two zones has different characteristics indicating different depositional conditions. The lower zone, for example, has a lower percentage of rudists (Fig. 12), indicating either a more restricted circulation condition on the shelf or deposition further away from the shelf edge. This has been shown in the discussion regarding the biofacies and the lithofacies in the Shuaiba. The few thin rudist-rich intervals within this zone were identified as storm beds that have been incorporated in this restricted setting due to storm events, which transported rudists and rudist fragments from the buildups at the shelf edge to this environment. The upper zone has a higher average rudist content and has more and thicker rudist-rich intervals. Upper zone deposition occurred in a more open environment (less restricted) and proximal to the rudist buildups. These rudist-rich intervals were identified as bioherms that developed in the shelf setting and were separated by interbiohermal sediments that are represented by

the thin rudist-poor intervals. Above a depth of 608.00 m in the core, the formation becomes highly enriched in rudists. This observation supports the general shallowing upward trend which was discussed in the previous section.

Algae.- The high abundance of the green algae in GN-23, identified as *Bacinella* and *Lithocodium* (Johnson, 1969), supports the interpretation of the depositional environment as a shallow, calm shelf setting. Green algae thrive in such a setting which provides protection and light for photosynthetic process. The trend observed in both zones (Fig. 13) indicates the occurrence of a cyclicity in algal abundance, which increases at the beginning and then decreases toward the top of each zone. This may represent of a gradual decrease in the energy of the environment followed by an increase toward the top. In general, the upper zone appears to be deposited in an open setting or proximal to the shelf edge with higher energy levels inferred from its lower average percentage of algae (Fig. 13) and higher average rudist content (Fig. 12). The cross-plot of rudists versus algae (Fig. 34) clearly shows the inverse relation between these allochems. This relation supports the observation made in the course of discussing the lithofacies present in GN-23.

Orbitulina and Other Allochems.- The cyclicity in abundance of these allochems versus depth is very obvious (Fig. 14). However, the trend in this case is opposite to the variability trend observed in the algal abundance in both the lower and upper zones of the Shuaiba (Fig. 13). The abundance of *Orbitulina* and other allochems increases gradually from the bottom and then decreases toward the top of each zone. The upper zone possesses a higher average percentage of these allochems. If higher abundance of these allochems is taken to be an indication of a more open, nutrient-rich environment, then the

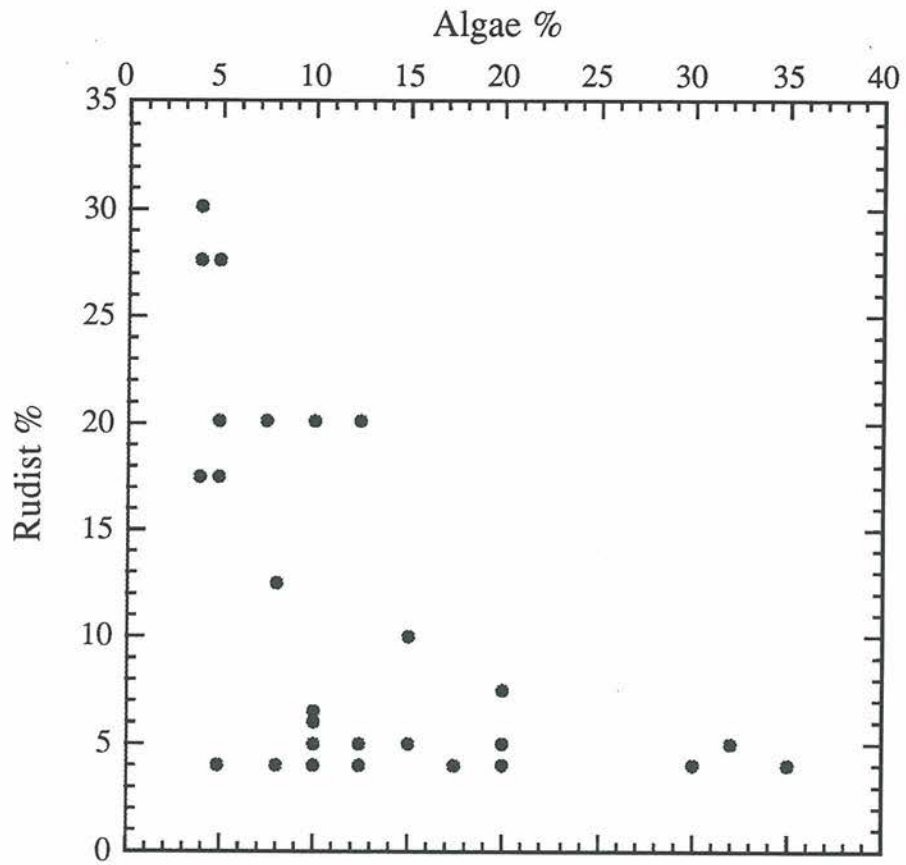


Figure 34. Cross-plot of rudist versus algal abundance in the Shuaiba Formation GN-23 core. See text for discussion.

circulation conditions during the deposition of the upper zone were better than the lower zone. This is consistent with the discussion regarding the depositional environment of the Shuaiba Formation in previous parts of this section.

Controls on Reservoir Properties

This section discusses and interprets the variability of reservoir properties in the Shuaiba Formation in GN-23. Reservoir characteristics of the lithofacies in the Shuaiba, which divide GN-23 into two zones, will be reviewed and interpreted in order to tie them to the depositional environment interpretation. Controls on these properties will be discussed in order to develop a useful strategy in exploitation of the Shuaiba formation in Ghaba North Field.

Reservoir Characteristics of the Lower and Upper Zones of the Shuaiba.- As discussed previously, the lower zone extends from the bottom of GN-23 core to a depth of about 619.45 m. This zone is represented by the section from the bottom of the first interval to the top of the eighteenth interval. It is dominated by the foram and the algae-foram-rudist fragment biofacies. It is represented by the inner shelf lithofacies. On the other hand, the upper zone extends from about 619.45 m to the top of the Shuaiba Formation in GN-23. This zone is represented by the section from the bottom of the nineteenth to the top of the thirty-first interval. It is dominated by the rudist-*Orbitulina* biofacies. It is represented by the outer-shelf lithofacies. Reviewing the variability plots of total measured porosity, macroporosity, microporosity, and horizontal permeability versus depth in Figures 15, 16, 17 and 19, respectively, it appears that the upper zone, in general, possesses the best

reservoir characteristics. The upper zone has higher averages of total measured porosity, macroporosity, microporosity and horizontal permeability. The causes for such observations will be evident when discussing the controls on these reservoir properties. It is important to notice that the upper zone, which is represented by the outer shelf lithofacies, contains less algae (Fig. 13), more rudists (Fig. 12) and more *Orbitulina* and other allochems (Fig. 14) than the upper zone. Variability of the allochemical constituents of the lower and upper zones has been discussed in the previous section. This variability is attributed to the depositional conditions that dominated during deposition of each zone. Obviously, sedimentology, allochemical constituents and biofacies forming the lithofacies of the Shuaiba Formation, which are dependent on the depositional conditions, play an important role in determining the quality of the reservoir. The Shuaiba Formation, in general, possesses very high total measured porosity (PDO, 1990). However, examining cores, plugs and thin sections of the Shuaiba it appears that macroporosity is very low in the lower zone and becomes higher in the upper zone. The cores and samples of the Shuaiba are dripping with oil from bottom of the cores to the top, with heavier hydrocarbon staining toward the top. Therefore, the majority of hydrocarbons in the Shuaiba have to be held in the microporosity, which accounts for the difference between total measured porosity and macroporosity. Microporosity of the formation was investigated in this study by the SEM.

The Shuaiba Formation has been described as a chalky limestone (Gallagher et al., 1990) due to its micritic texture. Chalky textured limestone petroleum reservoirs in the Mesozoic and Tertiary deposits of the Middle East are very common (Wilson, 1975). The chalky texture is due to abundant and disseminated microporosity existing within the micritic matrix of typical carbonate platform sediments (Moshier, 1989A). SEM

observations of broken sample surfaces from GN-23 (Fig. 29) reveal that the matrix of the Shuaiba Formation is composed of euhedral to subhedral micro-rhombic calcite spar. The microporosity appears to be an intercrystalline type porosity. Moshier (1989B) and Budd (1989) discussed the origin and reviewed the processes of formation of microporosity and micro-rhombic calcite matrix in the Shuaiba Formation and other Lower Cretaceous formations in the United Arab Emirates. Further discussion regarding the origin, nature and diagenesis of micro-rhombic calcite matrix and microporosity in GN-23 will be conducted in a separate section. The Shuaiba Formation in this core possesses high porosities, which are attributed to the microporosity of the micro-rhombic calcite matrix; however, there is an observed variability in this microporosity with depth in both zones of the Shuaiba (Fig. 17). This matter will be discussed in a following section. Development of secondary moldic porosity in the upper zone, due to the leaching of rudists and rudist fragments, enhanced the horizontal permeability of the matrix, thus increasing the reservoir quality and capacity to hold hydrocarbons. In addition to the role played by the depositional environment in determining reservoir properties, there is a diagenetic environment role which enhances these properties.

Controls on Microporosity.- The similarity between the plot of microporosity versus depth (Fig. 17) and the plot of total measured porosity versus depth (Fig. 15) and the presence of a positive linear relationship between the two properties (Fig. 35) are indicative of the responsibility of microporosity for the storage capacity of most of hydrocarbons in this reservoir. Variability of microporosity in the lower and the upper zones of the Shuaiba, which is observed in Figure 17, can be understood by correlating it to variability of allochemical constituents and by using cross-plots of allochemical constituents versus microporosity. Figure 17 shows that there is a trend observed in

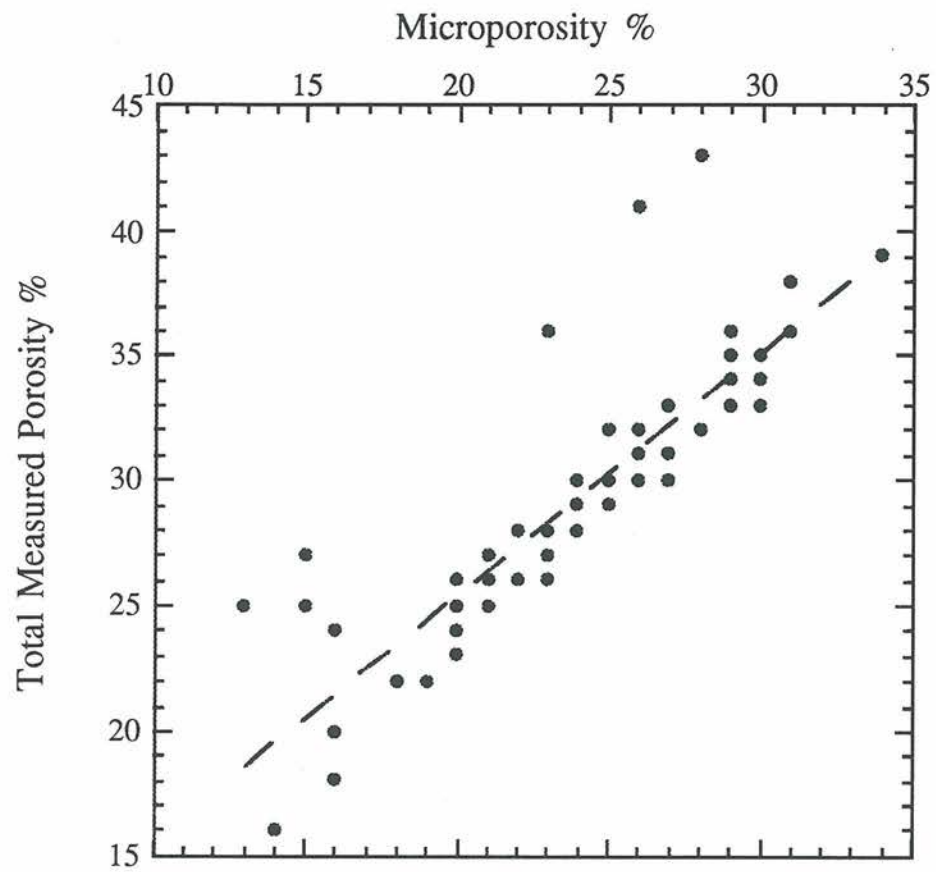


Figure 35. Cross-plot of total measured porosity versus microporosity in the Shuaiba Formation GN-23 core. Dashed line represents the overall trend.

microporosity in both zones. In this trend, microporosity decreases gradually from the base until the middle and then increases toward the top of each zone. The observed decrease in microporosity corresponds to a decrease in *Orbitulina* and other allochems (Fig. 14) and an increase in algal abundance (Fig. 13). The increase in microporosity toward the top of the zones, however, corresponds to an increase in *Orbitulina* and other allochems and a decrease in algal abundance. The positive correlation between microporosity and the abundance of *Orbitulina* and other allochems is further clarified in Figure 36, which shows a positive linear relationship between the two. On the other hand, the cross-plot of microporosity versus rudists abundance (Fig. 37) shows a negative linear relationship. Thus, in general, variability of microporosity in the Shuaiba Formation is correlated with the abundance of *Orbitulina* and other allochems. This is due to the presence of intraparticle microporosity in *Orbitulina* and small benthic forams, which increases microporosity percentages.

Further analysis of microporosity variability in the Shuaiba in GN-23 was done by choosing five samples for SEM investigation. These samples were chosen because they correspond to alternating intervals of high and low microporosity (Fig. 17). These samples and their properties are listed in Table 1.

SEM observations of these samples support the presence of microporosity as intercrystalline porosity within the micro-rhombic calcite matrix of the Shuaiba. These micro-rhombs of calcite reflect some limited dissolution due to their partially smoothed edges and corners. Sample #19, which corresponds to an extensively cemented rudstone interval, possesses relatively low microporosity due to the presence of a neomorphic

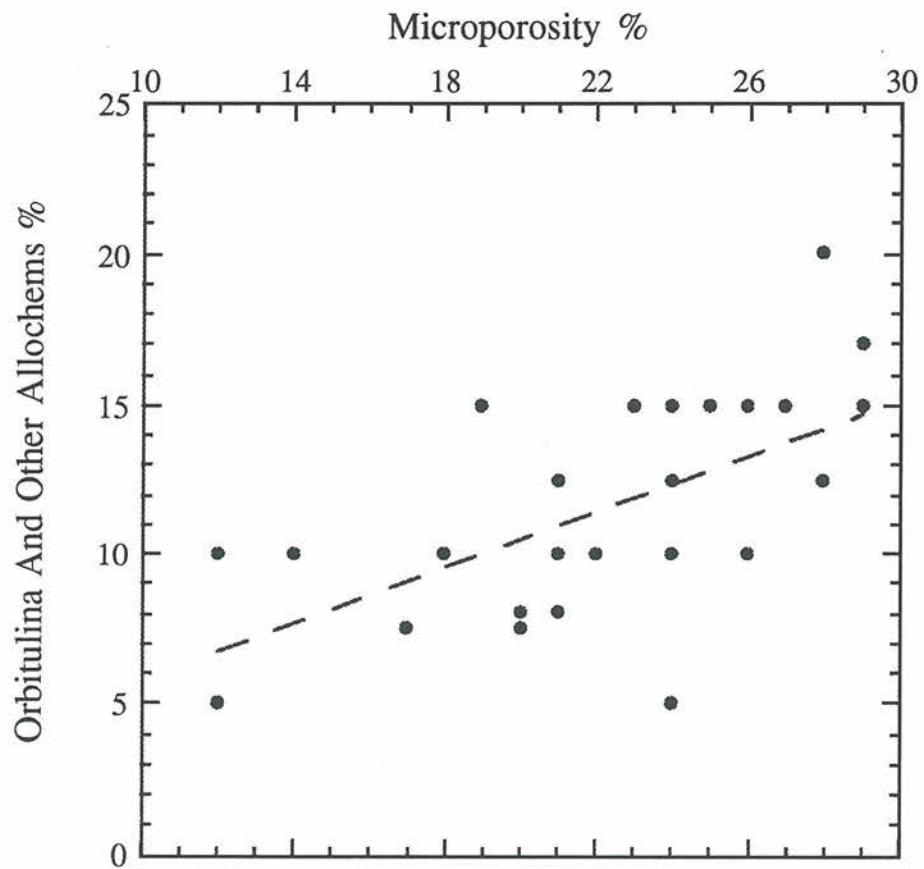


Figure 36. Cross-plot of *Orbitulina* plus other allochems abundance versus microporosity in the Shuaiba Formation GN-23 core. Dashed line is the overall trend.

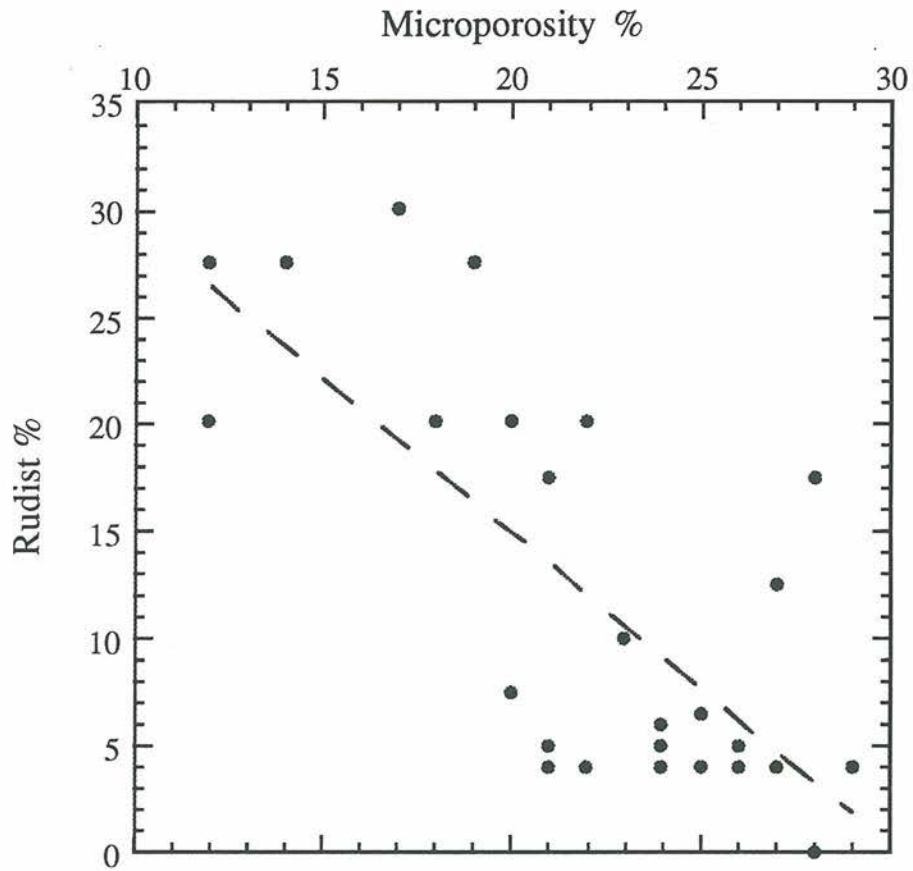


Figure 37. Cross-plot of rudist abundance versus microporosity in the Shuaiba Formation GN-23 core. Dashed line is the overall trend.

calcite microspar that heals microporosity of the matrix (Fig. 31). Sample #77 shows very high macroporosity but relatively low microporosity. This is due to the presence of

Table (1)

Depths and Reservoir Properties of the SEM Samples

Sample #	Depth (m)	Total Porosity	Macroporosity	Microporosity	Horizontal Perm.
2	643.66	33%	3%	30%	6.8 md
19	633.60	16%	2%	14%	1 md
47	618.49	35%	5%	30%	14 md
77	601.06	25%	12%	13%	43 md
81	598.83	41%	15%	26%	230 md

two types of textures in the matrix; a crystal mosaic texture and a blocky-crystal framework texture (Fig. 30 and 29, respectively). The former shows little microporosity, whereas the latter possesses high microporosity values. Further discussion regarding

origin and interpretations of microporosity and micro-rhombic calcite matrix will be conducted in the diagenesis section.

Controls On Macroporosity.- The fact that the upper zone possesses a higher average macroporosity than the lower zone (Fig. 16) is consistent with the higher rudist content in the upper zone than in the lower (Fig. 12). The relation between rudist abundance and macroporosity is very obvious in Figure 38, which shows a clear positive linear relationship between the two. On the other hand, the cross-plot of macroporosity versus algal abundance (Fig. 39) indicates, in general, that highest macroporosity values correspond to lower algal content in the formation. Therefore, it is obvious that the macroporosity is controlled primarily by rudist abundance in the Shuaiba Formation. Macroporosity of the Shuaiba is a secondary moldic porosity which developed due to leaching of rudists and rudist fragments by undersaturated diagenetic fluids. The upper zone possesses higher macroporosity than the lower zone and values of macroporosity increase toward the top of the upper zone. This is due to the presence of abundant rudists and rudist fragments of caprinid and caprotinid types rather than monopleurid rudists. Because caprinid and caprotinid rudists have aragonitic rather than calcitic original mineralogy, it takes a longer period of time to stabilize these rudists to low-Mg calcite (LMC) in the diagenetic environment (Borgomano, 1991). Therefore, leaching of these rudists is much easier than rudists which stabilize to LMC at a faster rate. The upper zone is capped by a regional unconformity, separating the Shuaiba Formation from the Nahr-Umr Shales (Harris et al., 1984), which acted as a subaerial exposure surface from which potential diagenetic fluids invaded the Shuaiba. Thus, the lower zone possesses

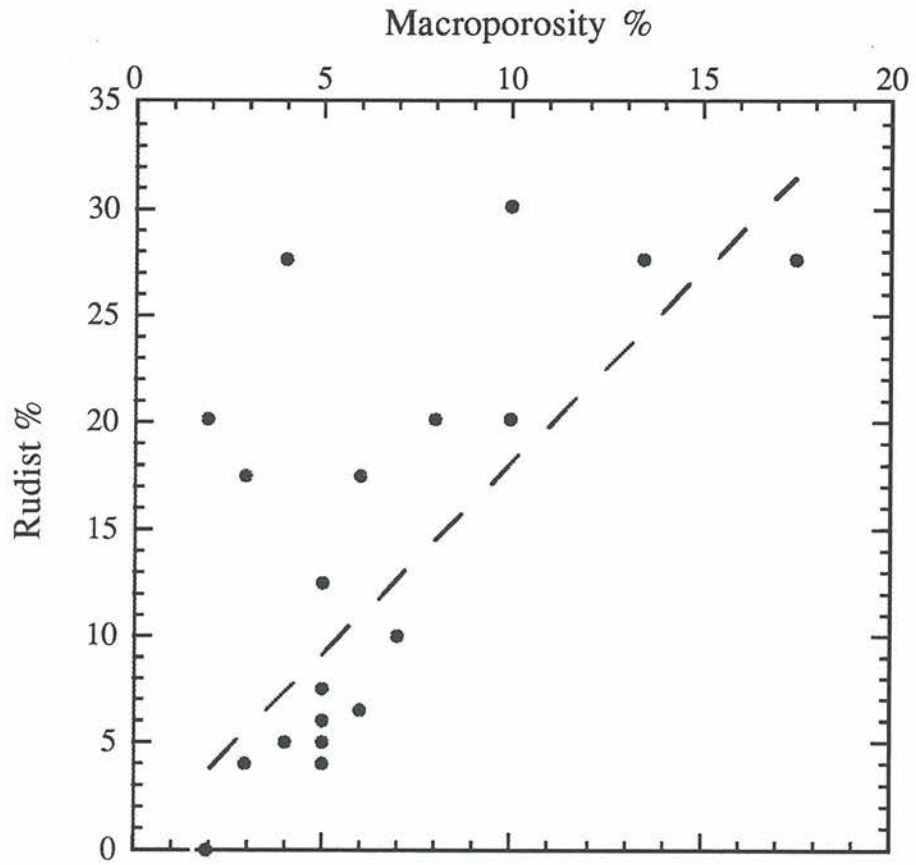


Figure 38. Cross-plot of rudist abundance versus macroporosity in the Shuaiba Formation GN-23 core. Dashed line is the overall trend.

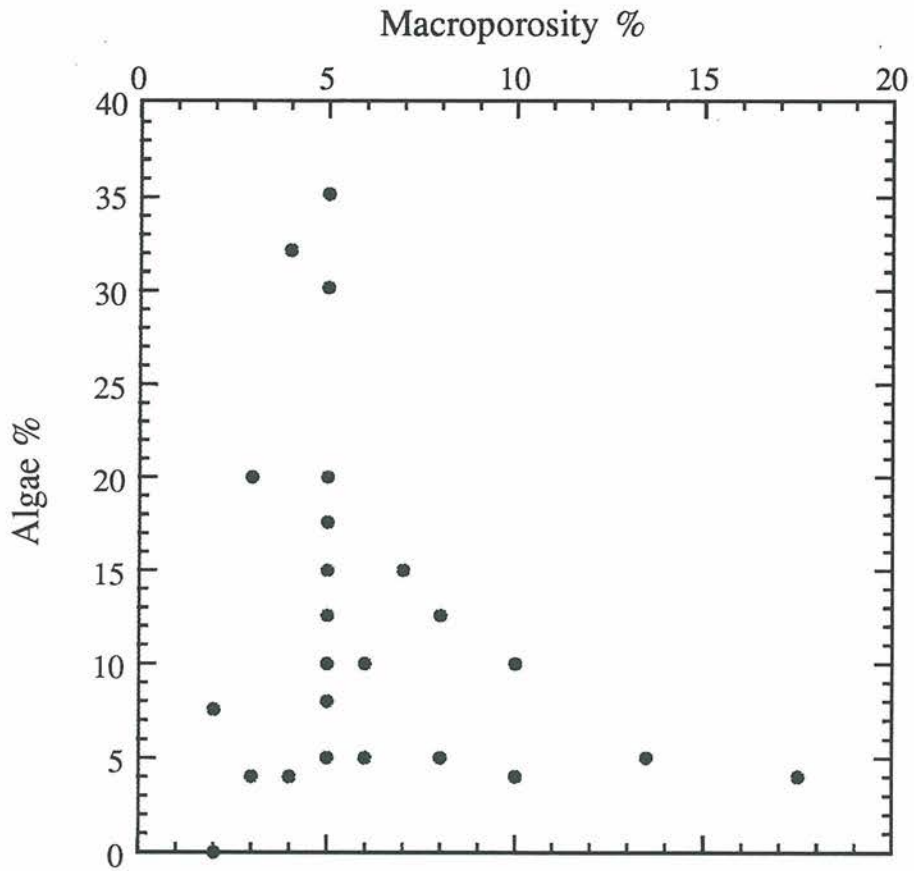


Figure 39. Cross-plot of algal abundance versus macroporosity in the Shuaiba Formation GN-23 core. See text for discussion.

lower macroporosity values because it either contained less amounts of rudists and less amounts of favorable rudists for leaching, or it was far from the reach of undersaturated meteoric fluids which caused leaching of rudists in the upper zone.

Controls On Horizontal Permeability.- Examination of the plot of horizontal permeability versus depth (Fig. 18) gives an obvious impression that the Shuaiba Formation, in general, possesses low permeability values. This is due to the micritic nature of the formation, which is consistent with deposition on a protected shelf. However, when considering the plot with horizontal permeability values of above 35 md removed (Fig. 19), it becomes clear that this plot is analogous to the plot of macroporosity versus depth (Fig. 16). Higher permeability values in the upper zone and the increase in these values toward the top of the zone correspond to the increase in macroporosity and effective porosity, defined as the inter-connected pores. This has to do with leaching of rudists and rudist fragments, where leaching of rudists creates moldic porosity and leaching of rudist fragments and micro-debris of allochems enhances the connectivity of the pore system (Borgomano, 1991). The relationship between rudist abundance, macroporosity and horizontal permeability is clear because there is a general trend of increasing the permeability with increasing rudist abundance and macroporosity observed in Figures 40 and 28, respectively. The increase in rudists abundance also means an increase in the amount of coarse-grained constituents of the formation at the expense of fine-grained materials, thus enhancing the permeability of the matrix. Anomolously high values of horizontal permeability are observed near the top of the formation in Figure 18. This is due to the presence of open fractures. In general, the increase in microporosity and total measured porosity causes an increase in horizontal permeability as observed in Figures 41 and 42, respectively. This is because the increase

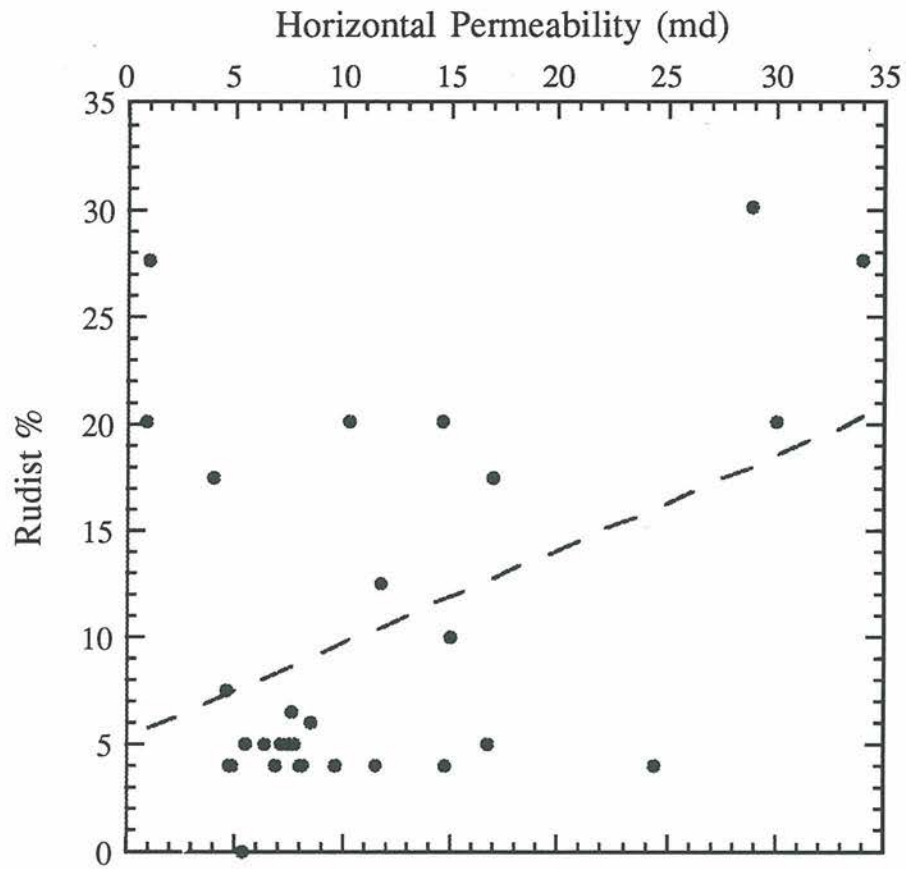


Figure 40. Cross-plot of rudist abundance versus horizontal permeability in the Shuaiba Formation GN-23 core. Dashed line is the overall trend.

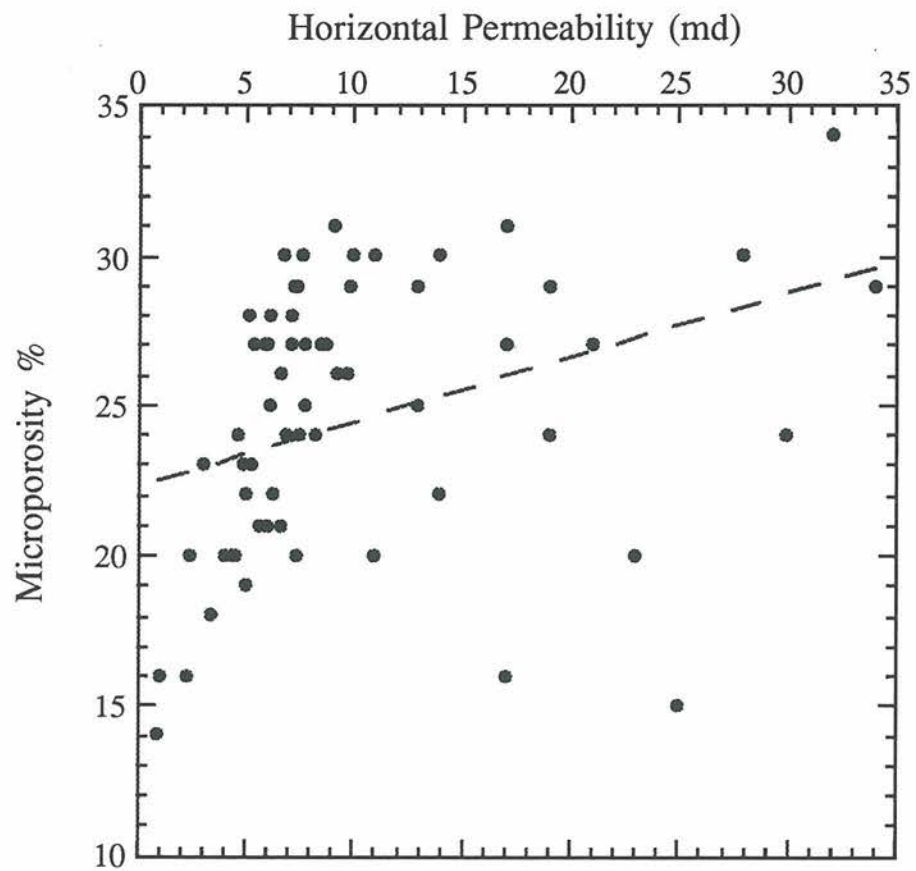


Figure 41. Cross-plot of microporosity versus horizontal permeability in the Shuaiba Formation GN-23 core. Dashed line is the overall trend.

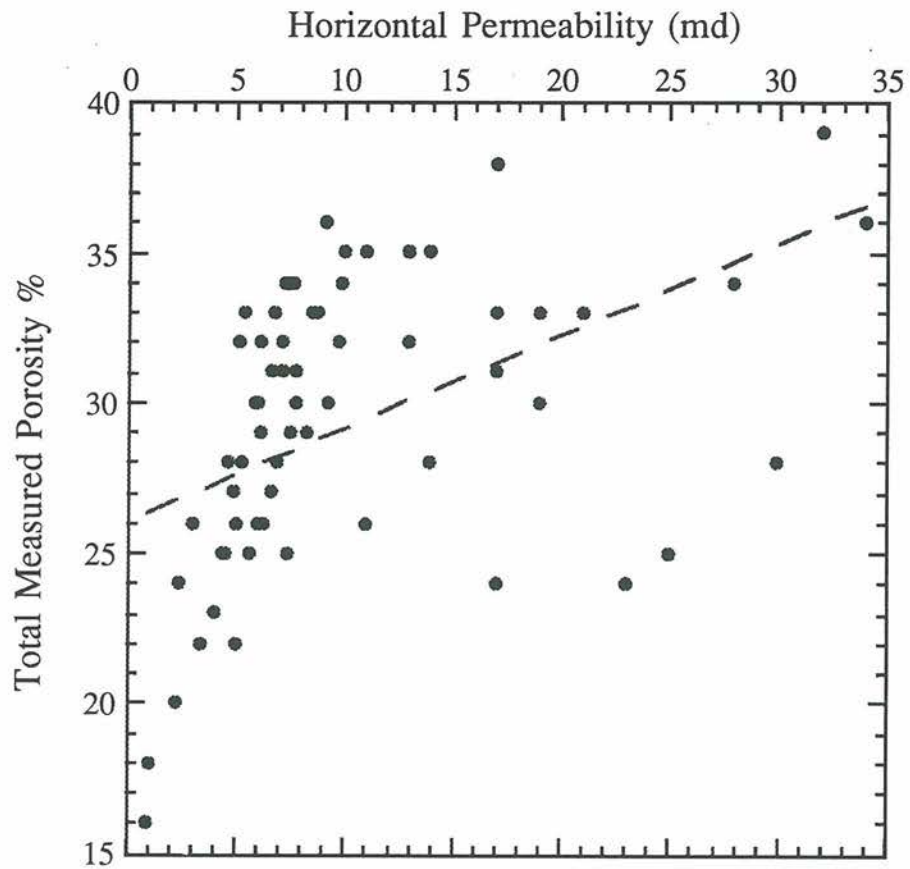


Figure 42. Cross-plot of total measured porosity versus horizontal permeability in the Shuaiba Formation GN-23 core. Dashed line is the overall trend.

in microporosity means enhancement of the matrix pore system, and thus the permeability.

Diagenesis of the Shuaiba Formation in GN-23

Origin of diagenetic features observed in the Shuaiba GN-23 core will be discussed in this section. Moreover, the relation of these features to each other will be reviewed in order to obtain a whole-picture understanding of diagenesis in the formation. Stable isotopic data will be reviewed in a stratigraphic context. Finally, the diagenetic history of the Shuaiba and its control on the evolution of reservoir properties will be presented by combining the stable carbon and oxygen isotopic data with the implication of diagenetic features on the history of the formation.

Diagenetic Features of the Shuaiba in GN-23

Conditions which led to the development of diagenetic features of the Shuaiba will be discussed herein. These conditions will be inferred from occurrence and characteristics of diagenetic features. Relative timing of development of these features will then be obtained.

Cements in the Shuaiba Formation.- Paucity in cementation in the Shuaiba Formation is obvious from the core, plugs and thin sections. This is due to the nature of sediments deposited in Ghaba North area during the Aptian. Due to deposition in a shelfal lagoon behind a barrier which rimmed an intrashelf basin, or as localized rudist buildups on a

paleohigh, the Shuaiba is characterized by wackestone and micritic nature. Therefore, there was little interparticle macro-pore spaces to start with. The presence of rubbly intervals in the core is indicative of the paucity of cementation. Cementation, although not abundant, occurs as fine-crystalline and coarse-crystalline calcite cements. These two types differ in their nature and occurrence. The fine-crystalline calcite cement fill small inter- and intraparticle porosity which is, in general, primary in nature. These are intraparticle pores of algae and forams, as well as shelters and borings. These cements are formed of subhedral to euhedral crystals and show a trend of increasing crystal size toward the center of the pores. This might indicate that these pores were empty or were cemented by marine cements originally (HMC and aragonite) and then were stabilized to LMC and/or cemented by LMC in a meteoric diagenetic realm early in the formation history. This is inferred because there are no cross-cutting relationships with compaction features, such as broken fragments or spalled micrite envelopes, in these cements. The presence of microfractures, which cut through allochems and are cemented by a fine-crystalline calcite cement, indicates that these are of a different generation and were precipitated in the fractures during later event after the formation of microfractures.

The coarse-crystalline calcite cements occur primarily in secondary moldic porosity or primary macroporosity such as rudist internal pore spaces. These cements are generally equant-blocky, subhedral to euhedral, and show a trend of increasing crystal size toward the center of the pores. The presence of broken fragments of rudists, spalled micrite envelopes and brecciated fragments of matrix floating within these cements indicates that these are late cements. Higher abundance of these cements occurs below 619.45 m and corresponds to rudist-rich intervals.

Other Diagenetic Features.- Other diagenetic features present in the Shuaiba include hardgrounds and solution seams on the macro-scale, and micrite envelopes, calcite overgrowths, calcite microspar, and replacement, recrystallization and neomorphism of rudists and rudist fragments on the micro-scale.

Micrite envelopes outlining rudists and rudist fragments are very abundant in the Shuaiba Formation. These form by endolithic algae and fungi which scavenge the shells and fragments of allochems and work from the outside inward. This process mostly occur on the seafloor and results in the formation of very fine bores and tubes in these shells and fragments which then become filled by very fine micritic materials from the surrounding environment (James and Choquette, 1983). Later, when sediments undergo stabilization from metastable mineralogy (HMC and aragonite) to stable mineralogy (LMC), these rims of micrites possess abundant nucleation sites, thus allowing them to stabilize faster than the rest of the shell or fragments. Thus, exposing the sediment to undersaturated solutions with respect to metastable mineralogy before completion of the stabilization process causes leaching of metastable shell or fragment leaving behind stable micrite envelopes surrounding moldic porosity. In some cases, these molds become cemented by other saturated solutions in a later event. In other scenarios, micrite envelopes surround replaced and recrystallized or neomorphosed (when the process cannot be identified as replacement or recrystallization) shells and fragments. Formation of these micrite envelopes probably occurred early in the diagenetic history of the sediments. Thus, presence of broken micrite envelopes floating in a cement indicates that cement is late in timing, and was at least precipitated after compaction under a considerable depth.

Calcite overgrowths are abundant on echinoid plates in the Shuaiba. These were either developed in a phreatic diagenetic realm or in a late, relatively deep, diagenetic event.

The presence of a peloidal matrix accompanied by neomorphic calcite microspar in interpeloidal pore spaces is common in GN-23 core. This leads to reduction of total measured porosity due to reduction of microporosity. This microspar forms as a result of compaction and diagenesis of the initial muddy materials which occurred originally in interpeloidal pore spaces (Moshier, 1989A; his Fig. 11). Textural changes of the initial unconsolidated muds, by changing porosity and crystal size, leads to development of micrite ($< 4 \mu\text{m}$) or microspar crystals ($4 - 20 \mu\text{m}$). Coalescive aggrading neomorphism could also transform micrite to microspar (Moshier, 1989A). Therefore, this neomorphic calcite microspar is a normal product of compaction and overburden pressure effects on muddy materials, which were deposited within these interpeloidal pore spaces.

Abundant hardgrounds occur throughout the Shuaiba GN-23 core. These hardgrounds are an early diagenetic feature. Hardgrounds form on the seafloor by precipitation of marine cements into pores of the sediment (James and Choquette, 1983). In the Shuaiba, hardgrounds were developed mostly by marine cementation of intraparticle pores in algal-rich facies, thus developing a substrate for the establishment of rudist-rich facies. Presence of abundant hardgrounds is indicative of active marine diagenetic realms, which precipitate cements during periods of low depositional rates and breaks in sedimentation (Hartmans, 1986). These hardgrounds might act as barriers to vertical flow pathways if they were not fractured, thus compartmentalizing the reservoir.

The presence of solution seams is indicative of late burial diagenesis. In addition, it indicates that there has been a considerable shortening of the formation due to the chemical compaction processes. Solution seams can act as conduits for diagenetic solutions and pathways for hydrocarbon migration (Choquette and James, 1987).

Rudist Leaching and Macroporosity Development.- Rudists, as mentioned earlier, are a major constituent of the Shuaiba and are represented by different taxa with different original mineralogies (Fig. 33). Rudists and rudist fragments which have HMC original mineralogy (such as monopleurids) are more easily and rapidly stabilized to LMC than rudists with aragonitic original mineralogy (caprinids and caprotinids) (Borgomano, 1991). Aragonitic rudists are more subjected to dissolution rather than stabilization. Saturation with respect to LMC is attained much faster in sediments containing mixed stabilized and unstabilized constituents due to higher solubilities of metastable mineralogies relative to LMC. This mechanism is fabric-selective and is termed "mineral controlled alteration" which acts in low activity phreatic realms (low water/rock ratio) (James and Choquette, 1984). However, if the phreatic realm was very active or all the constituents of the sediment were already stabilized, then alteration of the sediment will occur depending on the nature of the fluid (saturated or undersaturated). This process is non-fabric selective and is termed "water controlled alteration". Leaching here might occur if there were large volumes of undersaturated fluids flowing through the sediment (high water/rock ratio) (James and Choquette, 1984). This process then proceeds in the sediment depending on saturation state, flow rates, porosity, permeability and grain size. Rudists and rudist fragments in rudist-rich or poor intervals below 619.45 m boundary, which separates the lower zone from the upper zone in the Shuaiba GN-23 and coincides with a hardground, are preserved and extensively cemented. Above 619.45 m only some

are preserved and the majority show development of moldic porosity, which increases in abundance with proximity to the subaerial exposure surface at 609.45 m and the regional unconformity at the top of the Shuaiba. Therefore, this indicates that there was more than one diagenetic event that affected the sediments of the Shuaiba Formation at this locality. This will be discussed later when interpreting the isotopic data.

Development of the Micro-Rhombic Calcite Matrix and Microporosity.- Development of the micro-rhombic calcite matrix in the Shuaiba is a very important event because intercrystalline microporosity of this matrix is responsible for most of hydrocarbons storage capacity in the reservoir. This micro-rhombic calcite has previously been identified in the Shuaiba formation in the United Arab Emirates by Moshier (1989B) and Budd (1989). A majority of lime mud accumulating in modern shallow-platform settings is formed from post-mortem disintegration of calcareous green algae, and bioerosion and abrasion of skeletal debris (Moshier, 1989A). It has been found that the production of aragonite needles from algae is sufficient to account for mud abundance in the Bight of Abaco, Bahamas (Neumann and Land, 1975). Moreover, Wells and Illing (1964) have studied the whittings phenomena in the Persian Gulf and have indicated the importance of spontaneous inorganic marine precipitation of lime mud particles. The nature of the micro-rhombs, regarding their crystal habit and the fact that they are not original sedimentary particles and are made of separate crystals, is indicative that these micro-rhombs and microporosity were formed by a process related to dissolution and reprecipitation of CaCO_3 (Budd, 1989). Therefore, calcite rhombohedrons are the products of stabilization of original metastable lime mud accumulated in this setting. However, the diagenetic environment in which stabilization occurred has been debated by Moshier (1989B) and Budd (1989). Based on geochemical data, Moshier (1989B)

suggested that microporosity of the Shuaiba and other Lower Cretaceous formations in the United Arab Emirates formed by stabilization in a closed-system of marine pore waters. On the other hand, Budd (1989) argued for the development of micro-rhombic calcite by meteoric fluids through a two-step process involving subaerial exposure and at shallow burial diagenesis. In this study, the diagenetic environment of micro-rhombic calcite matrix development in the Shuaiba at Ghaba North will be interpreted using isotopic, petrographic and stratigraphic data. This discussion will be conducted later. The blocky-crystal framework texture and the crystal mosaic texture of the matrix have been discussed by Moshier (1989A, B). In general, blocky-crystal framework texture possesses higher microporosity and permeability, whereas crystal mosaic texture possesses lower values of both. Moreover, dissolution along crystal boundaries creates secondary intercrystalline microporosity and enhances permeability due to enlargement of interconnected porethroats (Moshier, 1989A). The development of framework texture versus mosaic texture was also discussed by Moshier (1989A; his Figure 11). He suggested that a framework texture developed by stabilization of wet, unconsolidated lime muds. Additional cementation and compaction of crystals of the framework resulted in formation of the mosaic texture with less microporosity. In addition, he suggested that framework texture forms in low water/rock ratio systems, whereas crystal mosaic texture forms in a high water/rock ratio (open) system. His argument was that open systems will introduce excess carbonate for thorough cementation. However, this is not always the case because in some cases these open systems transport carbonate out of the system rather than delivering it in.

Stable Carbon and Oxygen Isotopic Analysis

Figure 32 is a cross-plot of $\delta^{13}\text{C}$ and $\delta^{18}\text{O}$ (‰ PDB) of both the matrix and late coarse-crystalline calcite cements. Apart from late cement sample #49, which has a $\delta^{13}\text{C}$ of +9.73 and a $\delta^{18}\text{O}$ of -6.19 (‰ PDB), all other samples fall within the ranges of +3.11 to +5.95 $\delta^{13}\text{C}$ and -8.25 to -4.1 $\delta^{18}\text{O}$ (‰ PDB). Enriched (positive) $\delta^{13}\text{C}$ values are indicative of a rock-buffered carbon isotopic composition. Depleted (negative) $\delta^{18}\text{O}$ values are indicative of alteration by meteoric waters. These data could be interpreted in different ways. For instance, Moshier (1989B) interpreted the $\delta^{13}\text{C}$ range of +3.4 to +4‰ and the $\delta^{18}\text{O}$ range of -4 to -5‰ of the micro-rhombic calcite matrix of the Shuaiba in the Saja Field in the United Arab Emirates, as indicative of stabilization of matrix in a closed system with marine pore-waters. Because a range of -2 to -2.5‰ PDB was reported for $\delta^{18}\text{O}$ of Aptian marine calcite (Scholle and Arthur, 1980; Moldovanyi and Lohmann, 1984), he suggested that the more depleted $\delta^{18}\text{O}$ values of his are the result of dissolution/precipitation through a process of replacement of original matrix materials during diagenesis. Thus, Moshier (1989B) suggested that the Shuaiba matrix was depleted by 1.5 to 2‰ relative to its precursor marine sediment. On the other hand, Budd (1989) interpreted the $\delta^{13}\text{C}$ range of micro-rhombic calcite matrix of +3.1 to 4.5‰ PDB to be primary and unaltered by diagenesis. However, the $\delta^{18}\text{O}$ range of -4.5 to -6‰ PDB was interpreted by Budd as a reflection of alteration by meteoric waters. Therefore, one could interpret the $\delta^{13}\text{C}$ and $\delta^{18}\text{O}$ data of the Shuaiba matrix in Ghaba North Field as indicative of stabilization in a system with marine pore-water composition. Moreover, it can be seen that there is a covariance between $\delta^{13}\text{C}$ and $\delta^{18}\text{O}$ in Figures 43 and 44, where, in general, $\delta^{13}\text{C}$ and $\delta^{18}\text{O}$ become more depleted with depth. Thus, it can be argued that this depletion is a result of temperature fractionation of the isotopes with

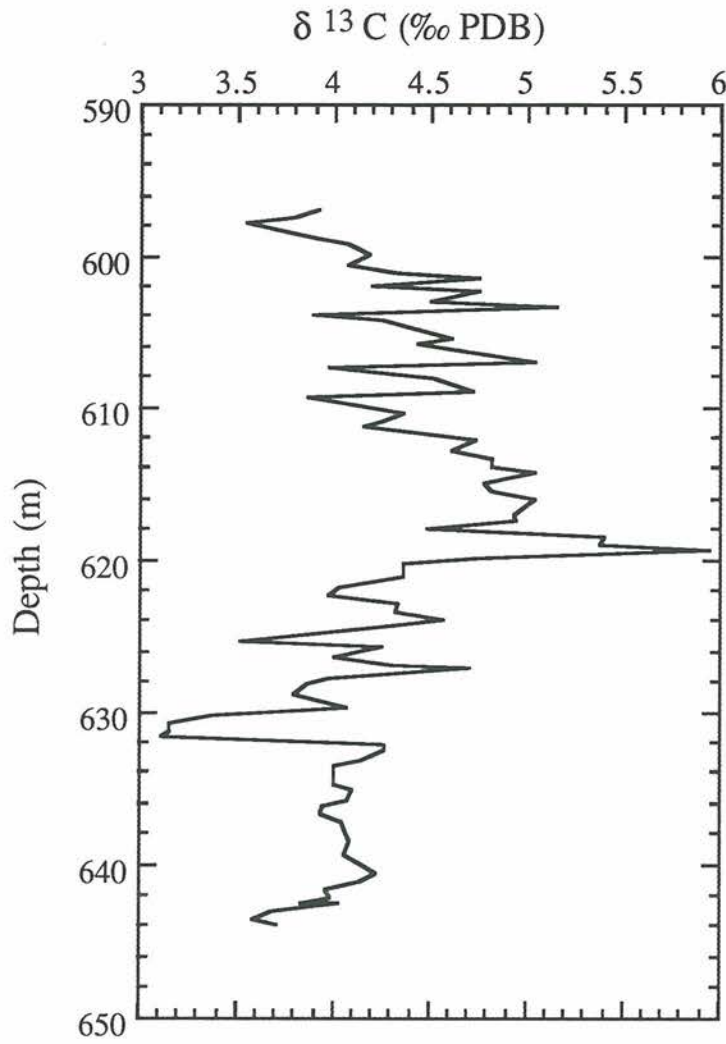


Figure 43. Variation of the Shuaiba matrix $\delta^{13}C$ values with depth in GN-23 core. See text for discussion.

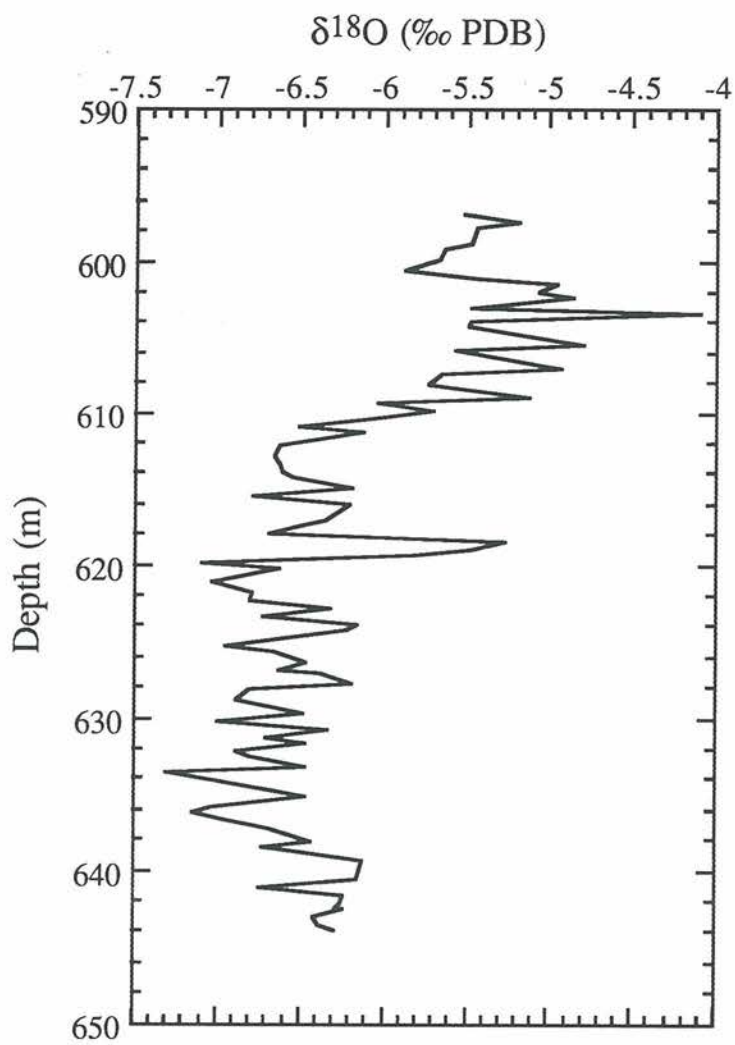


Figure 44. Variation of the Shuaiba matrix $\delta^{18}\text{O}$ values with depth in GN-23 core. See text for discussion.

depth and time. However, a more realistic interpretation of this data could be developed if petrographic and stratigraphic evidence was incorporated, along with stable isotopic data, in this interpretation. First of all, unlike the case with Moshier (1989B), there is ample evidence for subaerial exposure and communication with meteoric waters in GN-23 in Ghaba North Field. In fact, there are two surfaces of potential importance for this argument; the subaerial exposure surface observed at 609.45 m and the regional unconformity at the top of the Shuaiba. Other evidence come from extensive leaching beneath these surfaces and from the texture of calcite cements observed in the formation.

A close look at Figure 32 indicates that micro-rhombic calcite matrix isotopic data can be separated into two groups rather than one. These are the samples with $\delta^{18}\text{O}$ values more depleted than -6‰ PDB and the samples with $\delta^{18}\text{O}$ more enriched than -6‰ PDB. These data likely suggest that the calcite rhombohedra developed in more than one event. If this is the case, it explains the spread in the $\delta^{18}\text{O}$ values of the Shuaiba and the narrower range observed in the $\delta^{13}\text{C}$ values. Thus, it explains the deviation of data from the pattern suggested by Allan and Matthews (1977; 1982) for the variation expected in the carbon and oxygen isotopic compositions of limestones during fresh water diagenesis. This pattern suggests that there should be a narrower range of $\delta^{18}\text{O}$ and a wider range of $\delta^{13}\text{C}$ values. This is because water possesses a large reservoir for oxygen relative to the rock (Lohmann, 1988). Thus, most of the oxygen incorporated in a diagenetic product will be sourced from water. On the other hand, carbon reflects a combination of sources, such as soil-gas CO_2 , precursor CaCO_3 , and atmospheric CO_2 . Thus, $\delta^{13}\text{C}$ reflects water-rock interaction and proximity to the soil zone and therefore varies with depth (Allan and Matthews, 1982; Lohmann, 1988). However, if there were more than one

diagenetic event affecting the sediments, then this pattern should not hold, because it will depend on the isotopic composition of the two different waters involved.

Variations of $\delta^{13}\text{C}$ and $\delta^{18}\text{O}$ with depth in the Shuaiba (Fig. 43 and 44) should be used together and in concordance with petrographic and stratigraphic observations. The two plots could be divided into three zones with different isotopic characteristics. The first zone starts from the bottom to a depth of 619.45 m. The second zone begins at 619.45 m and ends at 609.45 m. The third zone starts at 609.45 m and ends at the top of the Shuaiba at 596 m. Each one of these diagenetic zones will be discussed below.

Diagenetic Zone I.- Using the fundamentals of $\delta^{13}\text{C}$ and $\delta^{18}\text{O}$ data interpretation as stated in Allan and Matthews (1977; 1982) and Lohmann (1988), the Shuaiba isotopic data can be used to interpret the diagenetic environments that affected the formation. Variation of $\delta^{18}\text{O}$ values over the Shuaiba (Fig. 44) is indicative of more than one diagenetic event. This is because the $\delta^{18}\text{O}$ value should be relatively invariant if it reflects a single diagenetic event (Allan and Matthews, 1982). Thus, the first zone, which extends from the bottom of GN-23 core to a depth of 619.45 m, is distinguished from the rest of the Shuaiba by its nearly invariant $\delta^{18}\text{O}$ and $\delta^{13}\text{C}$ values. Interestingly, the 619.45 m boundary was also recognized as the stratigraphic boundary between the lower zone (interpreted as inner-shelf lithofacies) and the upper zone (interpreted as outer-shelf lithofacies) of the Shuaiba in GN-23. Moreover, this boundary was identified as a hardground. Since a -2 to -2.5‰ PDB was suggested for the $\delta^{18}\text{O}$ composition of calcitic sediments deposited from Aptian seawater (Scholle and Arthur, 1980; Moldovanyi and Lohmann, 1984), then $\delta^{18}\text{O}$ average of -6.7‰ PDB of the first zone is indicative of meteoric influence. If stabilization of the matrix occurred in marine pore-waters, then

$\delta^{18}\text{O}$ of the matrix should be around -4‰ PDB, which indicates depletion by 1.5 to 2‰ relative to its marine precursor (Moshier, 1989B). However, this is not the case in the Shuaiba matrix in Ghaba North, because it is more depleted than that. Therefore, it must reflect alteration by meteoric waters.

The $\delta^{13}\text{C}$ average of the first zone is around $+4\text{‰}$ PDB. This enriched carbon isotopic composition indicates that the micro-rhombic calcite matrix is rock-buffered. This means that the carbon incorporated in this diagenetic stabilization process was dominated by carbon sourced from the rock. Therefore, this might reflect a low water/rock ratio and stabilization far away from the reach of depleted soil gas. Presence of the hardground at 619.45 m reflects a period of time during which the depositional rate was low. Moreover, this hardground could have acted as a seal between the sediments below it and seawater. Since the $\delta^{18}\text{O}$ values reflect a meteoric water influence, I suggest that the matrix of this zone has been stabilized in meteoric waters or mixed meteoric and marine water. Freshwater may have been driven below the hardground and through the shelf sediments by a high hydraulic head. Tongues of freshwater may extend many tens of kilometers seaward beneath continental shelves in strongly dynamic systems (James and Choquette, 1984). A modern analog exists where submarine freshwater springs discharge from the west Florida continental shelf, about 45 km from the coast (Fanning et al., 1981). These springs represent a discharge of waters whose origin is the exposed Florida Platform.

Therefore, I suggest that matrix stabilization in the lower diagenetic zone started early, during a separate event than matrix stabilization of the upper Shuaiba zone. Additional evidence for this interpretation comes from the fact that there is no evidence

for leaching below 619.45 m. This indicates that all rudists and rudist fragments of the lower zone were stabilized to LMC before subaerial exposure events observed in the upper Shuaiba zone occurred.

Diagenetic Zone II.- This zone extends from 619.45 m to 609.45 m. The $\delta^{18}\text{O}$ averages about -6.4‰ PDB. Apart from the $\delta^{18}\text{O}$ value at the base of this zone, other values are almost constant and then become enriched toward the top of the zone. This top occurs at 609.45 m and happens to be an erosional surface. Using the isotopic evidence, it is interpreted as a subaerial exposure surface due to the fact that $\delta^{18}\text{O}$ values vary above it and below it (Allan and Matthews, 1982). Increasing the depletion of $\delta^{13}\text{C}$ toward this surface is indicative of incorporation of more amounts of carbon from soil-gas during the stabilization process. One can argue that the $\delta^{13}\text{C}$ is still enriched (about $+3.8\text{‰}$ PDB) at the surface. However, this can be explained as an indication of an arid climate with only limited plant and soil zone activity (Budd, 1989). Only minor influx of ^{12}C from the degradation of organics at the soil zone would be expected below the exposure surface. Moreover, it has been noted that soil-gas CO_2 in arid regions may be enriched in $\delta^{13}\text{C}$ by as much as 8‰ relative to soil gas in humid regions (Rightmire and Hanshaw, 1973). In addition, subsequent marine submergence of this surface might have caused erosion of the thin soil zone (with the most depleted $\delta^{13}\text{C}$) that developed under these arid conditions. The enrichment in $\delta^{18}\text{O}$ toward the surface is another indication of subaerial exposure. This enrichment occurs at the exposure surface because of oxygen fractionation due to evaporation, where light oxygen becomes enriched in vapor phase and residual oxygen becomes heavier isotopically.

Covariance of $\delta^{13}\text{C}$ and $\delta^{18}\text{O}$, where both become enriched toward the base of this zone, might represent a mixing zone diagenesis (Allan and Matthews, 1982) between the fresh water lens and seawater.

Stratigraphic evidence, represented by the presence of the erosional surface, and petrographic evidence, represented by extensive leaching of rudists and rudist fragments below the surface, are in concordance with the isotopic data. Thus, I envisage a localized subaerial exposure and development of a small freshwater lens in a rudist bioherm, which was established on a pre-existing high on the shelf.

Diagenetic Zone III.- This zone extends from 609.45 m to the regional unconformity which separates the Shuaiba from the overlying Nahr-Umr Formation. The $\delta^{18}\text{O}$ and $\delta^{13}\text{C}$, again, show a pattern indicative of subaerial exposure and meteoric diagenesis. The presence of extensive leaching and moldic secondary porosity, especially below the unconformity, is further support for subaerial exposure at the end of Shuaiba time. The occurrence of a boundary at 600.4 m in this zone is obvious from $\delta^{13}\text{C}$ and $\delta^{18}\text{O}$ variation plots with depth. Sharp enrichment in $\delta^{13}\text{C}$ and $\delta^{18}\text{O}$ directly below 600.4 m and depletion trend of these above it toward the top is a pattern indicative of a vadose-phreatic boundary (Allan and Matthews, 1982). The Shuaiba above 600.4 m possesses very high macroporosity and abundant unconsolidated rubbly intervals, thus indicative of leaching and lack of extensive cementation, which are characteristics of vadose diagenesis.

Isotopic Analysis of Late Coarse-Crystalline Calcite Cements.- Petrographically, it has been shown, from cross-cutting relationships, that these cements are late and postdate

compaction. Apart from sample #49, other samples have a $\delta^{18}\text{O}$ average of -8‰ PDB and a $\delta^{13}\text{C}$ average of $+3.3\text{‰}$ (Figs. 45 and 46, respectively). Since this cement is observed to partially fill secondary moldic porosity in the upper Shuaiba zone, where these calcite crystals clearly appear growing in these molds (Fig. 27), it is obvious that this cement was precipitated after the development of molds, which were developed by dissolution associated with subaerial exposure events. Therefore, these cements might have precipitated after deposition of Nahr-Umr, relatively late in the burial history of the Shuaiba. Migration of hydrocarbons into the Shuaiba has prevented these cements from completely occluding moldic porosity. Hydrocarbons would not have been trapped in the Shuaiba in Ghaba North unless Nahr-Umr Shales had sealed the Shuaiba and the structure had already been developed. Thus, coarse-crystalline calcite cement precipitated after the formation of the anticlinal trap at Ghaba North, which occurred due to uplifting by salt movements. Post compaction nature and isotopic composition of the coarse-crystalline calcite cement indicate a burial origin. However, time constrain on the development of this late cement indicates that the Shuaiba during that time was not deeply buried.

Sample #49 occurs at 617.43 m and has a $\delta^{18}\text{O}$ value of -6.19‰ PDB and an anomalously enriched $\delta^{13}\text{C}$ value of $+9.73\text{‰}$ PDB. Stable carbon and oxygen analyses of this sample were repeated but the result was identical. Both the $\delta^{18}\text{O}$ and $\delta^{13}\text{C}$ values of the sample are enriched; $\delta^{18}\text{O}$ by about 2‰ and $\delta^{13}\text{C}$ by about 6‰ , relative to other late cement samples taken from GN-23 from depths below 619.45 m (Fig. 45 and 46). Sample #49 is the only sample with significant amount of cement for isotopic analysis above 619.45 m. Cement in this sample occurred as a filling of an internal pore space in a rudist shell. Extremely enriched $\delta^{13}\text{C}$ values in late carbonate cements might result

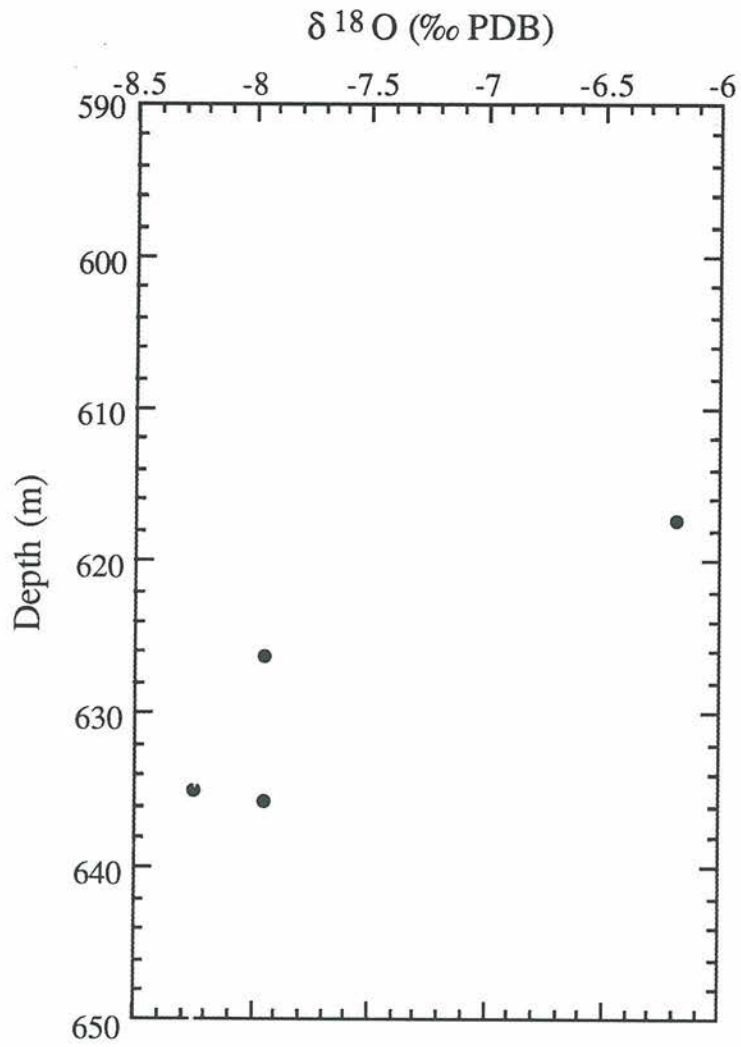


Figure 45. Depth plot of $\delta^{18}\text{O}$ of late calcite cements in the Shuaiba Formation GN-23 core.

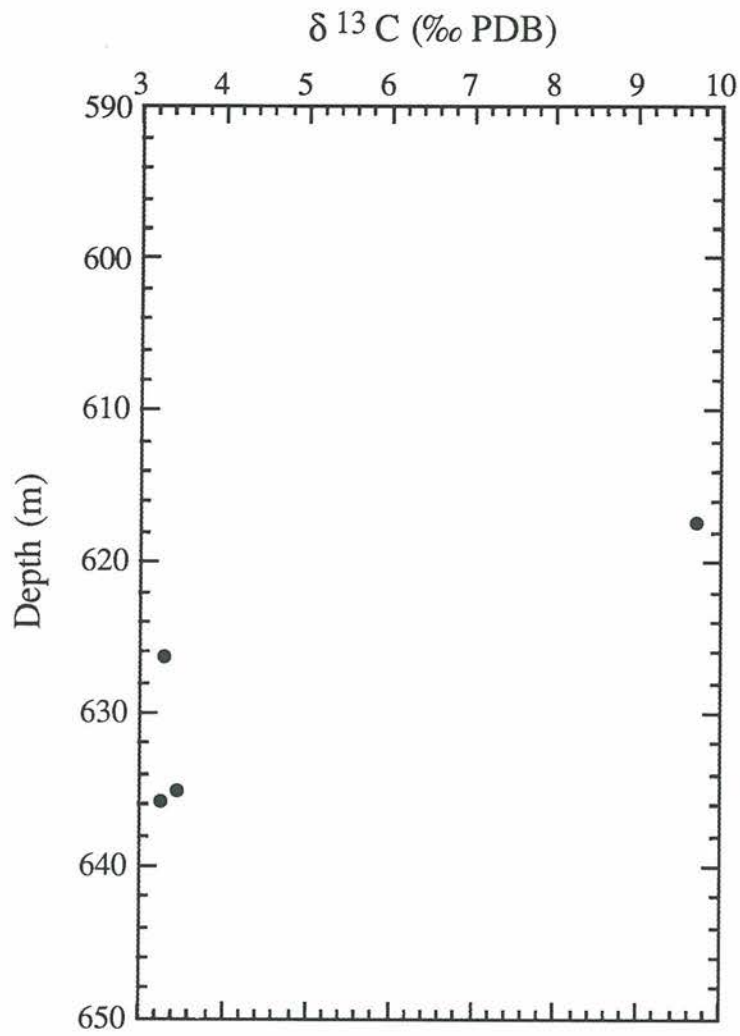


Figure 46. Depth plot of $\delta^{13}\text{C}$ of late calcite cements in the Shuaiba Formation GN-23 core.

from methane generation and escape (Hudson, 1977). $\delta^{13}\text{C}$ enrichment occurs due to preferential incorporation of ^{12}C in methane when formed by thermal cracking of kerogen, thus depleting methane and enriching the residual in ^{13}C (Faure, 1986). Reduction of CO_2 in deep burial settings generates depleted methane and enriched residual ΣCO_2 . Consumption of CO_2 during this process derives the following reaction to the left :



This leads to precipitation of CaCO_3 with an enriched $\delta^{13}\text{C}$. Although this sample is interesting, it is a minor component overall and only represents a localized event which seems to have not affected the isotopic composition of other Shuaiba samples.

Paragenetic Sequence of the Shuaiba Formation in GN-23

Following deposition of the lower depositional zone in a shallow inner-shelf setting and development of hardground (619.45 m), matrix and allochems of the lower zone were stabilized in a confined water aquifer which drove meteoric waters under the shelf. Stabilization was finished before the subaerial exposure at 609.45 m took place. This subaerial exposure led to development of a freshwater lens. Meteoric waters were responsible for creation of secondary moldic porosity, stabilization of the matrix to micro-rhombic calcite, and development of microporosity in the second diagenetic zone. Dissolution only affected unstabilized rudists and rudist fragments. This leaching event only affected sediments above the 619.45 m boundary. This indicates that sediments below this depth were already stabilized before this event and/or the freshwater lens was small and the sediments below 619.45 m were below the reach of undersaturated

solutions. Finally, by the end of Shuaiba time, a subaerial exposure event took place and led to creation of more moldic porosity. In addition, this exposure led to stabilization of the matrix in an unconfined meteoric diagenetic environment.

A transgression event led to deposition of Nahr-Umr Formation over the regional unconformity. Following establishment of the anticlinal trap at Ghaba North Field, late coarse-crystalline calcite cement precipitated in secondary moldic porosity and primary internal pore spaces within rudists shells. This event was followed by development of subvertical extensional fractures in the Shuaiba due to rejuvenation of salt movement in the Ghaba Salt Basin. The last event was migration of hydrocarbons into the Shuaiba reservoir, which inhibited total cementation of the macroporosity.

Lithology and Reservoir Properties of the Shuaiba Formation in other Wells in Ghaba North Field

In this section, results observed in the other cores available from the field will be discussed. The results obtained are regarding sedimentology, deposition, and reservoir properties. This discussion will help in understanding lateral variations of the Shuaiba across the field. Furthermore, correlation of the Shuaiba Formation between GN-13, GN-2, GN-1 and GN-23 will develop a strategy for extending reservoir property variations across the field, which is important for development of the Ghaba North Shuaiba reservoir.

The Shuaiba Formation in GN-13

Based on sedimentological and allochemical constituents, it is obvious that GN-13, in general, is characterized by deposition in a low-energy, restricted to partially restricted setting. The Shuaiba here contains abundant wackestones and green algae (*Bacinella* and *Lithocodium*). Apart from the presence of rudists in the interval between 646.05 m and 645.30 m, in which they occur with gastropods overlying a scour, there are hardly any rudists elsewhere in this core. The few that are present occur as scattered rudist fragments in a wackestone matrix. This indicates that the depositional setting at this locality was distally located from the shelf edge and rudist buildups. In addition, energy was low and circulation was restricted to partially restricted to account for the facies observed. The interval with the scour may represent a tidal channel cutting through sediments of this setting. Presence of a normally graded thin wackestone interval, with fine to very fine grains, represents deposits of a storm event. The lack of any coarse-grained constituents in this interval, such as rudists and rudist fragments, may be due to long transportation distance, because this interval is representative of a distally located depositional site on the shelf.

Lack of any considerable macroporosity in the Shuaiba in this core is due to the scarcity of rudists. As discussed above, the presence of considerable amounts of aragonitic rudists provides potential for leaching and creation of secondary moldic porosity in the Shuaiba. However, the Shuaiba here is described as a high porosity (due to the presence of microporosity) and low permeability reservoir.

The Shuaiba Formation in GN-2

The Shuaiba Formation in this core is representative of a low- to moderate-energy, partially restricted depositional setting. This interpretation is based on the presence of wackestone intervals alternating with rudist floatstones. The presence of these floatstones with bioclastic wackestones may be indicative of high energy conditions alternating with low energy conditions. Alternatively, the rudist floatstones may represent proximity to bioherms and the wackestones may then represent interbiohermal deposits.

Occurrence of some leaching in rudists enhanced macroporosity and permeability of the Shuaiba in this core relative to GN-13. However, most of hydrocarbon is still contained in microporosity of the reservoir.

The Shuaiba Formation in GN-1

The Shuaiba in this core is represented by deposits of a low-energy, restricted to partially restricted setting, which give way to more open, relatively high-energy deposits toward the top of the core. This is inferred from vertical variation trends of rudist and algal abundances. The lower part of the core is represented by burrowed wackestone facies, minor algal nodule facies, and algal boundstone facies. These give way, at about 625.40 m, to rudist floatstones and rudstones interrupted by thin wackestone intervals. Thus, it is obvious that rudist abundance increases toward the top, whereas algal abundance decreases in the same direction. This is indicative of conditions of less restriction to circulation and a locality more proximal to rudist bioherms and buildups.

Larger amounts of rudists and rudist fragments are transported to settings on the shelf proximal to shoal areas and shelf edge than distally located settings.

Macroporosity increases toward the top of the core as well, indicating that macroporosity is controlled by rudist abundance. However, it is important that the rudists present are of the caprinid and caprotinid types, which are susceptible to leaching due to the fact that their original mineralogy is aragonitic (Borgomano, 1991).

Correlation of the Shuaiba Formation Across Ghaba North Field

Sedimentologic and petrographic observations, from the four cores available from the field, will be used as a criteria for correlation of the Shuaiba Formation across the field. Due to the fact that this study concentrates on GN-23 (which is the most recently drilled, longest, and most complete core), the other cores will be correlated to this core and among themselves. Lateral variations in the formation then will be easily recognized.

Correlation of the Cores.- Due to the fact that GN-13, GN-2, and GN-1 cores have low recoveries, only general correlation lines can be drawn in the field. Based on the extensive examination of GN-23 in this study, three biofacies and two lithofacies were identified in the Shuaiba Formation. The biofacies are the foram biofacies, the algae-foram-rudist fragment biofacies, and the rudist-*Orbitulina* biofacies. The first and second biofacies were recognized in the inner shelf lithofacies, which covers the lower zone in GN-23, whereas the third biofacies was observed in the outer shelf lithofacies, which is represented by the upper zone of GN-23.

Considering sedimentologic and petrographic results obtained from GN-13, it appears that this core contains the foram and the algae-foram-rudist fragment biofacies. Moreover, the lithology is indicative of the inner shelf lithofacies as identified in GN-23. Stratigraphically, the Shuaiba cored in GN-13 is equivalent to the lower part of the lower zone described in GN-23. This is inferred from the fact that the Shuaiba in GN-13 is composed of wackestone facies with algal nodules alternating with a few floatstones of rudist fragments. Similarly, the Shuaiba in GN-2 contains the foram and the algae-foram-rudist fragment biofacies. Therefore, it represents the inner shelf lithofacies as well. However, the Shuaiba in the GN-2 is equivalent to the upper part of the lower zone of the Shuaiba in GN-23. This is based on the presence of rudist floatstone intervals alternating with wackestone intervals with algal nodules and some algal boundstone facies, which is similar to the upper part of the lower zone of the Shuaiba in GN-23. The Shuaiba of GN-1 contains the algae-foram-rudist fragment biofacies and the rudist-*Orbitulina* biofacies. Therefore, it contains parts equivalent to the inner shelf and outer shelf lithofacies. The boundary between the two Shuaiba lithofacies in GN-1 can be placed at about 625.40 m. Below this depth, the Shuaiba represents the inner shelf lithofacies and is equivalent to the upper part of the lower zone in GN-23. The outer shelf lithofacies is represented by the Shuaiba above 625.40 m and is equivalent to the lower part of the upper zone in GN-23.

General Lateral Trends Observed in the Shuaiba Cores.- Based on the correlation of the four cores, general variation trends can be observed between the cores. For example, there is a general trend of increasing rudist abundance from GN-13 through GN-2 and GN-1 toward GN-23 (see Fig. 9 for locations). In general, this northeast trend in rudist abundance in the field indicates the direction in which rudist buildups have developed

upon shoals on the wide shelf of the Shuaiba. These rudist buildups are located further in northeast direction because they were not encountered in the above mentioned cores. The identification of the Shuaiba in GN-13 as an equivalent to the lower part of the lower zone of the Shuaiba in the GN-23, based on sedimentologic and petrographic evidence, supports the interpretation of the lithofacies as an inner shelf. Due to the presence of tidal channel deposits in GN-13 (the interval described from 646.05 m to 645.30 m), GN-13 was located in a landward direction relative to the other cores. However, the Shuaiba in GN-2 was deposited in an offshore direction relative to GN-13. GN-2 is equivalent to the upper part of the lower zone in GN-23 and represents an inner shelf lithofacies. The Shuaiba in GN-1 is recognized to be equivalent to the upper part of the lower zone and the lower part of the upper zone in GN-23. GN-1 possesses a vertical variation in rudist and algal abundance, and contains facies similar to those described in GN-23. Therefore, GN-1 represents a locality further in the offshore direction relative to the previous wells. The Shuaiba in GN-23 contains an inner shelf lithofacies overlain by an outer shelf lithofacies. GN-23 possesses more abundant rudists, which are identified to form rudist bioherms toward the top of the formation. This indicates that GN-23 is proximally located to rudist buildups, which might have developed upon shoals or preexisting highs on the shelf or rimmed an intrashelf basin in central Oman or an extension of the intrashelf basin of Abu Dhabi.

The Shuaiba Formation in all four cores is characterized by the presence of high microporosity, which is responsible for most of the hydrocarbon storage capacity of the reservoir. However, macroporosity increases in a northeast trend as might be expected from the above discussion. This may be due to two reasons; first, the increase in rudist abundance in the northeast direction. Second, the Shuaiba in the northeast direction may

have been stratigraphically higher in the field than in the opposite direction. The increase in rudist abundance toward GN-23 is obvious, and the presence of rudists favorable for leaching, such as caprinids and caprotinids, seems to increase in that direction and vertically as well. These types of rudists are the main framework-builders, and thus are abundant in the direction of the buildups (Hamdan and Alsharhan, 1991). On the other hand, other types of rudists such as monopleurids, which have a original calcitic mineralogy and thus stabilize easily (Borgomano, 1991), predominate in the shelf lagoon and display a patchy distribution vertically and laterally (Hamdan and Alsharhan, 1991). Therefore, these might be the dominant rudists in a southwest direction in Ghaba North. In addition, stratigraphically higher positioning of the Shuaiba in the northeast direction provides better chances for development of meteoric diagenetic environments and creation of secondary moldic porosity after rudists. It is widely accepted that the occurrence of depositional relief beneath the unconformity, which separates the Shuaiba Formation from the overlying Nahr-Umr, provides better opportunity for reservoir development in the Shuaiba (Wilson, 1975). The presence of macroporosity enhances permeability of the reservoir, due to development of interconnected pore system due to leaching of rudist debris (Borgomano, 1991), thus enhancing the productivity of the reservoir.

CONCLUSIONS AND RECOMMENDATIONS

The Lower Cretaceous (Aptian) Shuaiba Formation in Ghaba North Field was studied in this thesis in order to understand the depositional environment and establish the diagenetic history of the formation. In addition, observing variations in reservoir characteristics, stratigraphically and across the field, was an important part of this study. Summary and conclusions about these aspects will be considered in this section.

The Shuaiba Formation in Ghaba North was deposited during the Early Aptian. It consists of two zones, the lower and upper. The lower zone represents deposition in a shallow inner-shelf setting with restricted to partially restricted water circulation. The upper zone represents deposition in a shallow outer-shelf setting with more open (less restricted) circulation conditions. The Shuaiba, in general, shows a shallowing upward trend. This indicates that deposition of the upper zone in the Ghaba North region was becoming more proximal to rudist buildups in the shelf. These buildups were probably established on paleohighs or were rimming an intrashelf basin in central Oman, resembling the intrashelf basin of Abu Dhabi or an extension of that intrashelf basin. Correlation of the cores available from the field indicates that there is a trend of increasing energy conditions and proximity to buildups, although the buildups were not encountered in the cores. This trend is in the northeast direction in the field and is established by correlating GN-13, GN-2, GN-1 and GN-23, which occurs in the northeastern sector of the field. This indicates that the paleo-strandline was to the southwest of Ghaba North Field.

Favorable reservoir characteristics of the Shuaiba decrease, in general, with depth and toward the GN-23 well. Development of secondary moldic porosity has a great influence on enhancing reservoir properties; however, the matrix microporosity is responsible for most of the reservoir hydrocarbon holding capacity. The upper Shuaiba zone possesses higher macroporosity and horizontal permeability, and thus better reservoir quality. Microporosity of the Shuaiba is present as intercrystalline porosity within micro-rhombic calcite matrix. In both the lower and upper Shuaiba zones, microporosity decreases from the bottom until a minimum and then increases toward the top of each zone. The decrease in microporosity occurs due to development of crystal mosaic texture in the matrix rather than blocky-crystal framework texture. Presence of neomorphic calcite microspar in interpeloidal pore spaces in peloidal matrices also reduces microporosity of the Shuaiba. In addition, microporosity in the Shuaiba is controlled by abundance and distribution of *Orbitulina* and other allochems versus algae. Microporosity in the Shuaiba decreases with increasing algal abundance.

There are three diagenetic zones identified in the GN-23 core. These are distinguished due to different stable carbon and oxygen isotopic compositions of the matrix and supported by stratigraphic and petrographic evidence. These zones are indicative of different diagenetic events and the complexity of the Shuaiba diagenetic history. The first zone covers the lower Shuaiba zone, which extends from the bottom of GN-23 to the hardground which occurs at a depth of 619.45 m. The second zone extends from this hardground to the subaerial exposure surface identified at 609.45 m. The third zone starts from the 609.45 m exposure surface to the top of the Shuaiba, which happens to be a regional unconformity and an exposure surface. From isotopic evidence, presence of subaerial exposure surfaces, and the action of leaching, it can be concluded that

meteoric waters were the main diagenetic fluids that developed the diagenetic features of the Shuaiba Formation at Ghaba North. It is also concluded that the matrix was stabilized, and thus the microporosity was formed, in meteoric diagenetic environments. The development of moldic secondary porosity in rudists and rudist fragments was controlled by the presence of abundant rudists, original mineralogy of the rudists, and by proximity of rudist-rich facies to subaerial exposure surfaces.

Macroporosity and leaching of rudists increases from GN-13 to GN-2, and GN-1 to GN-23; in a trend resembling the trend observed in proximity to rudist buildups. These trends are toward the northeast of Ghaba North Field. This indicates that the northeastern sector of the field occurred stratigraphically higher than the southwestern sector. Thus, the Shuaiba sediments in the northeastern sector were affected more by leaching due to invasion of undersaturated fluids. These sediments were placed in vadose and meteoric phreatic environments. However, lesser amounts of secondary moldic porosity might be also due to lack of significant amount of unstabilized rudists and rudist fragments in the southwestern sector of the field due to being distally located from rudist buildups during deposition.

Stabilization of the Shuaiba matrix, development of moldic macroporosity associated with the exposure surfaces, and establishment of the anticlinal trap in Ghaba North occurred relatively fast. Presence of partially cemented molds by coarse-crystalline calcite cement indicates that hydrocarbons migrated into the reservoir soon after precipitation of this late cement. Hydrocarbon migration thus prevented occlusion of porosity by cementation or compaction under heavy overburden pressures at deep burial depths.

Recommendations

This study of the Shuaiba Formation is very useful for a Ghaba North Field development plan. First of all, it should be noted that development of a petroleum reservoir in the Shuaiba at Ghaba North is a function of development of micro-rhombic calcite matrix and intercrystalline microporosity. However, enhancement of reservoir quality occurred by development of moldic secondary porosity. At Ghaba North, the upper Shuaiba possesses the best reservoir characteristics. Moreover, these reservoir characteristics are, in general, best toward the northeast direction in the field. However, it should be noted that production plans are also controlled by structure of the field and the oil-water contact.

Since a rudist buildup was not encountered by cores available from the field, and since there is a trend of increasing proximity to rudist buildups, it is recommended to explore for the buildups to the northeast of Ghaba North Field. This will require a regional study of the Shuaiba Formation and correlation over the existing wells in the fields in order to understand the geometry and verify the existence of an intrashelf shelf basin and a rimming rudist buildup. Importantly, the presence of two subaerial exposure surfaces, observed in GN-23, increases the potential of the Shuaiba Formation as an exploration target. The subaerial exposure surface at 609.45 m in GN-23, although it might be a localized exposure event, suggests that such an event might have occurred in other localities due to growth of rudist bioherms or buildups above sea level and subsequent development of freshwater lenses. Thus, if the location of buildups is inferred to occur to the northeast of Ghaba North Field, then higher chances for development of such exposure events exist there. Development of secondary moldic porosity should be

denoted by an amplitude decrease in the top Shuaiba seismic reflectors, thus reducing the ordinary velocity contrast between the higher velocity limestone of the Shuaiba and the overlying lower velocity Nahr-Umr shale (Frost et al., 1983).

The Shuaiba Formation in Ghaba North is very heterogeneous. This is due to the complexity of depositional environments and facies mosaics contained. Presence of highly cemented thin rudist-rich intervals in the lower Shuaiba might act as impermeable layers to vertical flow movements if not fractured. Stabilization of the matrix and development of microporosity in meteoric diagenetic environments have created a highly porous reservoir. This porosity, however, is reduced by presence of neomorphic calcite microspar in the intervals with peloidal matrices and by development of crystal mosaic matrix textures instead of framework textures. Crystal mosaic textures form by additional compaction and/or cementation of blocky-crystal framework textures. In GN-23, this decrease in microporosity, and thus in permeability, occurs toward the middle of both the lower and upper Shuaiba zones. Variation of microporosity should be considered in any development plan of the Shuaiba in Ghaba North Field.

REFERENCES CITED

- Aldabal, M. A., and Alsharhan, A. S., 1989, Geological model and reservoir evaluation of the Lower Cretaceous Bab member in the Zacum Field, Abu Dhabi, United Arab Emirates; *Society of Petroleum Engineers*, 18007, p. 797-809.
- Allan, J. R., and Matthews, R. K., 1977, Carbon and Oxygen isotopes as diagenetic and stratigraphic tools in surface and subsurface data, Barbados, West Indies; *Geology*, V. 5, p. 16-20.
- Allan, J. R., and Matthews, R. K., 1982, Isotope signatures associated with early meteoric diagenesis; *Sedimentology*, V. 29, p. 797-817.
- Alsharhan, A. S., 1985, Depositional environment, reservoir units evolution, and hydrocarbon habitat of Shuaiba Formation, Lower Cretaceous, Abu Dhabi, United Arab Emirates; *American Association of Petroleum Geologists Bulletin*, V. 69, p. 899-912.
- Alsharhan, A. S., 1987, Geology and reservoir characteristics of carbonate buildup in giant Bu Hasa oil field, Abu Dhabi, United Arab Emirates; *American Association of Petroleum Geologists Bulletin*, V. 71, p. 1304-1318.
- Alsharhan, A. S., and Kendall, C. G., 1986, Precambrian to Jurassic rocks of the Arabian Gulf and adjacent areas; *American Association of Petroleum Geologists Bulletin*, V. 70, p. 977-1002.

- Alsharhan, A. S., and Nairn, A. E., 1986, A review of the Cretaceous formations in the Arabian Peninsula and Gulf: Part 1. Lower Cretaceous (Thammama Gp.) stratigraphy and paleogeography; *Journal of Petroleum Geology*, V. 9, p. 365-392.
- Alsharhan, A. S., and Nairn, A. E., 1988, A review of the Cretaceous formations in the Arabian Peninsula and Gulf: Part 2. Middle Cretaceous (Wasia Gp.) stratigraphy and paleogeography; *Journal of Petroleum Geology*, V. 11, p. 89-112.
- Borgomano, J. R., 1991, Quick-look sedimentological study on selected Shuaiba cores; *PDO Exploration Laboratory Note*, No. 24, 5 p.
- Budd, D. A., 1989, Micro-rhombic calcite microporosity in limestones: a geochemical study of the lower Cretaceous Thammama Group, United Arab Emirates, *In*: C. R. Hanford, R. G. Loucks and S. O. Moshier (Eds.), *Nature and Origin of Micro-rhombic Calcite and Associated Microporosity in Carbonate strata*; *Sedimentology Geology*, V. 63, p. 293-311.
- Choquette, P. W., and James, N. P., 1987, Diagenesis 12. diagenesis in limestones-3, the deep burial environment, *Geoscience Canada*, V. 14, p. 3-35.
- Clarke, M. H., 1988, Stratigraphy and rock unit nomenclature in the oil-producing area of interior Oman; *Journal of Petroleum Geology*, V. 11, p. 5-60.
- Clarke, M. W., 1990, *Oman's geological heritage*, Stacey International Publishers, 247 p.
- Connaly, T. C., and Scott, R. W., 1985, Carbonate sediment-fill of an oceanic shelf, Lower Cretaceous, Arabian Peninsula, *In*: P. D. Crevello and P. M. Harris (Eds.),

- Deep Water Carbonates; *Society of Economic Paleontologists and Mineralogists*, core workshop, 6, p. 266-302.
- Engel, S., 1989, Al Huwaisah Field gamma ray correlation of the Shuaiba Formation; *PDO Exploration Note*, No. 109, 5 p.
- Fanning, K. A., Byrne, R. H., Breland II, J. A., Betzer, P. R., Willard, S. M., Elsinger, R. J., and Pyle, T. E., 1981, Geothermal springs of west Florida continental shelf: evidence for dolomitization and radionuclide environments; *Earth and Planetary Science Letters*, V. 52, p. 345-354.
- Faure, G., 1986, *Principles of isotope geology*; Wiley, New York, 589 p.
- Freake, J. R., and Witt, W. G., 1972, A revised depositional model of the Shuaiba Formation in Central Oman; *PDO Geological Report*, No. 94, 11 p.
- Frikken, H. W., 1982, Reservoir geological investigation of cores from the Shuaiba Formation in well Ghaba North-13, Central Oman; *KSEPL Report*, No. 63, 27 p.
- Frost, S. H., Bliefrick, D. M., and Harris, P. M., 1983, Deposition and porosity evolution of a Lower Cretaceous rudist buildup, Shuaiba Formation of eastern Arabian Peninsula, In: P. M. Harris (Ed.), Carbonate Buildups; *Society of Economic Paleontologists and Mineralogists*, core workshop, 4, p. 381-410.
- Gallagher, J., Mercadier, C., Mcfadyen, K., and Meij, R., 1990, Ghaba North Shuaiba incremental development; *Petroleum Development Oman Report*, No. Pef/90/146, 16 p.

- Hamdan, A. R., and Alsharhan, A. S., 1991, Paleoenvironments and paleoecology of the rudists in the Shuaiba Formation (Aptian) United Arab Emirates; *Journal of African Earth Sciences*, V. 12, p. 569-581.
- Harris, P. M., Frost, S. H., Seiglie, G. A., and Schneidermann, N., 1984, Regional unconformities and depositional cycles, Cretaceous of the Arabian Peninsula; *American Association of Petroleum Geologists*, Memoir 36, p. 67-80.
- Hartmans, R. F., 1986, Fahud-223 core and Shuaiba reservoir geological model, Fahud oil field, Oman; *PDO Production Geology Report*, No. 43, 18 p.
- Hudson, J. D., 1977, Stable isotopes and limestone lithification; *Journal of Geological Society of London*, V. 133, p. 637-660.
- James, N. P., and Choquette, P. W., 1983, Diagenesis 6. limestones - the sea floor diagenetic environment; *Geoscience Canada*, V. 10, p. 162-179.
- James, N. P., and Choquette, P. M., 1984, Diagenesis 9. limestones - the meteoric diagenetic environment; *Geoscience Canada*, V. 11, p. 161-194.
- Johnson, J. H., 1969, *A review of the Lower Cretaceous algae*; Professional Contributions of the Colorado School of Mines, No. 6, 180 p.
- Lohmann, K. C., 1988, Geochemical patterns of meteoric diagenetic systems and their application to studies of paleokarst, *In*: P. W. Choquette and N. P. James (Eds.), *Paleokarst*, Springer-Verlag, New York, p. 55-80.

- Mattes, B. W., and Wynne, S. B., 1984, Sedimentology, diagenesis and reservoir distribution in carbonate of the Lower Cretaceous Shuaiba Formation, northern central Oman; *KSEPL Report*, No. 267, 47 p.
- McCrea, J. M., 1950, The isotope chemistry of carbonates and a paleotemperature scale; *Journal of Chem. Phys.*, V. 18, p. 849-857.
- Mercadier, C. G., 1990, Geological review of the Ghaba North Field; *PDO Geological Report*, No. PE/90, 12 p.
- Moldovanyi, E. P., and Lohmann, K. C., 1984, Isotopic and petrographic record of phreatic diagenesis: Lower Cretaceous Sligo and Cupido Formations; *Journal of Sedimentary Petrology*, V. 54, p. 972-985.
- Moshier, S. O., 1989A, Microporosity in micritic limestones: a review, *In*: C. R. Hanford, R. G. Loucks and S. O. Moshier (Eds.), Nature and Origin of Micro-rhombic Calcite and Associated Microporosity in Carbonate Strata; *Sedimentary Geology*, V. 63, p. 191-213.
- Moshier, S. O., 1989B, Development of microporosity in a micritic limestone reservoir, Lower Cretaceous, Middle East, *In*: C. R. Hanford, R. G. Loucks and S. O. Moshier (Eds.), Nature and Origin of Micro-rhombic Calcite and Associated Microporosity in Carbonate Strata; *Sedimentary Geology*, V. 63, p. 217-240.
- Murris, R. J., 1980, Middle East: stratigraphic evolution and oil habitat; *American Association of Petroleum Geologists Bulletin*, V. 64, p. 597-618.

- Neumann, A. C., and Land, L. S., 1975, Lime mud deposits and calcareous algae in the Bight of Abaco, Bahamas: a budget; *Journal of Sedimentary Petrology*, V. 45, p. 763-786.
- Petroleum Development Oman, 1990, Core analysis for well Ghaba North-23, Oman; *Core Laboratories Report*, 31 p.
- Petroleum Development Oman, 1991, *Production Reference Data Book*, PDO internal report.
- Petroleum Development Oman, 1992, Ghaba North Field; *Production Reference Data Book*, V. 1, 27 p.
- Powers, R. W., Ramirez, L. F., Remond, C. D., and Elberg, E. L., 1966, Geology of the Arabian Peninsula: Sedimentary geology of Saudi Arabia; *United States Geological Survey Professional Paper*, 560 (D), 147 p.
- Pratt, B. R., and Smewing, J. D., 1993, Early Cretaceous platform-margin configuration and evolution in the Central Oman Mountains, Arabian Peninsula; *American Association of Petroleum Geologists Bulletin*, V. 77, p. 225-244.
- Rightmire, C. T., and Hanshaw, B. B., 1973, Relationship between the carbon isotope composition of soil CO₂ and dissolved carbonate species in ground waters; *Water Resour. Res.*, V. 9, p. 958-967.
- Scholle, P. A., and Arthur, M. A., 1980, Carbon isotope fluctuation in Cretaceous pelagic limestones: Potential stratigraphic and petroleum exploration tool; *American Association of Petroleum Geologists Bulletin*, V. 64, p. 67-87.

Scoffin, T. P., 1987, *An introduction to carbonate sediments and rocks*; Blackie, New York, 274 p.

Uitentuis, E., 1981, Ghaba North Field production geological review; *PDO Internal Report*, 10 p.

Well, A. J., and Illing, L. V., 1964, Present day precipitation of Calcium Carbonate in the Persian Gulf, *In*: L. M. Van Straaten (Ed.), *Deltaic and Shallow Marine Deposits*; Elsevier, Amsterdam, p. 429-435.

Wilson, J. L., 1975, *Carbonate facies in geologic history*; Springer - Verlag, New York, 469 p.

APPENDIX 1

The Shuaiba GN-23 Petrographic Data			
Interval #	Samples No.s	Thickness (m)	Depths (m)
1	1,2,3	1.7	644.8-643.1
2	4,5,6,7	1.6	643.1-641.5
3	8,9,10	2.3	641.5-639.2
4	11,12,13,14	2.4	639.2-636.8
5	15,16	1.5	636.8-635.3
6	17,18	1.55	635.3-633.75
7	19	0.25	633.75-633.5
8	20	0.8	633.5-632.7
9	21	0.3	632.7-632.4
10	22,23,24,25	1.9	632.4-630.5
11	26,27	1	630.5-629.5
12	28	1.2	629.5-628.3
13	29	0.3	628.3-628.0
14	30,31,32	1.5	628.0-6269.5
15	33,34	1.05	626.5-625.45
16	35,36,37,38,39	2.65	625.45-622.8
17	40,41,42	1.65	622.8-621.15
18	43,44	1.7	621.15-619.45
19	45,46	0.4	619.45-619.05
20	47	1	619.05-618.05
21	48,49,50	1.05	618.05-617.0
22	51,52,53,54	2.6	617-614.4
23	55	0.75	614.4-613.65
24	56,57	0.88	613.65-612.77
25	58,59,60,61	2.35	612.77-610.42
26	62,63	0.97	610.42-609.45
27	64	1.33	609.45-608.12
28	65,66,67	1.32	608.12-606.8
29	68,69,70,71,72,73,74	4.63	606.8-602.17
30	75,76,77,78	1.77	602.17-600.4
31	79,80,81,82,83,84	4.4	600.4-596.0

Interval #	Average Depths	Rudists %	Algae %	Orbitulinas And Other Allochems %
1	643.95	-	-	20
2	642.3	< 5	20	10
3	640.35	5	20	< 10
4	638	5	15	10
5	636.05	5_10	20	< 10
6	634.53	5_7	10	10_15
7	633.63	20	5_10	5
8	633.1	< 5	10_15	10_15
9	632.55	< 5	> 35	5
10	631.45	5	10	10
11	630	< 5	30	10
12	628.9	5	10_15	15
13	628.15	25_30	< 5	10
14	627.25	5	15	15
15	625.98	15_20	< 5	10
16	624.13	5_8	10	15
17	621.93	10_15	< 10	15
18	620.3	< 5	10	> 15
19	619.25	15_20	5	10_15
20	618.55	< 5	10_15	15
21	617.53	20	10_15	10
22	615.7	< 5	15_20	15
23	614.03	20	5	5_10
24	613.2	< 5	5	15
25	611.6	5	> 30	10
26	609.94	30	< 5	5_10
27	608.79	< 5	< 10	15
28	607.46	20	10	10
29	604.49	10	15	15
30	601.29	25_30	5	10
31	598.2	25_30	< 5	15

	Measured			Horizontal
Interval #	Porosity %	Macroporosity %	Microporosity %	Permeability (md)
1	30	< 3	28	5.5
2	29	3	26	4.8
3	26	5	21	5.6
4	31	5	26	6.4
5	25	5	20	4.7
6	29	5	24	8.6
7	16	> 3	12	1
8	26	5	21	5
9	29	5	24	8.2
10	31	5	26	7.8
11	27	5	22	8
12	29	5	24	7.6
13	18	> 3	14	1.1
14	31	5	26	7.2
15	24	3	21	4.1
16	31	6	25	7.7
17	32	5	27	11.8
18	34	5	29	9.7
19	34	6	28	17
20	34	5	29	11.6
21	30	8	22	14.7
22	32	5	27	14.8
23	28	8	20	30
24	32	7	25	7
25	28	3_5	24	16.8
26	27	8_12	17	29
27	32	5	27	24.5
28	28	10	18	10.3
29	30	7	23	15
30	25	12_15	12	34
31	36	15_20	19	375

APPENDIX 2

Colorado School of Mines Stable Isotope Data							
Project:		Shuaiba					
Date:		Aug-93					
Standard Gas:		CYM-1					
Whole Rock Analysis							
Sample	Depth (m)	δ 45/44	s	δ 13C (PDB)	δ 46/44	s	δ 18O (PDB)
23-1	643.95	5.918	0.02	3.71	-0.253	0.016	-6.28
23-2	643.66	5.802	0.015	3.59	-0.37	0.011	-6.39
23-3	643.15	5.898	0.015	3.69	-0.389	0.005	-6.41
23-4	642.55	6.223	0.008	4.03	-0.21	0.013	-6.23
23-5	642.46	6.039	0.007	3.84	-0.263	0.019	-6.28
23-6	642.16	6.177	0.015	3.99	-0.238	0.013	-6.26
23-7	641.58	6.158	0.016	3.96	-0.215	0.01	-6.24
23-8	641.06	6.306	0.013	4.14	-0.725	0.009	-6.74
23-9	640.6	6.406	0.006	4.23	-0.139	0.015	-6.16
23-9d	640.6	6.45	0.011	4.29	-0.59	0.014	-6.61
23-10	639.42	6.252	0.016	4.06	-0.096	0.014	-6.12
23-11	638.5	6.264	0.013	4.09	-0.704	0.014	-6.72
23-12	638.15	6.256	0.011	4.08	-0.416	0.013	-6.43
23-13	637.25	6.214	0.002	4.04	-0.676	0.017	-6.69
23-14	636.82	6.113	0.01	3.94	-0.914	0.014	-6.93
23-15	636.18	6.118	0.011	3.95	-1.12	0.014	-7.14
23-16	635.8	6.243	0.009	4.08	-1.017	0.011	-7.03
23-17	635.18	6.282	0.01	4.10	-0.452	0.003	-6.47
23-18	634.8	6.185	0.016	4.01	-0.622	0.01	-6.64
23-19	633.6	6.156	0.011	4.00	-1.291	0.012	-7.31
23-20	633.18	6.314	0.006	4.14	-0.449	0.017	-6.47
23-21	632.63	6.423	0.003	4.27	-0.793	0.017	-6.81
23-21d	632.63	6.435	0.004	4.26	-0.27	0.012	-6.29
23-22	632.15	6.422	0.014	4.27	-0.87	0.014	-6.88
23-23	631.7	5.349	0.009	3.11	-0.435	0.011	-6.46
23-24	631.35	5.38	0.013	3.15	-0.672	0.015	-6.70
23-25	630.77	5.388	0.016	3.15	-0.31	0.008	-6.34
23-26	630.35	5.584	0.004	3.38	-0.975	0.005	-7.00
23-27	629.78	6.257	0.004	4.08	-0.46	0.019	-6.48
23-28	628.84	5.984	0.013	3.80	-0.865	0.013	-6.88
23-29	628.13	6.05	0.008	3.87	-0.796	0.01	-6.81
23-30	627.88	6.175	0.009	3.98	-0.17	0.007	-6.19
23-31	627.18	6.857	0.008	4.71	-0.371	0.007	-6.38
23-32	626.9	6.474	0.013	4.31	-0.619	0.014	-6.63
23-33	626.35	6.186	0.007	4.00	-0.45	0.006	-6.47
23-34	625.77	6.412	0.02	4.25	-0.638	0.016	-6.65
23-35	625.4	5.72	0.016	3.52	-0.932	0.019	-6.95

23-36	624.32	6.496	0.019	4.32	-0.201	0.014	-6.22
23-37	623.87	6.73	0.01	4.57	-0.136	0.006	-6.15
23-38	623.47	6.487	0.015	4.33	-0.72	0.017	-6.73
23-38d	623.47	6.584	0.005	4.42	-0.233	0.009	-6.25
23-39	622.85	6.51	0.012	4.34	-0.292	0.007	-6.31
23-40	622.42	6.158	0.019	3.98	-0.796	0.013	-6.81
23-41	621.9	6.2	0.017	4.03	-0.764	0.014	-6.78
23-42	621.15	6.509	0.01	4.37	-1.016	0.007	-7.03
23-43	620.33	6.521	0.01	4.36	-0.61	0.015	-6.62
23-44	619.87	6.875	0.008	4.76	-1.078	0.019	-7.09
23-45	619.34	8.032	0.011	5.95	0.195	0.009	-5.81
23-46	619.08	7.511	0.004	5.38	0.54	0.019	-5.47
23-46d	619.08	7.071	0.003	4.93	-0.047	0.007	-6.06
23-47	618.49	7.534	0.007	5.40	0.754	0.018	-5.26
23-48	617.93	6.635	0.005	4.49	-0.68	0.011	-6.69
23-49	617.43	7.071	0.009	4.95	-0.485	0.016	-6.50
23-50	617.03	7.07	0.008	4.94	-0.337	0.016	-6.35
23-51	616	7.165	0.01	5.04	-0.203	0.01	-6.21
23-52	615.58	6.953	0.012	4.83	-0.779	0.016	-6.79
23-53	614.96	6.93	0.014	4.78	-0.162	0.014	-6.18
23-54	614.28	7.172	0.008	5.05	-0.53	0.011	-6.54
23-55	613.95	6.951	0.014	4.82	-0.598	0.007	-6.61
23-55d	613.95	7.148	0.003	5.01	-0.095	0.017	-6.11
23-56	613.37	6.96	0.009	4.83	-0.606	0.009	-6.62
23-57	612.96	6.756	0.011	4.62	-0.634	0.009	-6.65
23-58	612.11	6.871	0.009	4.74	-0.605	0.018	-6.62
23-59	611.34	6.334	0.017	4.15	-0.109	0.005	-6.13
23-60	611	6.427	0.013	4.26	-0.491	0.013	-6.51
23-61	610.44	6.533	0.009	4.36	-0.048	0.006	-6.07
23-62	609.87	6.316	0.008	4.11	0.316	0.007	-5.71
23-63	609.45	6.075	0.014	3.87	-0.015	0.015	-6.04
23-63d	609.45	6.06	0.013	3.85	-0.038	0.018	-6.06
23-64	608.97	6.906	0.007	4.72	0.897	0.016	-5.12
23-65	608.09	6.697	0.005	4.52	0.283	0.014	-5.73
23-66	607.4	6.191	0.008	3.98	0.365	0.01	-5.66
23-67	607.05	7.213	0.007	5.04	1.083	0.017	-4.93
23-68	605.95	6.624	0.014	4.44	0.447	0.007	-5.57
23-69	605.48	6.814	0.002	4.61	1.217	0.015	-4.80
23-70	604.27	6.452	0.005	4.25	0.518	0.018	-5.50
23-71	603.97	6.114	0.01	3.89	0.546	0.006	-5.48
23-72	603.35	7.345	0.016	5.16	1.916	0.007	-4.10
23-73	603.03	6.687	0.006	4.50	0.55	0.011	-5.47
23-74	602.37	6.948	0.019	4.76	1.164	0.012	-4.86
23-75	601.95	6.418	0.01	4.20	0.958	0.01	-5.07
23-76	601.45	6.946	0.007	4.76	1.061	0.017	-4.96
23-76d	601.45	6.894	0.014	4.71	0.812	0.012	-5.21
23-77	601.06	6.519	0.009	4.32	0.578	0.009	-5.44
23-78	600.65	6.271	0.007	4.07	0.143	0.016	-5.88
23-79	599.9	6.378	0.014	4.18	0.354	0.011	-5.67

23-80	599.28	6.275	0.011	4.07	0.386	0.008	-5.64
23-81	598.83	6.14	0.005	3.92	0.545	0.023	-5.48
23-82	597.75	5.782	0.009	3.54	0.573	0.012	-5.45
23-83	597.37	6.031	0.015	3.79	0.841	0.011	-5.19
23-84	596.85	6.138	0.018	3.92	0.493	0.005	-5.53
Secondary Cements Analysis							
				∂ 13C			∂ 18O
Sample	Depth	∂ 45/44	s	(PDB)	∂ 46/44	s	(PDB)
	(m)						
23-16 s	635.8	5.445	0.006	3.26	-1.935	0.011	-7.95
23-17 s	635.18	5.64	0.004	3.48	-2.231	0.013	-8.25
23-33 s	626.35	5.47	0.006	3.29	-1.935	0.02	-7.95
23-49 s	617.43	11.571	0.013	9.73	-0.219	0.007	-6.19

T - 4522

AUTHOR: ABDULRAHMAN AL-BASTAKI

PLATE 5

Photographic Record of the Shuaiba Formation GN-23 Core

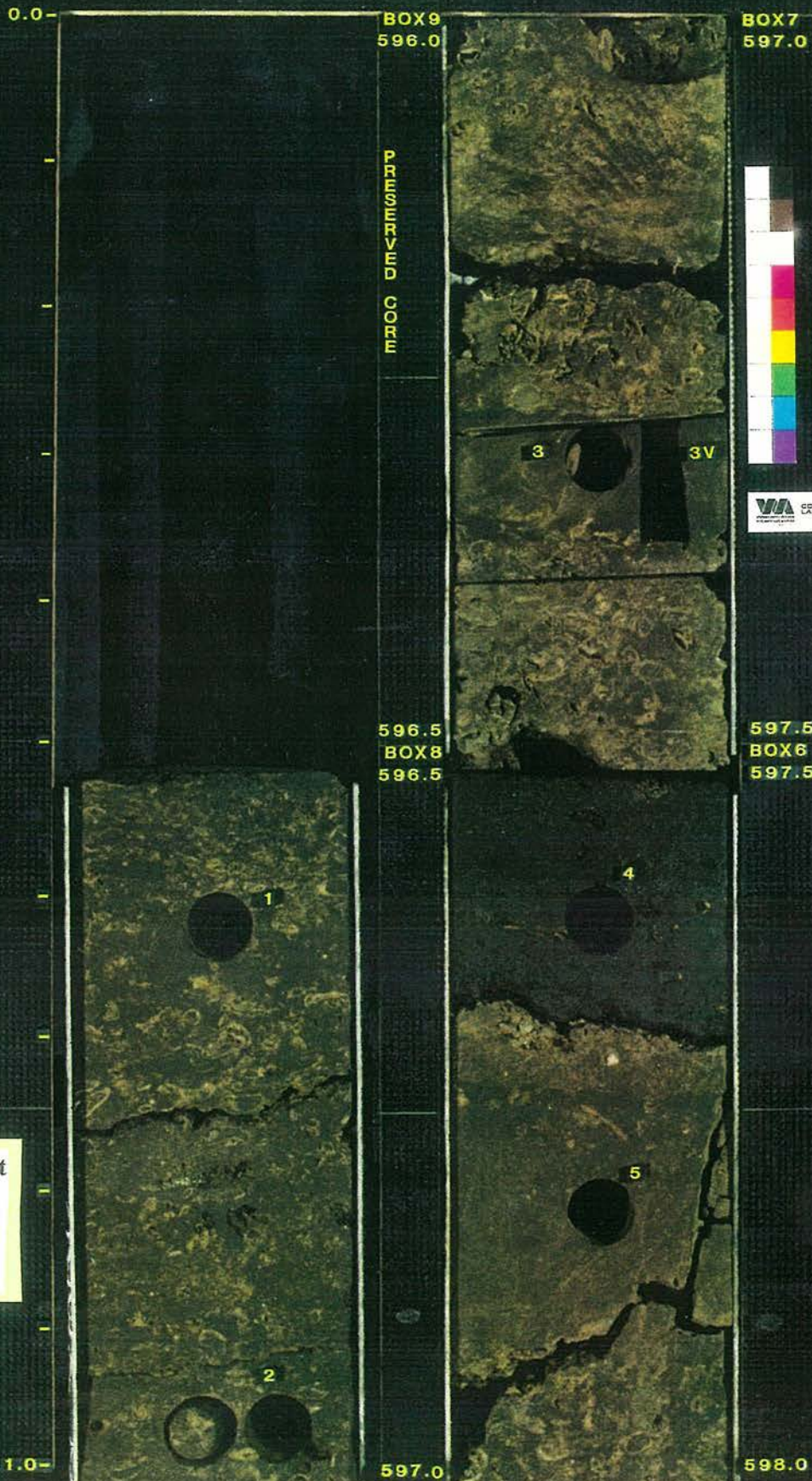
COMPANY PDO
WELL GHABA NORTH-23

CORE 1 594.0 - 600.4M



COMPANY PDO
WELL GHABA NORTH-23

CORE 1 594.0 - 600.4M



Extensive Rudist
Leaching And
Very Heavy
Hydrocarbon
Staining

COMPANY PDO
WELL GHABA NORTH-23

CORE 1 594.0 - 600.4M

0.0-

BOX5
598.0

BOX3
599.0

2WC

7



VA CORE LABORATORIES

598.5
BOX4
598.5

599.5
BOX2
599.5

8

8

1.0-

599.0

600.0

COMPANY PDO
WELL GHABA NORTH-23

CORE 1 594.0 - 600.4M

0.0-

BOX 1
600.0



600.4



VIA
CORE
LABORATORIES

1.0-

COMPANY PDO
WELL GHABA NORTH-23

CORE 2 600.4 - 606.8M

0.0-

BOX 14
600.40

BOX 12
601.21

PREPARED CORE



601.67
BOX 11
601.67

600.92
BOX 13
600.92



601.21

3WC

602.17

8

1.0-

COMPANY PDO
WELL GHABA NORTH-23

CORE 2 600.4 - 606.8M

0.0-

BOX 10
602.17

BOX 8
603.17



602.67

603.67

BOX 9
602.67

BOX 7
603.67



1.0-

603.17

604.17

COMPANY PDO
WELL GHABA NORTH-23

CORE 2 600.4 - 606.8M

0.0-

BOX 6
604.17

BOX 4
605.17



16



17



604.67

605.67

BOX 5
604.67

BOX 3
605.67

P
R
E
M
I
U
M
C
O
R
E



4WC

1.0-

605.17

606.17

COMPANY PDO
WELL GHABA NORTH-23

CORE 2 600.4 - 606.8M

0.0-

BOX 2
606.17

18

606.40
BOX 1
606.40

19

606.80

1.0-



COMPANY PDO
WELL GHABA NORTH-23

CORE 3 606.8 - 613.2M

0.0-

BOX 13
606.80

BOX 11
607.70

20V

20

21

24

24V

25

607.20
BOX 12
607.20

608.20
BOX 10
608.20

22

23

PRESERVED CORE

607.70

1.0-

608.70



COMPANY PDC
WELL GHABA NORTH-23

CORE 3 606.8 - 613.2M

0.0-

BOX9
608.70

BOX7
609.70



VIA CORE LABORATORIES

609.20
BOX8
609.20

610.20
BOX6
610.20



610.70

Subaerial Exposure
Surface At The
Top Of A Rudist
Boundstone Facies.
Note Leaching Of
Rudists Below This
Surface

COMPANY PDO
WELL GHABA NORTH-23

CORE 3 606.8 - 613.2M

0.0-

BOX 1
612.70



613.20



1.0-

COMPANY PDO
WELL GHABA NORTH-23

CORE 4 813.2 - 819.5M

0.0-

BOX 13
813.20

BOX 11
814.20

40

42

42V

41

43

44

813.70

BOX 12
813.70

814.70

BOX 10
814.70

6WC

45

46

1.0-

814.20

815.20



COMPANY PDO
WELL GHABA NORTH-23

CORE 4 613.2 - 619.5M

0.0-

BOX9
615.20

BOX7
616.20

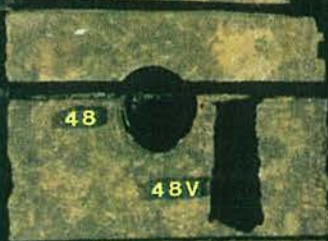
PRESERVED CORE



47

615.70
BOX8
615.70

616.70
BOX6
616.70



48

48V



49



50

1.0-

618.20

617.20

51

COMPANY PDO
WELL GHABA NORTH-23

CORE 4 613.2 - 619.5M



COMPANY PDO
WELL GHABA NORTH-23

CORE 4 813.2 - 819.5M

0.0-

BOX 1
819.20



819.50

A Hardground With Borings Separating The Overlying Cemented Rudist Rudstone From The Underlying Wackestone



1.0-

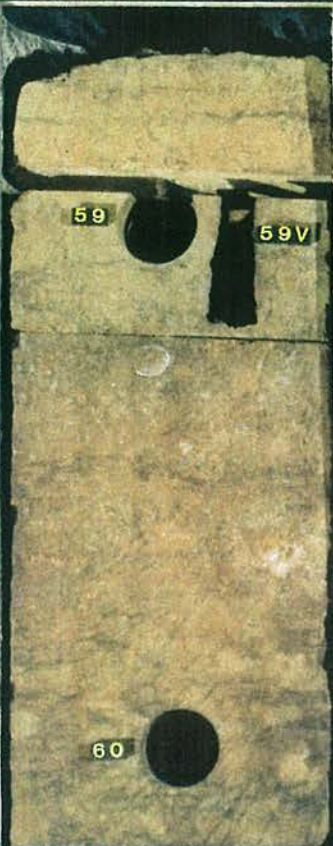
COMPANY PDO
WELL GHABA NORTH-23

CORE 5 619.6 - 626.0M

0.0-

BOX 13
619.60

BOX 11
620.60



59

59V

60



PRESERVED CORE



620.10
BOX 12
620.10

621.10
BOX 10
621.10



61

62



63

64

1.0-

620.60

621.60

COMPANY PDO
WELL GHABA NORTH-23

CORE 5 619.6 - 626.0M



COMPANY PDO
WELL GHABA NORTH-23

CORE 5 819.8 - 828.0M

0.0-

BOX 5
823.80

BOX 3
824.80



REVISIONS

1	0.00	0.00	0.00
2	0.00	0.00	0.00
3	0.00	0.00	0.00
4	0.00	0.00	0.00
5	0.00	0.00	0.00
6	0.00	0.00	0.00
7	0.00	0.00	0.00
8	0.00	0.00	0.00
9	0.00	0.00	0.00
10	0.00	0.00	0.00



Very Well Developed
Solution Seams

824.10
BOX 4
824.10

825.10
BOX 2
825.10



1.0-

824.60

825.60

COMPANY PDO
WELL GHABA NORTH-23

CORE 5 619.6 - 626.0M

0.0-

BOX 1
625.60

77

77V

78

79

626.00



1.0-

COMPANY PDO
WELL GHABA NORTH-23

CORE 6 626.0 - 632.4M

0.0-

BOX 13
626.00

BOX 11
627.00

9WC

82

83V

83

626.50

627.50

BOX 12
626.50

BOX 10
627.50

80

84

81

85

85V

1.0-

627.00

628.00



COMPANY PDO
WELL GHABA NORTH-23

CORE 6 626.0 - 632.4M

Extensively Cemented
Thin Rudist Rudstone
Interval

0.0-

BOX 9
628.00

BOX 7
629.00



628.50
BOX 8
628.50

629.50
BOX 6
629.50



1.0-

629.00

630.00

COMPANY PDO
WELL GHABA NORTH-23

CORE 6 626.0 - 632.4M

0.0-

10WC

BOX5
630.00

BOX3
631.00

94

95

630.50

631.50

BOX4
630.50

BOX2
631.50

92

92V

96

93

97V

97

1.0-

631.00

632.00



COMPANY PDO
WELL GHABA NORTH-23

CORE 6 626.0 - 632.4M

0.0-

BOX 1
632.00



632.40



VA CORE LABORATORIES

1.0-

COMPANY PDO
WELL GHABA NORTH-23

CORE 7 632.4 - 638.8M

0.0-

BOX 13
632.40

BOX 11
633.40

99

99V

103

103V

100

104

632.90

633.80

BOX 12
632.90

BOX 10
633.80

101

102

634.40

1.0-

633.40

634.40



COMPANY PDO
WELL GHABA NORTH-23

CORE 7 632.4 - 638.8M

0.0-

BOX9
634.40

BOX7
635.40



WC11



107

Algal Boundstone
Facies



108

634.90

635.90

Solution Seams And
Horse-tail Compaction
Features

BOX8
634.90

BOX6
635.90



105



109

109V



106

635.40

636.40

1.0-

COMPANY PDO
WELL GHABA NORTH-23

CORE 7 632.4 - 638.8M

0.0-

BOX 5
636.40

BOX 3
637.40



110



111

111V

636.90

637.90

BOX 4
636.90

BOX 2
637.90



112



WC12



113

637.40

638.40

1.0-

PRESERVED CORE



COMPANY PDO
WELL GHABA NORTH-23

CORE 7 632.4 - 638.8M

0.0-

BOX 1
638.40

114

638.80



1.0-

COMPANY PDO
WELL GHABA NORTH-23

CORE 8 638.8 - 644.8

0.0-

BOX 12
638.80

BOX 10
639.76



639.26
BOX 11
639.26

640.26
BOX 9
640.26



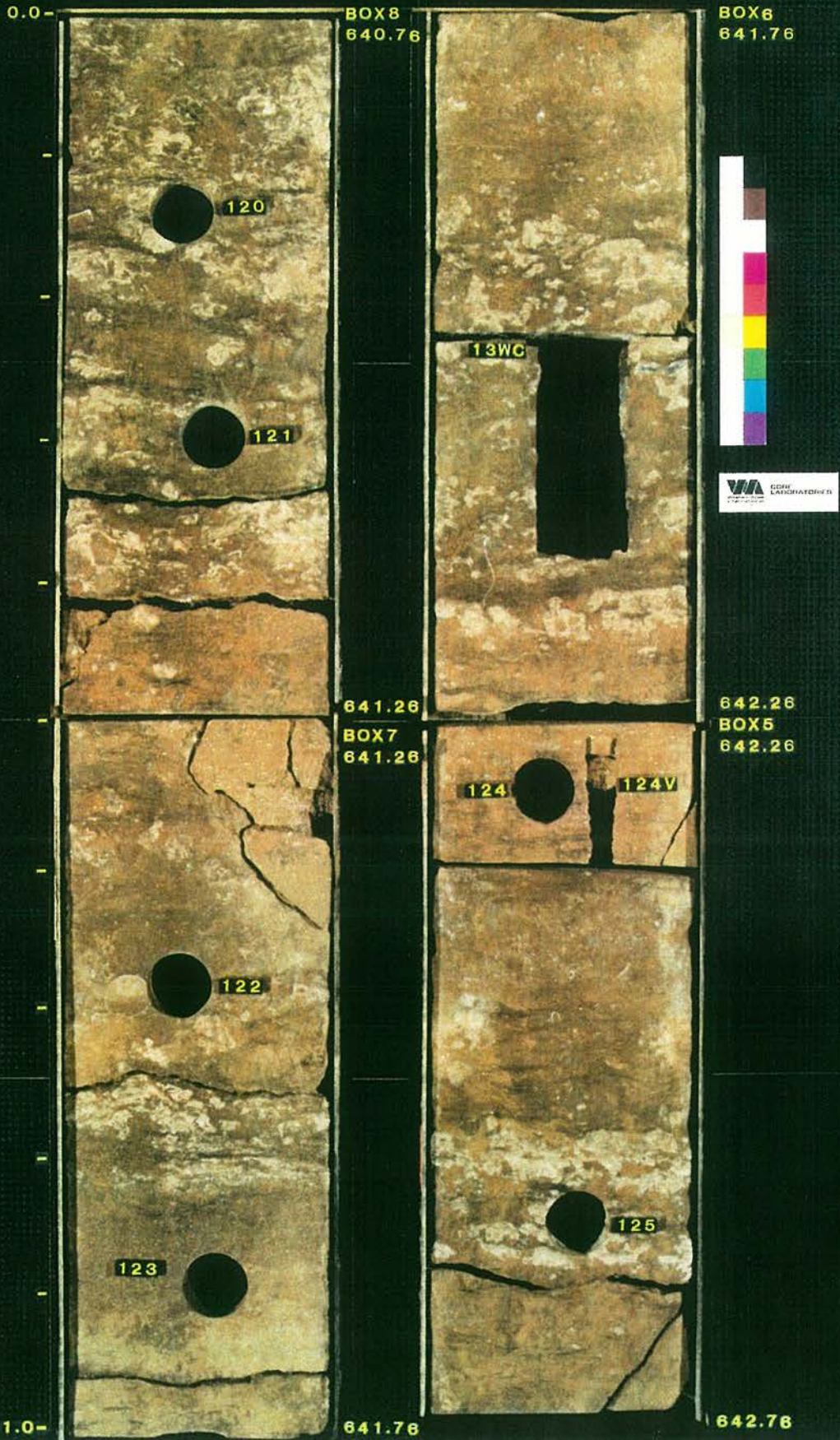
1.0-

639.76

640.76

COMPANY PDO
WELL GHABA NORTH-23

CORE 8 638.8 - 644.8M



COMPANY PDO
WELL GHABA NORTH-23

CORE 8 638.8 - 644.8M

0.0-

BOX 4
642.76

BOX 2
643.76

Subvertical Extensional
Fracture

126

130

127

131

643.26

644.26

BOX 3
643.26

BOX 1
644.26

128

129

643.76

644.80

1.0-

PRESERVED CORE

